

Zeitschrift: IABSE reports = Rapports AIPC = IVBH Berichte
Band: 66 (1992)
Rubrik: Experimental studies

Nutzungsbedingungen

Die ETH-Bibliothek ist die Anbieterin der digitalisierten Zeitschriften auf E-Periodica. Sie besitzt keine Urheberrechte an den Zeitschriften und ist nicht verantwortlich für deren Inhalte. Die Rechte liegen in der Regel bei den Herausgebern beziehungsweise den externen Rechteinhabern. Das Veröffentlichen von Bildern in Print- und Online-Publikationen sowie auf Social Media-Kanälen oder Webseiten ist nur mit vorheriger Genehmigung der Rechteinhaber erlaubt. [Mehr erfahren](#)

Conditions d'utilisation

L'ETH Library est le fournisseur des revues numérisées. Elle ne détient aucun droit d'auteur sur les revues et n'est pas responsable de leur contenu. En règle générale, les droits sont détenus par les éditeurs ou les détenteurs de droits externes. La reproduction d'images dans des publications imprimées ou en ligne ainsi que sur des canaux de médias sociaux ou des sites web n'est autorisée qu'avec l'accord préalable des détenteurs des droits. [En savoir plus](#)

Terms of use

The ETH Library is the provider of the digitised journals. It does not own any copyrights to the journals and is not responsible for their content. The rights usually lie with the publishers or the external rights holders. Publishing images in print and online publications, as well as on social media channels or websites, is only permitted with the prior consent of the rights holders. [Find out more](#)

Download PDF: 31.12.2025

ETH-Bibliothek Zürich, E-Periodica, <https://www.e-periodica.ch>



EXPERIMENTAL STUDIES

Leere Seite
Blank page
Page vide

Lessons to be Learned from the History of Suspension Bridge Suspenders

Leçons tirées des expériences réalisées avec les suspentes
de ponts suspendus

Lehren aus den Erfahrungen mit Aufhängungen in Hängebrücken

Blair BIRDSALL
Consulting Eng
Allendale, NJ, USA



Blair Birdsall, born 1907, obtained his Civil Engineering masters degree at Princeton University, Princeton, NJ. During 31 years at John A. Roebling's Sons Co. and 27 years with the consulting firm Steinman Boynton Gronquist & Birdsall, he has specialized in the design and construction of cable supported bridges.

SUMMARY

A review of laboratory results as compared with stress ranges in current use over many years suggests a relaxation in the conservative approach to design for fatigue.

RÉSUMÉ

L'auteur présente une rétrospective de résultats de laboratoire comparés aux tendances pratiquées depuis plusieurs années. Il suggère d'assouplir la méthode conservatrice du dimensionnement à la fatigue des câbles de suspension.

ZUSAMMENFASSUNG

Eine Rückschau auf Labortestergebnisse im Vergleich zu den Spannungsniveaus, die tatsächlich über viele Jahre auftreten, legt nahe, das konservative Vorgehen bei der Ermüdungsbemessung von



LESSONS TO BE LEARNED FROM THE HISTORY OF SUSPENSION BRIDGE SUSPENDERS

In reflecting on the subject of fatigue, as related to cyclic axial tension on wire tension members, the writer has been impressed by the inexactitude of the data base on which design judgments are made. The results of laboratory tests typically show a wide scatter of cycles to "failure". (Here "failure" is in quotation marks because each researcher has his own criterion for failure, or for discontinuance of a test). Also, the number of cycles selected for design purposes on a given structure is, at best, an educated guess.

In the presence of all these uncertainties, it is not surprising that designers take a very conservative approach, selecting an S-N curve which is at or near the lower boundary of the scatter of test results, and then applying a factor of safety by limiting the maximum permissible stress range to a percentage (e.g. 75% or 80%) of the range taken from the curve.

As more and more experience gets into the record, and better testing procedures are developed, designers will probably be inclined to relax this conservatism to some degree. The writer has also been impressed that, although thousands of tons of suspender ropes on suspension bridges have been undergoing millions of cycles of stress during more than 100 years of service, there has not come to his attention a single case of wire fracture or retirement from service which has been attributed to the results of cyclic axial tension. Admittedly, the cyclic stress range in this service has been relatively small. On the other hand, the writer suspected that the scatter of test results for this construction of wire rope (galvanized wire assembled in six helically wound strands wound helically about a core consisting of another strand or a small stranded wire rope) would demonstrate a relatively low endurance limit. (Defined as the maximum stress range which can be repeated indefinitely without failure.) Some researchers have even concluded that a rope of such construction has no endurance limit.

The original intended purpose of this paper was that of placing on the record a full review of test results and a wide spectrum of design and actual stress ranges on existing bridges. However, the task turned out to be so time consuming that, when the time came to draw the line on further research in order to meet the deadline for submission of papers, it had been far from finished to the writer's satisfaction. Thus, this will, to some extent, be in the nature of an interim report, presented in the hope that some institution devoted to research will agree that the intended result has validity, and will decide to finish the job.

In search of test results, an attempt was made to achieve a full review of literature on the subject, with the aid of many persons, whose generous responses are gratefully acknowledged. The literature abounds with fatigue tests on individual wires, spiral strands, and parallel wire strands, but relatively little appears for stranded cables, which are the subject of this paper. However, it was possible to uncover seven research projects whose results are pertinent. The sources are given below under "References". Correlation of these results was difficult. There was no consistency in the method of plotting (i.e. logarithmic vs. natural). Where stress ranges are expressed as percentages, the question "percentage of what?" is often not clearly answered. The criterion for failure or discontinuance of test is often not clear. Making reasonable assumptions, where necessary, and making a careful attempt to reduce all data to natural scale, the writer has produced seven curves, numbered from one to seven, corresponding to the number of the "Reference" from which each was obtained. For ease of reading, these curves are first presented on three separate charts, as indicated below:

Figure 1: This presents curves 1 & 2.



Curve 1 is taken from Fig. 4 of reference 1, It represents the only two lines on that chart which deal with ropes of the subject type, It is an average of those two lines, which are very close and similar. Failure is defined as the failure of 5% of the wires. This line represents an average of test results, not a bottom boundary of scatter.

Curve 2 is taken from Fig. 9 of reference 2. It represents the dashed line and is the boundary of test results based on failure defined as "5 broken wires".

It is interesting to note that, although separated vertically by approximately 10% of ultimate strength, the curves have very similar forms. This implies the likelihood of a failure to correlate data adequately well (e.g. ultimate strengths or failure criteria). There is also the difference between "average of scatter" and "lower boundary".

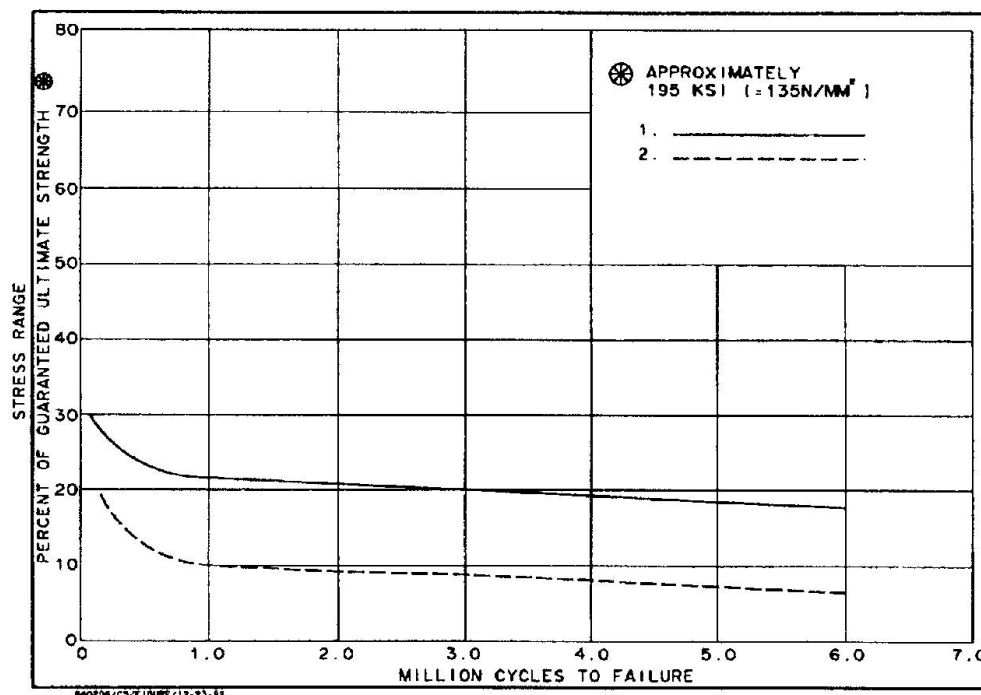


FIGURE 1

Figure 2: Here are presented curves 6 & 7.

Curve 6 is taken from Fig. 8 of reference 6. It represents the curve for 5% wire breakage and is the average of test scatter.

Curve 7 is taken from Fig. 9 of reference 7. It represents the average of test results and the criterion for failure is not given. Again we have two curves of similar form, separated by almost 10% of ultimate strength, and, again, the most likely cause is imperfection of correlation of data.

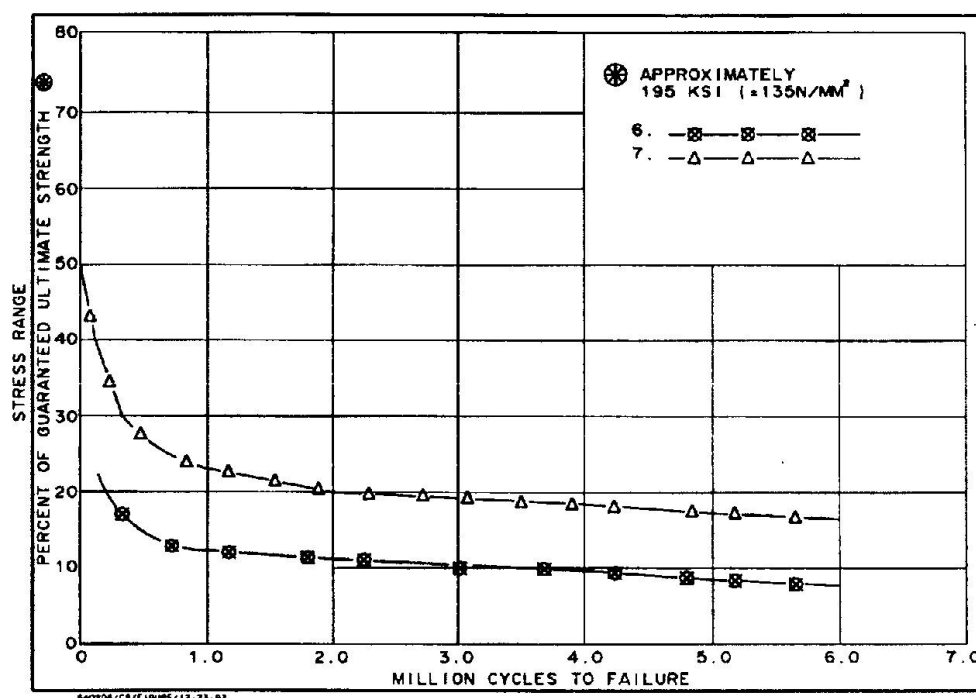


FIGURE 2

Figure 3: Here are presented Curves 3, 4, & 5.

Curve 3 is taken from Fig. 8 of reference 3. It represents an average of test results wherein the criterion for failure was the fracture of one strand.

Curve 4 is taken from Fig. 4 of reference 4. It represents a judgmental statement of the safe lower boundary of a fatigue spread developed from the study of many ropes including the suspenders of the Golden Gate Bridge.

Curve 5 is taken from Fig. 4 of reference 5. It represents the average of test results on the suspenders of the George Washington Bridge. The criterion for failure seems to have been excess elongation.

It can be seen that these results represent a scatter between the extremes of curves 1 & 7 on the high side, and curves 2 & 6 on the low side.

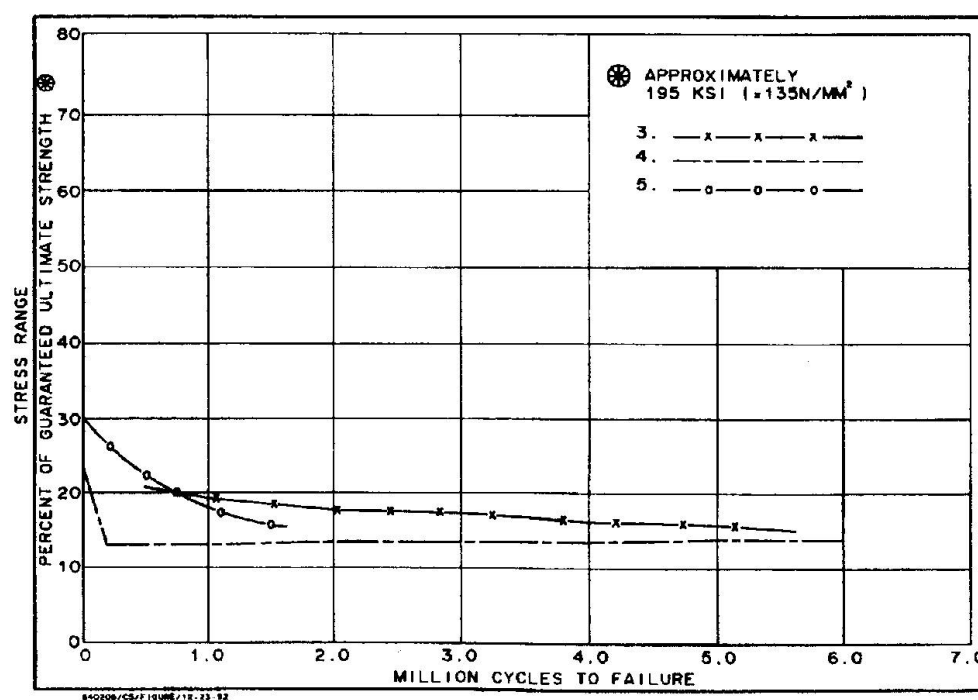


FIGURE 3



Figure 4: Here all 7 curves have been plotted to provide the visual representation of the range of all the data,

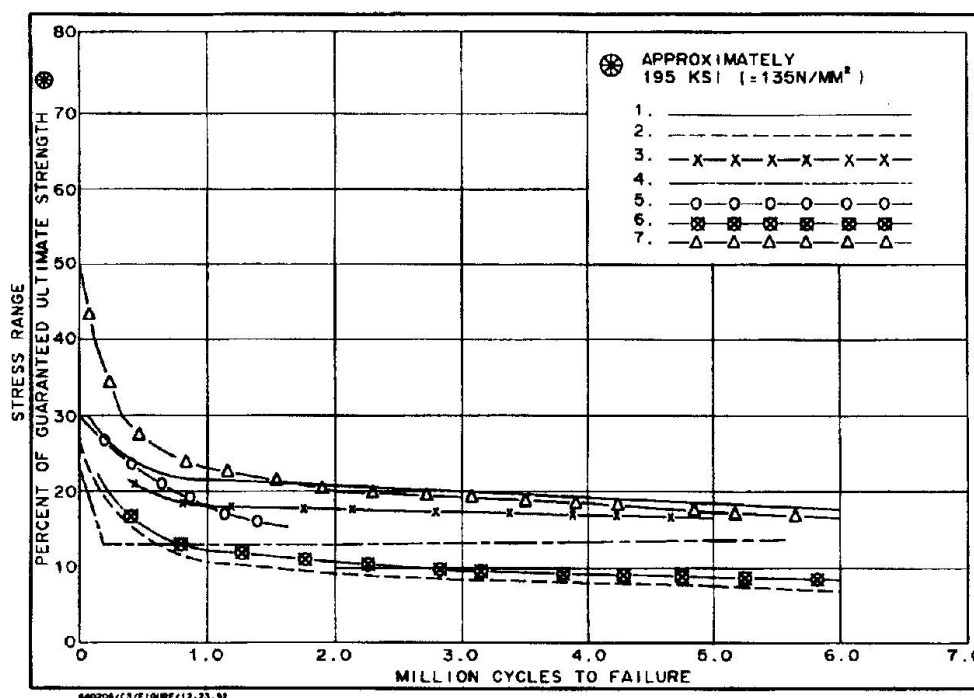


FIGURE 4

The above represents the limit of the data which the writer has been able to collect and analyze in the available time. It probably represents a fair sampling of currently existing reports and literature. What is needed from further research is a fine tuning of this type of data, -- either by going into greater depth in the analysis of existing data, in order to make sure that it is properly correlated and comparable, or by additional experimental research aimed specifically at obtaining data which is germane to the subject of this paper, or both,

Now let us turn to the input representing existing practice in the design stress range of suspenders. A partial list is presented in Table 1. This, also, is not as complete as the writer would like. It turned out to be very difficult to dig up this data out of old files. However, the spread of values seems to be broad enough to reach some tentative conclusions from this study.

TABLE 1

DESIGN STRESS RANGE OF SUSPENDER ROPES OF SEVERAL BRIDGES

BRIDGE	LOCATION	STRESS RANGE*
George Washington	New York	5
Walt Whitman	Philadelphia	10
Throg's Neck	New York	10
Maysville	Kentucky	12
Odgenburg	N.Y.-Canada	14
Davenport	Iowa-Illinois	14
Verrazano	New York	8
Forth Road	Scotland	12

*Percent of guaranteed strength (from several sources, including the writer's own files)



Figure 5 is a repetition of Figure 4, with the addition of the cross-hatched band which represents the above spread of extant stress ranges. This indicates that many suspenders have been operating successfully, without known fatigue breaks, at stress ranges above the minimum values for fatigue life developed from the literature. This does not mean, of course, that one should consciously take such liberties with experimental fatigue life. There can be many reasons for this apparent overlap. It is likely that serious consideration of fatigue was not included in the design. If the subject was given any consideration, it would probably have been discounted because of the low range of stress. The overlap could mean simply that the actual incidence of the maximum design stress range was not great enough to require dependence on the endurance limit.

However, it does lead one to believe that it would be adequately conservative to accept the lower portions of the test scatter as permissible design stress ranges, without the application of any further factor of safety. Hopefully, further tests and experience may lead to an even more relaxed approach.

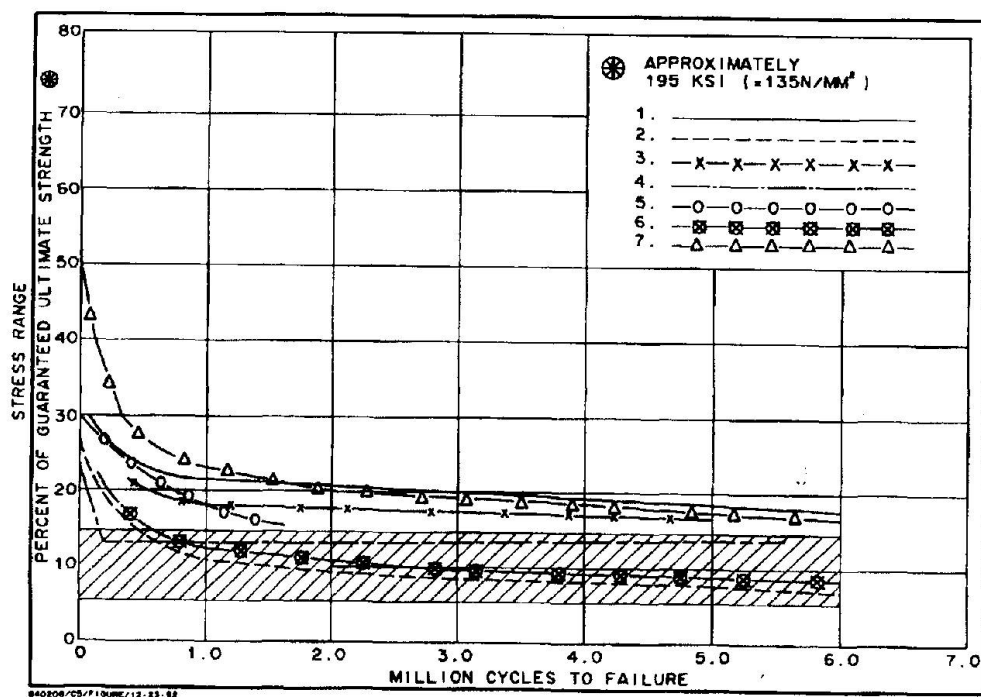


FIGURE 5

CONCLUSIONS AND RECOMMENDATIONS.

This study leads the writer to make the following suggestion for determining safe design stress range for cyclic axial tension on any type of steel wire tension member, be it a single wire, a bundle of parallel wires for use in a cable stayed bridge, spiral strands, or stranded cable:

Find the static stresses for the member, using all the criteria for loadings and allowable stresses selected for the design of the particular structure. Using the widest spectrum available of test data for the type of member, find the lower border of the scatter of test results which contains 95% of the test results. (This is suggested to avoid being misguided by the occasional extreme apparent test result.) If the design stress range is equal to, or below, the range obtained from the border curve, accept the design without further factor of safety.



It is the writer's hope that this discussion will motivate others to think along the same lines, and that a consensus will develop eventually in favor of a less ultra-conservative approach than many are taking now.

ACKNOWLEDGEMENTS

Grateful acknowledgement is given to the following persons for their generous contributions of their time and their files to help in this investigation:

G.P. Tilly, Head, Structures Group, British Transport and Road Research Laboratory;

Takeshi Mitamura, General Manager, Bridge Engineering & Construction Dept, Kobe Steel, Japan;

Stig Berge, University of Trondheim, Norway;

W.A. Lucht, P.E., Consulting Engineer, Danville, California;

Mohammed Raoof, of South Bank Polytechnic, London;

David Bradshaw, Bridon Ropes;

Dr. Fritz Leonhard, Stuttgart, Germany, and Dr. Jorg Schlaich, Stuttgart.

REFERENCES

1. HANZAWA MITSUGU et. al. Fatigue Behavior of Large Diameter Wire Ropes. Paper No. OTC 3999, 13th. Annual Offshore Technology conference.
2. G.P. TILLY. Performance of Bridge Cables. 1st, Oleg Kerensky Memorial Conference June 1988--London.
3. STIG BERGE. Axial Stiffness and Fatigue Strength of 76mm Dia. Steel Rope. Report MK/R 87. Department of Marine Technology, The Norwegian Institute of Technology, University of Trondheim, Norway.
4. W.A. LUCHT and F.W. DONECKER. Factors Affecting Wire Rope Life in a Marine Environment. Report No. OTC 2924. 9th Annual Offshore Technology Conference, Houston, Texas, May 2-4 1977.
5. I.P. GOULD. Suspender Ropes on George Washington Bridge Pass Rigid Tests. CIVIL ENGINEERING (New York) July 1966 pp 52-55.
6. A. OKUKAWA. Tensile and Fatigue Tests of Hanger Ropes for Suspension Bridges. Technical Report of the Honshu-Shikoku Bridge Authority Vol. 2 No. 5 Sept. 1978.
7. MOHAMMED RAOOF. A Critical Review of Draft API Recommended Practice 2FPI Regarding Fatigue Life Estimation of Moorings. Bridon Reader, Civil and Structural Engineering Department, South Bank Polytechnic, London.

Leere Seite
Blank page
Page vide

Experimental Execution and Results of Fatigue Test with Prestressing Steel

Exécution et résultats d'essai de fatigue sur des aciers de précontrainte

Ausführung und Ergebnisse von Ermüdungsversuchen an Spannstahl

Volker ESSLINGER

Dr. Eng.

EMPA

Dübendorf, Switzerland



Volker Esslinger, born in 1939, graduated in Mech. Eng. at the Techn.Univ. of Stuttgart in 1964 and received his doctorate at the Fed. Inst. of Technology Zurich in 1968. In 1969 he was Res. Assoc. at Columbia Univ., New York City. Since 1971 he is Head of the Section for Fatigue/Service Loading at the EMPA in Dübendorf. He is also a lecturer at the ETH Zurich.

SUMMARY

The demand for quality tests of prestressing steels in fatigue with specimen as long as possible, create special requirements for the testing technique. These aspects are presented and, based on test results, individual influences of the fatigue test on prestressing wires and strands are discussed.

RÉSUMÉ

La nécessité de réaliser des essais de fatigue sur des éprouvettes d'une longueur aussi grande que possible, pour les aciers de précontrainte, n'est pas sans conséquence pour la technique d'essai. Ces aspects sont présentés et les divers facteurs d'influence des essais de fatigue sur des fils et des torons de précontrainte sont discutés sur la base de résultats d'essai obtenus.

ZUSAMMENFASSUNG

Die Forderung nach einer Qualitätsprüfung von Spannstählen unter Ermüdungsbeanspruchung mit möglichst langen Proben hat Folgen für die Prüftechnik. Diese Aspekte werden dargestellt, und anhand von Versuchsergebnissen werden einzelne Einflußgrößen der Ermüdungsprüfung von Vorspanndrähten und Spannlitzen diskutiert.



1. FATIGUE TESTING OF PRESTRESSING STEELS

1.1 Test frame

In fatigue tests of prestressing steels it is, according to Castillo [1] strongly recommended to use the longest possible elements, because this has the following advantages

- a better extrapolation to the real length of the element
- closer sample values to the zero-percentile curve
- shorter life and therefore lower costs
- more information at the same time
- the threshold value associated with the asymptotic independence assumption is more likely to be overcome.

Normally, the length of the "longest possible element" is given by the available fatigue testing machine. Commercially available fatigue testing equipment with a 250 kN-load capacity – this load range is well suitable for the quality test of single prestressing wires and strands – is frequently unsuitable in the sense of testing long elements in the meaning mentioned above. Therefore, the best way to deal with large values of length – say 1 meter or more – is to build a test frame which optimizes the conditions for the fatigue testing of elements made of prestressing steel. Such a frame was erected at the Swiss Federal Testing Laboratory (EMPA) and is shown in figure 1. The load limit of this frame is 400 kN. All parts of this test frame belong to a construction kit which serves the needs for a variety of fatigue test tasks. The frame is built up in sections of 2 m length and can easily be dismantled and reassembled in steps for a desired free clamping length of the tested specimen of about 2, 4, 6, 8 or 10 m. On both ends of these sections, identical base plates are attached. The base plate at the "fixed end" of the specimen holds the load measuring device with the clamping system in serie whereas the one at the "movable end" of the specimen holds the servo-hydraulic actuator with the displacement measuring device and with the other clamping system in serie.

The frame with the specimen is placed on the floor in a horizontal position which allows free access to the tested element for inspection during the test.

Wire specimen sometimes show multiple failures, that means that the first failure immediately causes a second failure at the next weak spot and then parts of the specimen are often released from the test frame. To prevent this, segments of plastic tubes should cover the specimen under test.

The specimen is tested symmetrically with regard to the central axis of the frame. For this reason, the load cell and the hydraulic actuator were especially developed with a passing hole in the center of 40 respectively 60 mm diameter, figure 2.

1.2 Measuring devices

Since fatigue tests on prestressing steel are characterized by high upper loads and relatively small load ranges – whereby the load range is primarily responsible for the fatigue of the element – the accuracy and stability of the load cell are of predominant importance for the consistency of the test results. The capacity of the used load cell should suit the highest loads needed and the overall error related to the nominal load should be less than $\pm 0.05\%$.

The deformation of the specimen during the load-controlled test is measured with a separate LVDT-displacement sensor which is attached to the hydraulic actuator. This signal also serves for monitoring the test and for shutting down the whole arrangement after failure of the prestressing wire or after failure of the first wire in strands. In some cases a shock sensor was used parallel to cut off the test in a reliable manner.

1.3 Loading equipment

The loading of the specimen is done by a servo-hydraulic actuator under load control with sinusoidal wave form. This control facilitates the adjustment of the test frequency and the wave form in one-step-tests (constant amplitude). Nevertheless, it should be noted that long specimen and high load ranges cause large amplitudes of deformation and in this case, the use of one or more servovalves with high flow rates is mandatory in order to obtain a reasonable value of the test frequency.

The stroke of the actuator is not only given by the deformation of the specimen under load, but also by the slipping of the specimen in the grips during set-up of the test. For the test of 10 m long specimen a stroke of 200 mm is adequate.

The hollow drilled piston of the actuator also allows to load the specimen without any restraint against torsional movement. Such a rotation around the axis of the specimen would occur in strands. There is no rotation in service and therefore, rotation is prevented during the test by a longitudinal guidance.

1.4 Clamping devices

To perform fatigue tests in an economical way, it is important to use a reliable and easy-to-use clamping system. One should be aware that independent of the mode of clamping, the probability of failure in the clamping region increases with shorter length of the specimen, and this is one more point to test the longest possible specimen. Also the best clamping system cannot prevent that once in a while the weakest point of a specimen is situated in the clamp and thus causes a failure in the clamping region.

The clamping system used for wires shown in [figure 3](#), and the clamps used for strands shown in [figure 4](#), permitted in the past to hold down the rate of failures in the clamp under 1/40.



For clamping the wire, three under 120° displaced wedges of 80 mm length with an adapted stiffness are used, together with a 0.5 mm aluminium sheet formed as a tube to protect the surface of the wire like a sheath. An additional action to prevent failures in the clamping region is to roll the surface of the wire in this range as to increase the hardness of the surface and to put the surface layers under compression. All these methods are advantageous to prevent fretting fatigue as a main cause for failures in the clamps. At the ends of the wire-specimen a punched head with a washer anchors the wire on the wedges.

The strands are clamped by two wedges of 200 mm length, shown in [figure 4](#). Inside the wedges are wooden inserts surrounding the whole specimen and forming a quasi hydrostatic pressure state under load; this causes the wood to yield around the six outer wires of the strand and to guarantee a continuous transfer of the loads into the specimen. To anchor the strand on the two wedges – which is especially important at the beginning of the test – a commercially available anchor head is used.

2. RESULTS OF FATIGUE TESTS ON PRESTRESSING STEELS

2.1 Influence on test position

In this test program only specimen with a 10 m length were fatigued in horizontal position; all other, shorter specimen were tested in vertical position. To check a possible influence of the test position on the initiation site of the crack, the location of the crack initiation was noted with respect to four 90°-sectors named 1 to 4 starting at the upright position and going clockwise around the section. For 27 wire specimen tested with a length of 10 m, the following assignment was observed

number of failures	5	7	8	7
in sector	1	2	3	4

A preferred position for the initiation with regard to a differentiation up/down with 12 failures in sectors 1/2 (up) and 15 failures in sectors 3/4 (down) is not clearly visible.

2.2 Periodicity of flaws

If a periodicity of flaws over the length stemming from fabrication is supposed, it should be noticed in a compilation of the succeeding distances of failures. For the 27 tested wire-specimen with a free clamping length of 10'410 mm, the frequency of occurrence of the distances between failures are given in tab. 1.

The intervals of the fracture distances not listed in table 1, did not show any fracture.

Tab 1: Frequency of occurrence for the distances between the fatigue failures in wire specimen of 10'410 mm free clamping length

fracture distance in m	1-2	4-5	6-7	7-8	8-9	9-10	10-11	11-12	13-14	14-15	15-16
frequency absolute	1	1	2	3	6	3	4	1	2	2	3
frequency relative in %	3.6	3.6	7.1	10.7	21.4	10.7	14.3	3.6	7.1	7.1	10.7

Two of these 27 wire-specimen failed simultaneously at two locations. A statistical treatment of the failure distances with respect to a supposed periodicity – also for the shorter specimen – should be done in future.

The percentage of the fracture surface developed under fatigue was for all tested wire-specimen about 25 to 30 %, more or less independent from the stress ranges (400 to 800 N/mm²).



2.3 Strands: type of fracture

The fatigue failures in the single wires of the tested 0.6 inch-strands are predominantly caused by fretting corrosion. A designation of these failures according to [tab. 2](#) and an allocation of the fracture types for the various tested proof length is given in [tab 3](#).

Tab. 2: Strands; designation of fracture types

Type No.	Crack started	
	in	from interface
1	outer wire	outside
2	outer wire	outer / outer wire
3	outer wire	outer / center wire
4	control wire	outer / center wire
5	combination of type 2 and 4	

Tab 3: Strands; number of failures according to type number (see [tab. 2](#))

Proof length in m	Type				
	1	2	3	4	5
0.5	3	7	1	3	-
1	6	5	1	1	-
2	2	8	2	1	3
10	1	11	-	1	4
Sum	12	31	4	6	7

Tab. 3 shows that in these tests the fatigue crack started mostly at the interface between the outer wires. It is striking that with a test length of 1 m the majority of cracks begun at the outer surface of the outer wires. Obviously, the surface of these strands was damaged during fabrication or transport.

2.4 Strands: influence of pretorsion

To show whether there is an influence of a pretorsion given on the specimen in a clamped condition, strands of test length 1040 mm were tested at a stress range of 350 N/mm².

The first group was screwed up and the second group screwed down by an angle of 180° before starting the test. The results are given in tab. 4.

Tab 4: Strand 0.6 inch diameter; effect of pretorsion.
Free length 1040 mm; upper stress $\sigma_u = 1239$ N/mm²
Stress range $\Delta\sigma = 350$ N/mm²; test frequency 3.5 Hz

Specimen No.	Handling	Number of cycles until fracture of first wire	Remarks
19	screw down	154'000	* fracture type 1
18	screw down	264'000	fracture type 1
20	screw down	2'000'000	runout
22	screw up	333'000	fracture type 1
21	screw up	495'000	fracture type 1

* fracture type according to tab. 2

Screwing up or down the strand specimen in a clamped condition before starting the test has no clear influence as can be seen in tab 4. The occurrence of fracture type 1 (outer wire / from outside) shows that the outer surface of the single wire became critical and not – as supposed – that the interfaces of the outer wires and hereby the fretting corrosion were predominantly influenced by the pretorsion.

2.5 Wires: influence of test frequency

An influence of the test frequency on the results of fatigue tests is mainly to be expected at relatively high stress ranges. The plastic strain range depends on the rate of loading and, therefore, also on the test frequency. This means that at a lower test frequency higher plastic strain ranges appear which lead to a shorter life. This effect should vanish the closer the stress range reaches the fatigue limit.

For verification of this influence, wires of 150 mm length were fatigued at relatively high stress ranges of 600 and 800 N/mm² and a test frequency of 3.5 Hz and 105 Hz. The results are shown in figure 5. On both, the higher and lower level of the stress range, the influence of the test frequency is clearly visible, in the sense of shorter lives at a lower test frequency.

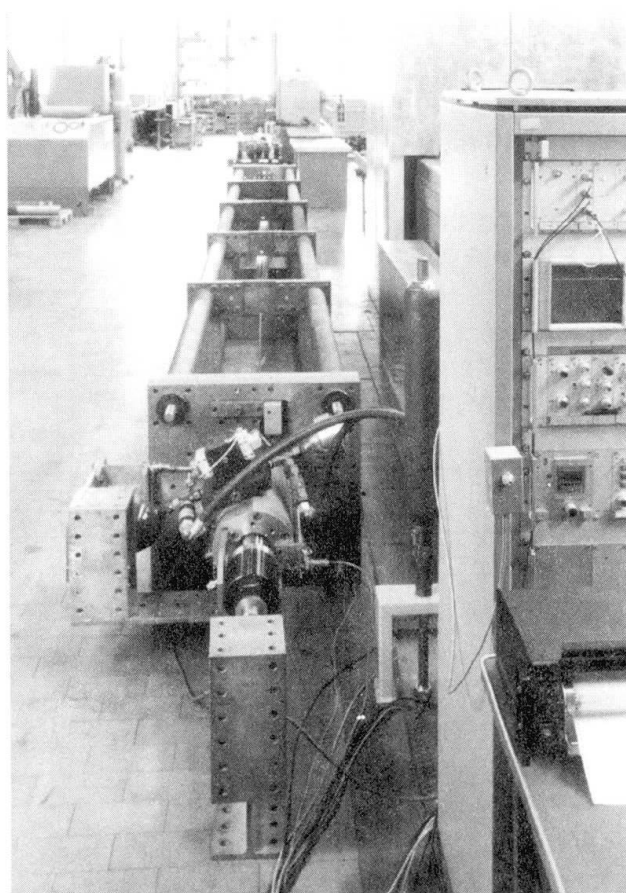


Figure 1: Test frame for fatigue tests of elements up to 10 m proof length

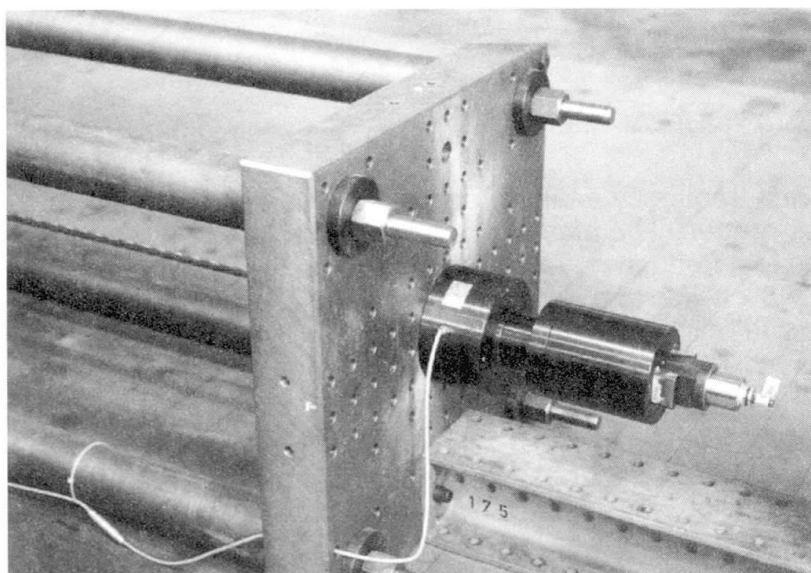


Figure 2: Arrangement of load cell and clamping system mounted on the base plate at the firm end of a fatigue test with a strand

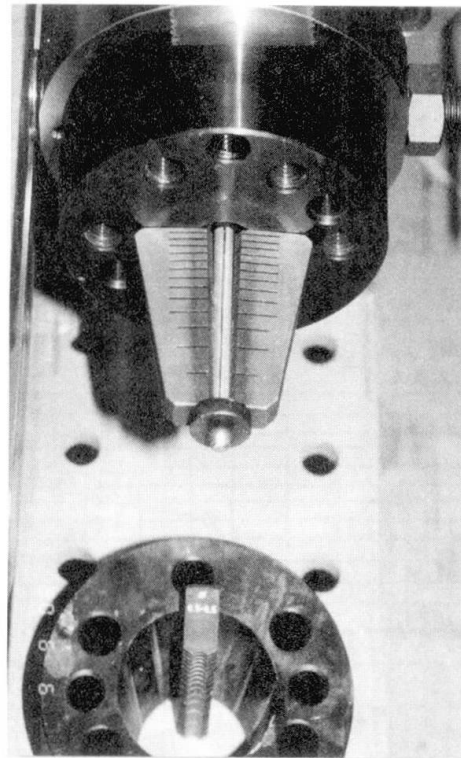


Figure 3: Clamping system for the 7 mm prestressing wire

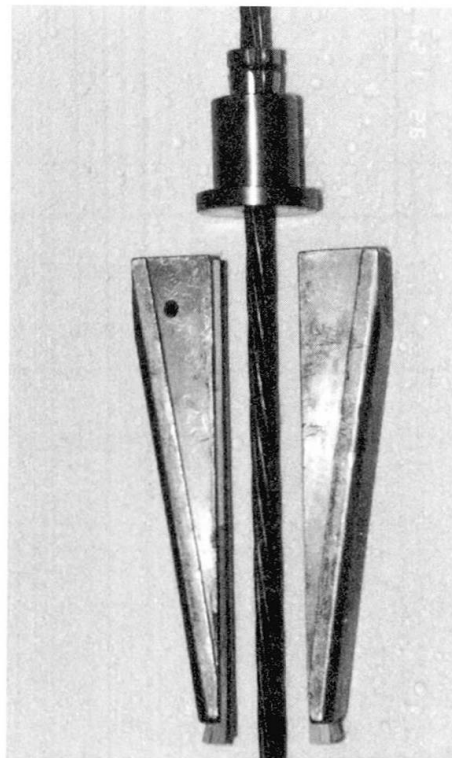


Figure 4: Clamping system for the 0.6 inch strand

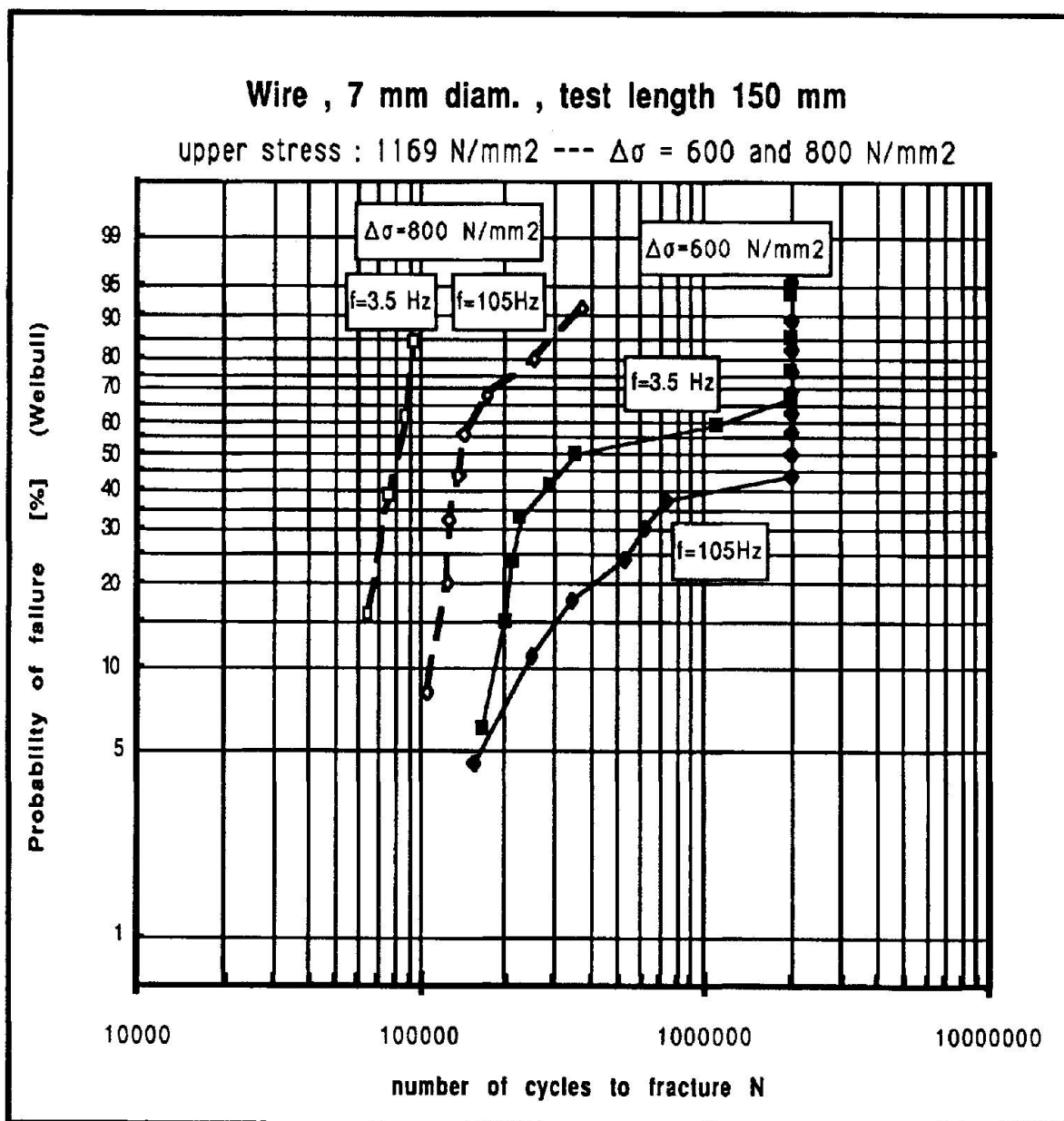


Figure 5: Influence of test frequency on results of fatigue tests on prestressing wire, 7 mm diameter

REFERENCES

- [1] Castillo, E. and A. Fernández-Canteli;
Statistical Models for Fatigue Analysis of long Elements;
IABSE Workshop Madrid, September 1992,
Length Effect on Fatigue of Wires and Strands.

Fatigue and Failure of a Flexed Locked Coil Wire Rope

Fatigue et défaillance de câbles clos soumis à une flexion forcée

Ermüdung und Versagen von verschlossenen Seilen unter
erzwungener Wechselbiegung

Georg KOPANAKIS

Mech Eng.
Swiss Fed. Inst. of Technology
Zurich, Switzerland



Georg Kopanakis, born 1952, received his Mechanical Engineer degree at the ETH Zurich. He is working at the Institute of Lightweight Structures and Ropeways of the Swiss Federal Institute of Technology.

SUMMARY

Investigations are currently being carried out on locked coil ropes both in service and in a specially constructed full-scale fatigue testing machine in order to examine the fatigue behaviour of a locked coil rope flexed at a roller chain. This paper describes the results of a part of this investigation.

RÉSUMÉ

Des essais de fatigue sont effectués pour étudier, dans la pratique ainsi qu'à l'aide d'un dispositif spécialement construit pour les essais en vraie grandeur, le comportement de câbles clos porteurs passant en flexion sur une chaîne à rouleaux. Ce travail décrit les résultats d'une partie de ces essais.

ZUSAMMENFASSUNG

Es werden Untersuchungen von verschlossenen Tragseilen in der Praxis und in einer speziell dafür konstruierten Prüfmaschine im Maßstab 1:1 durchgeführt, um das Ermüdungsverhalten von verschlossenen Seilen an Rollenketten zu ermitteln. Die vorliegende Arbeit beschreibt die Ergebnisse eines Teiles dieser Untersuchungen.



1. INTRODUCTION

In order to compensate potential load variations of the track rope of a reversible aerial tramway, due to fluctuating ambient temperature, cabin load and cabin position, a counterweight can be used. In most aerial tramways the track rope is directly deflected to the counterweight over a roller chain. The compensating movement of the counterweight causes a motion of the rope and the roller chain over the deflection saddle.

Over recent years, during regular nondestructive testing, a number of track ropes have been found to have an unexpected degree of damage within the areas subject to alternate stretching and bending at the roller chain.

The calculation of the multicomponental loading of a single wire in a bended steel wire rope is still not satisfactory, which makes a theoretical approach almost impossible. Therefore the Institute of Lightweight Structures and Ropeways of the Swiss Federal Institute of Technology Zurich started carrying out investigations of locked coil track ropes both in service and in a specially constructed full-scale fatigue testing machine in order to answer the following questions:

- how the damage nucleates and develops within the flexed area of the rope;
- whether there is a visible or acoustic indication, reliably warning of a critical amount of damage;
- to what extent the results of Gamma Ray Examination applied in this area are reliable, as well as
- how the fatigue behaviour of the track rope over roller chain is influenced by
 - * the rope itself (design & construction, lubrication)
 - * the ropeway installation (geometrical parameters of the deflection saddle and roller chain, number and length of the spans)
 - * the ropeway operation (trip frequency, cabin load).

2. EXPERIMENTAL PART

2.1 Test equipment (Fig. 1a & 2))

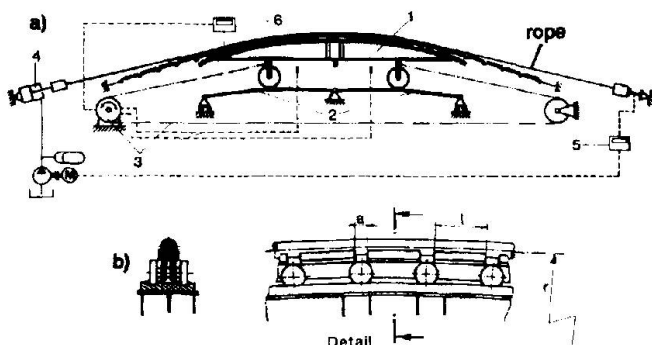


Fig. 1: Layout of the roller chain testing machine.

The testing machine consists of the following parts:

1. Saddle and roller chain (fabricated by the Swiss Ropeways Industry) fixed on a carriage
2. Track (of the carriage)
3. Drive system
4. Tensioning cylinder
5. Automatic control of the tensile force
6. Automatic control of the carriage velocity, influenced by rope temperature.

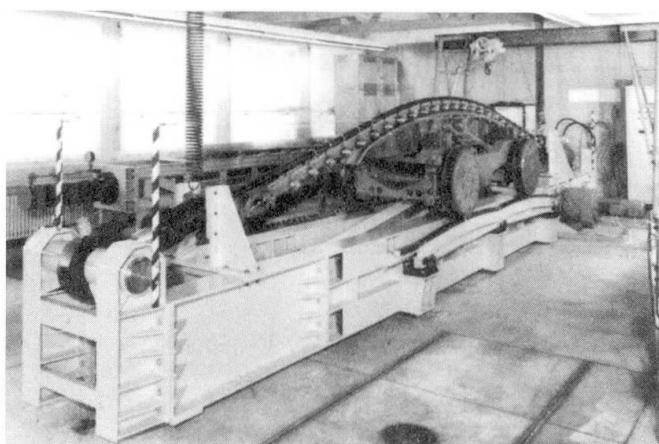


Fig. 2: View of the roller chain testing machine.

It has been designed to test ropes up to a diameter of 55 mm, reproducing the actual stress condition of a locked coil track rope flexed at a roller chain of a reversible tramway.

The rope specimen is bent over the roller chain and tensioned by the hydraulic cylinder. The shape of the carriage tracks has been calculated to invert the movement actually taking place in practice. Thus it is not the roller chain and the rope which roll over the saddle but the saddle which

slides under the fixed roller chain and rope.

For the application of additional lubricant, drip oil lubrication was used.

In order to perform the necessary regular NDT it is ensured that the rope can be totally clear of the roller chain along each flexed area under the regular service load.

2.2 Tests

The fatigue tests were conducted using specimens taken from two different ropes:

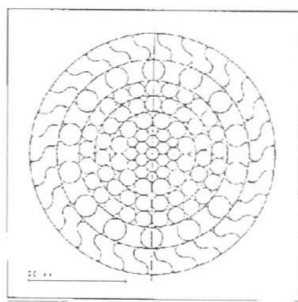


Fig. 3: Rope R1

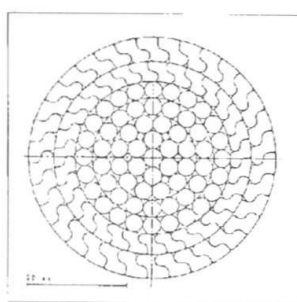


Fig. 4: Rope R2

R1: 50.7 mm diameter, 1 1/2 x locked coil rope of 1+6+(6+6)+12+19+25+14I+14x0+30xZ construction and minimum breaking load of 2640 kN (Fig. 3).

R2: 50 mm diameter, 2 x locked coil rope of 1+(6+6)+12+18+24+31Z+34Z construction and minimum breaking load of 2590 kN (Fig. 4).

The rope specimens have been manufactured with three different initial lubricants (L1, L2 & L3).

Two different saddle/roller chain sets have been tested:

- RK1: radius = 5500 mm ($r_1/d = 108.5$), link length = 185 mm, link distance = 40 mm, link form = curved ($r_{link} = r_{saddle}$), link lining = Polydur
- RK2: radius = 5000 mm ($r_2/d = 98.5$), link length = 360 mm, link distance = 45 mm, link form = curved ($r_{link} = r_{saddle}$), link lining = Polyacetate

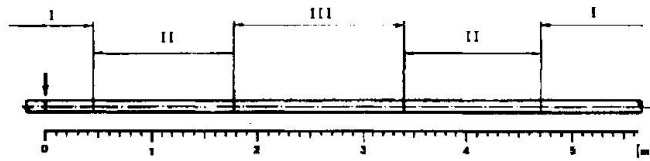


Fig. 5: Areas of the rope specimen

I: constantly stretched area (0 bc)
 II: flexed area (n bc)
 III: constantly bent area (1 bc)

The length of the flexed area adjusted for the tests comes to 1200 mm (~ 3 x the lay length of the outer layer) and the length of the constantly bent area to 1600 mm (~ 4 x the lay length of the outer layer) (Fig. 5).

A completed test numbered 600'000 bending cycles (bc) and lasted about three months. The frequency of bending

cycles chosen ensured that the temperature of the rope surface never exceeded 40°C during the tests.

The development of the number of wire breaks was followed by means of Gamma Ray Examination applied regularly during test life. In order to keep close to practice, the chosen NDT methods as well as the equipment required were those used on tramways for regular examinations. Thus an Ir¹⁹² source was used throughout all the experiments. After the end of each test the rope specimen was carefully dismantled and the damage found was registered.

Although the reproducibility of wire rope fatigue tests is mostly not high even when using one and the same rope, the tests mentioned here show that in this particular case of locally high resultant stress a high degree of consistency is possible (Fig. 6).

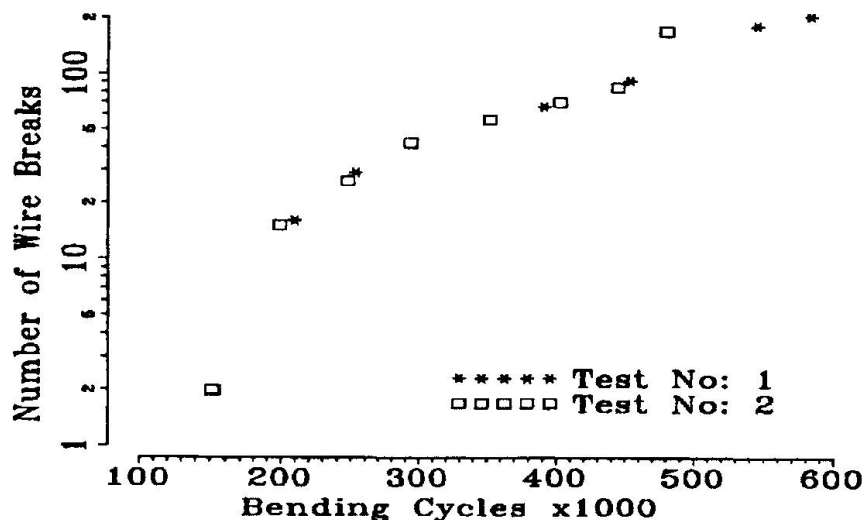


Fig. 6: The development of the number of wire breaks as a function of bending cycles, an example of the good reproducibility.

The plots in figures 6, 10, 11, 12 and 13 show the development of the number of wire breaks as a function of bending cycles. The number of wire breaks is plotted with a logarithmic scale on the Y axis, and the number of cycles is plotted with linear scale on the X axis. The straight lines drawn are an exponential approximation.

During the dismantling of the rope the relative position of the wires in the rope was registered in order to enable reconstruction of the local configuration in the surroundings of the breaks.



The areas of the first cracks as revealed by the Gamma Ray Examination were always of prime interest.

3. RESULTS OF THE TESTS

The first observation to be made is that the damage first starts and propagates in the second layer. The first wire breaks start in the "lower part" (i.e. at the rope side contacting the roller chain links) or/and in the "upper part" of the rope (i.e. the opposite rope side) (Fig. 1b).

Audible crackle emissions starting during an early stage of a test were always very soon followed by the first wire breaks occurring, as well as by a high amount of total damage at the end of a test.

However, the fact that during other tests no crackle emissions could be heard did not mean that no wire breaks occurred later. In those cases the damage started later without reaching a high amount, and the lubricant condition found after terminating the test was constantly better.

After the first breaks have occurred, more wire breaks follow almost in the same cross section. They first remain in the same layer, and they propagate ringwise.

Visible helical distortion - generated during service life - always indicated a concentration of wire breaks within the same area in the second layer.

Wire breaks in the first layer always followed previous advanced damage (i.e. all wires having multiple breaks) within this area in the second layer.

After terminating the test, the rope specimens were dismantled. The found state of the second layer described below was constantly repeated throughout the tests.



Fig. 7: A 60 mm long piece of O-wire ($d = 4.5$ mm) taken from the second layer, broken five times.

Almost all the wires of the second layer were found to have multiple breaks (Fig. 7), as well as several cracks next to the existing breaks (Fig. 8). An extreme local lack of lubrication within the contact areas of two wires of different layers (Fig. 9), and traces of frictional wear within these areas characterized the damage.

The amount of the fretting corrosion found depended on the quality and quantity of the lubricant used, i.e. in cases of a better lubricant - for this particular application - there was hardly any fretting corrosion to be found, which also resulted in a life improvement.

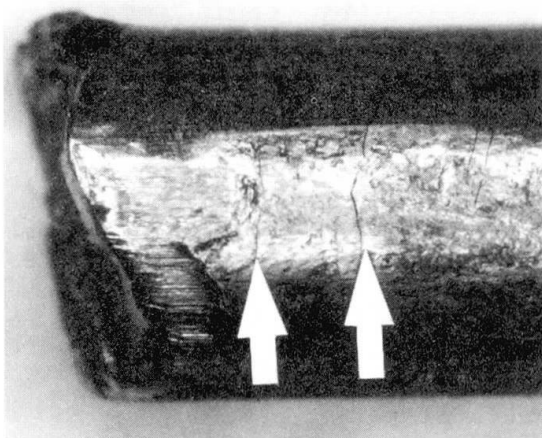


Fig. 8: A piece of an O-wire taken from the second layer with a fatigue break at the left. The arrows indicate the cracks nucleated next to the fatigue break.

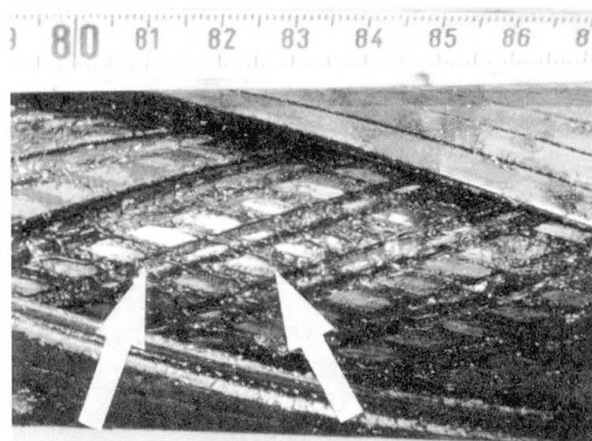


Fig. 9: Picture of the second layer after partly removing the first layer. The arrows indicate the contact areas with the wires of the first layer with visible local lack of lubrication.

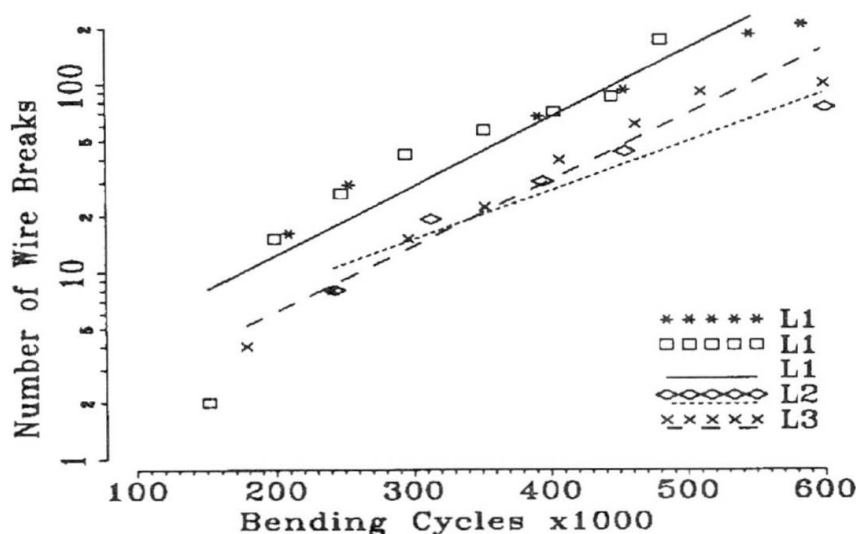


Fig. 10: The development of the number of wire breaks as a function of bending cycles; comparison between three initial lubricants.

Fig. 10 shows the comparison between three initial lubricants. The lubricants L2 and L3 have the same main component, being totally different to L1.

The influence of service relubrication depends on the compatibility with the initial lubricant, as well as on the ability to penetrate at least to the second layer of the locked coil wire rope.

An example is shown in Fig. 11. In this case a life increase of about 40 % has been achieved. Fig. 12 shows that if there is no compatibility between initial and service relubrication no significant improvement can be expected.

The above results show that the choice of the initial lubricant, as well as the application of a proper service relubricant, has significant influence on the fatigue behaviour of the rope under these resultant stress conditions.

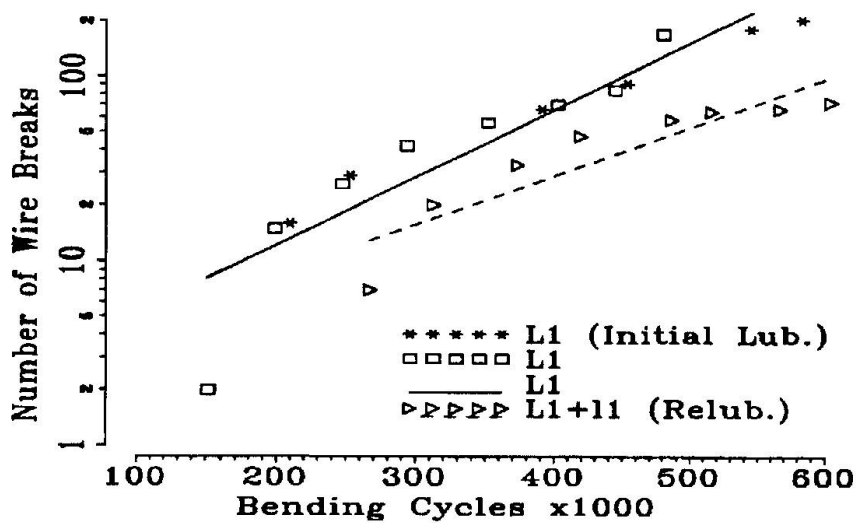


Fig. 11: The development of the number of wire breaks as a function of bending cycles; influence of service relubrication using a relubricant compatible with the initial lubricant.

All the above findings correspond well to the results of the metallographic examinations carried out by the Swiss Federal Laboratories for Materials Testing and Research, according to which, with the exception of some single wires, all the origins of the first cracks were situated within the intensive wear zones (Fig.14), mainly caused by high local pressure. On the other hand the crack

life increase due to the lubricant found here has led to the start of a detailed investigation of the influence of this parameter on fatigue behaviour.

The life expectancy of the rope construction R₂ (2 x locked coil) was, for this particular application and the ropes tested, almost 80% longer than that of R₁ (1 1/2 x locked coil) (Fig.13).

propagation is caused by combined bending and torsion and secondarily by tension.

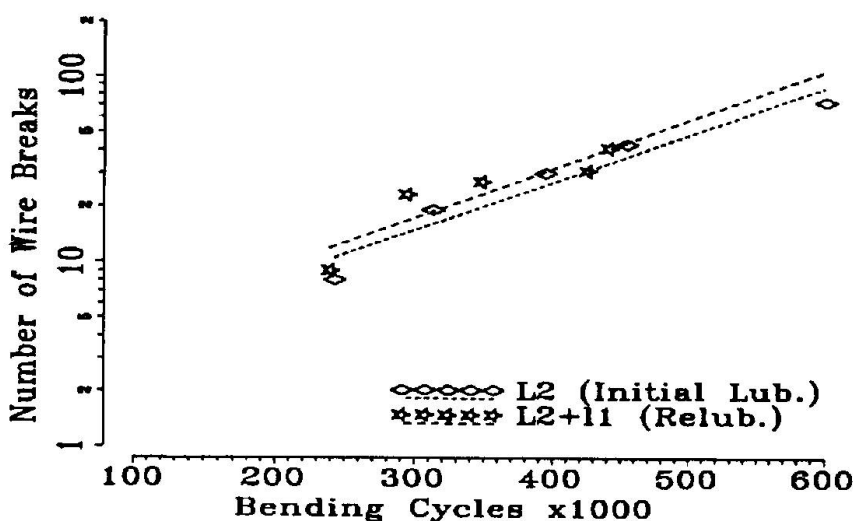
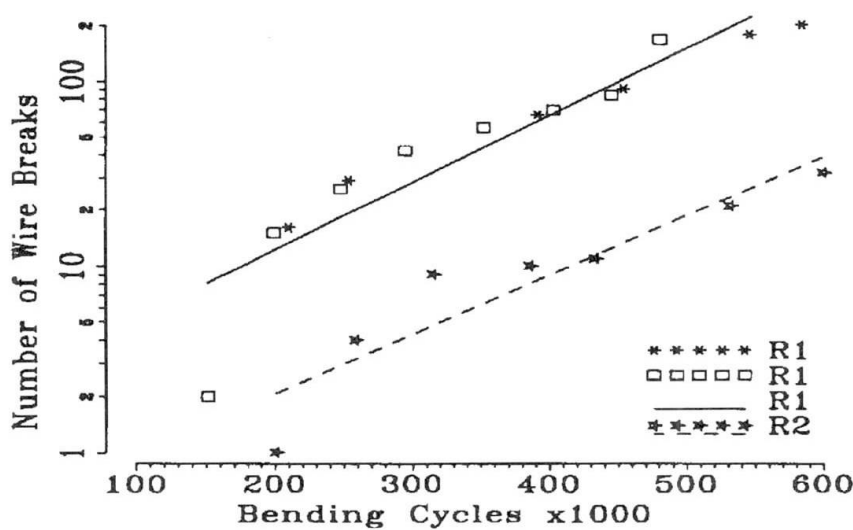


Fig. 12: The development of the number of wire breaks as a function of bending cycles; influence of service relubrication using a relubricant incompatible with the initial lubricant.

Finally the correspondence between the diagnosed (by NDT) sum of wire breaks and the actual figure has been found to be satisfactory.

Even in cases of considerable damage, 80% of the wire breaks have been identified. However, the existence of



numerous multiple wire breaks makes the correlation between the diagnosed number of wire breaks and the actual cross section loss practically impossible.

Fig. 13: The development of the number of wire breaks as a function of bending cycles; influence of the rope design and construction.

4. CONCLUSIONS

From this part of the investigations the following conclusions can be drawn:

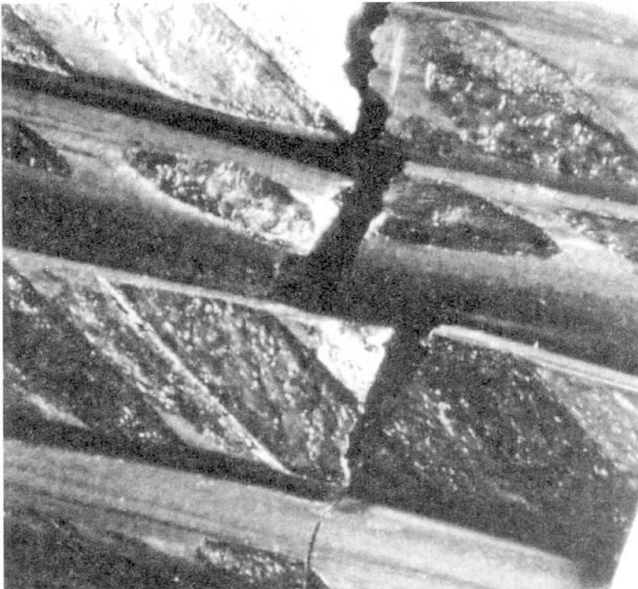


Fig. 14: Almost all the origins of the first cracks were situated within the intensive wear zones.

- The damage starts and first remains in the second layer. When this layer has reached a significant amount of damage, a visible damage in the first layer follows.
- Audible crackle emission indicates approaching damage, and visible helical distortion of the rope surface indicates existing wire breaks.
- The crack initiation in the second layer is a result either of friction wear combined with high pressure or of fretting.
- Improvement of the rope construction and lubrication results in a significant life improvement.

- If the application of Gamma Ray Examination is possible, satisfactory results can be expected for the diagnosed number and location of the wire breaks which occurred.



5. ACKNOWLEDGEMENTS

The author wishes to thank BAV (Swiss Federal Department of Traffic), the Swiss Rope and Ropeways Industry as well as SVS (Swiss Ropeways Association) for supporting this project.

Particular thanks are owed to EMPA (Swiss Federal Laboratories for Materials Testing and Research) for the very useful cooperation, namely for all the NDT and especially the detailed metallographic examinations done, as well as for all the useful information given.

6. BIBLIOGRAPHY

- CHAPLIN, C.R./
TANTRUM, N.R.H.: The Influence of Wire Break Distribution on Strength.
OIPEEC Round Table Conference, Glasgow, June 1985.
- CZITARY, E.: Seilschwebbahnen. Springer Verlag, 1962.
- KOPANAKIS, G.: -Zum Verhalten von Seilen an Rollenketten
Internationale Seilbahn-Rundschau, 1 (1990)
-On the Behaviour of Ropes on Roller Chains
International Aerial Lift Revue, 1 (1991).
- KOPANAKIS, G.: Fatigue Behaviour of Locked Coil Ropes over Roller Chains.
OIPEEC Technical Meeting "Safety, Acceptance and Discard of Ropes, Nantes, October 1991.
- LEIDER, M.: Die Bestimmung der Zusatzspannungen bei der Biegung von Drahtseilen und ihr Einfluss auf die Seillebensdauer.
Diss. TH-Karlsruhe, 1975.
- LUETHY, Th./
BLASER, E.: Radiographic Examination of Steel Wire Ropes.
OIPEEC Round Table Conference, Zurich, September 1989.
- OPLATKA, G.: Nachschmierung von Drahtseilen.
Draht 8 (1985).
- WOODTLI-Folprecht, J./
FICHTER, R.: Fraktographie von Brüchen an Seildrähten aus Stahl.
- Draht 5 (1975)
- Il Filo Metallico 3 (1976)
- Alambre 1 (1976)
- Le Tréfilé 2 (1976)
- WOODTLI, J. /
KOPANAKIS, G.: Fractographical Evaluation of Fatigue Damage in Locked Coil Ropes.
Fourth International Conference on Structural Failure, Product Liability and Technical Insurance, Vienna (A), July, 1992.

Leere Seite
Blank page
Page vide

Full-size Fatigue Test of Bridge Cables

Essais à fatigue sur des câbles d'un pont existant

Ermüdungsversuche an Original-Brückenkabeln

Chitoshi MIKI

Prof. of Civil Eng.
Tokyo Inst. of Techn.
Tokyo, Japan



Chitoshi Miki, born in 1947, received his doctoral degree from Tokyo Institut of Technology in 1979. He has been involved in research in fatigue and fracture of bridge structures.

Takeo ENDO

Exec. Dir.
Honshu-Shikoku Bridge Auth.
Tokyo, Japan



Takeo Endo, born in 1935, received his civil engineering degree from Waseda University in 1958. Since then he worked for the Ministry of Construction and now he is responsible for the design and construction of Honshu-Shikoku Bridges.

Atsushi OKUKAWA

Chief Eng.
Honsshu-Shikoku Bridge Auth.
Tokyo, Japan



Atsushi Okukawa, born in 1944, received his doctoral degree from University of Tokyo in 1973. He joined the Honshu-Shikoku Bridge Authority and has been involved in the design of many suspension bridges and cable-stayed bridges.

SUMMARY

Fatigue tests by axial tension and bending were carried out on specimens having the same thickness and anchorage structure as the cable system of an actual bridge and fatigue performances of various types of cable systems were studied.

RÉSUMÉ

L'article décrit les essais à la fatigue en traction et flexion axiales, effectués sur les échantillons qui, quant à la section et à la disposition d'ancrage, correspondent exactement à un système de câbles d'un pont existant. Ce faisant, il examine les propriétés que différents types de câbles peuvent présenter à la fatigue.

ZUSAMMENFASSUNG

Ermüdungsversuche in achsialem Zug und Biegung wurden an Proben durchgeführt, die bezüglich Dicke und Verankerungskonstruktion dem Kabelsystem einer vorhandenen Brücke entsprochen haben. Dabei wurden die Ermüdungseigenschaften unterschiedlicher Kabeltypen untersucht.



1. INTRODUCTION

The series of full-sized fatigue tests of cable systems including anchorages have been carrying out since 1974 at the Honshu-Shikoku Bridge Project which includes suspension bridges and cable stayed bridges of largest-in-the-world class is reported in this paper. Cables used as structural members of bridges are of the three varieties of main cable of suspension bridge, hanger rope, and diagonal stay cable of cable stayed bridge. Of these cables, the proportion of dead load in tensile force is large in the main cable of a suspension bridge and fatigue is not a problem in many cases. In case of hanger ropes, the proportion of live load making up tensile force becomes large, and there will be cases of fatigue being of concern. For hanger ropes of the Honshu-Shikoku suspension bridge, CFRC (Center Fit Rope Core) type, a form of strand rope is to be used.

As for stay cables of a cable stayed bridge, the proportion made up by live load is large. Especially, the Kojima-Sakaide route of the Honshu-Shikoku bridges has combination highway and railroad bridges and in case of a cable-stayed bridge of the route there is great tensile force variation due to train loads, and giving consideration to tensile fatigue is of importance. Locked coil rope (LCR), a type of spiral rope, or parallel wire strand (PWS) is often used for stay cables of cable stayed bridges.

As fatigue of cable and rope, fatigue due to bending is a problem besides fatigue due to axial force. For example, with stay cables of a cable stayed bridge, bending occurs in the anchored parts of the cables due to deflections produced in girders by application of live load and variations in sagging due to axial force. Furthermore, deflection oscillations are induced in cables by wind and these may also be a cause of fatigue.

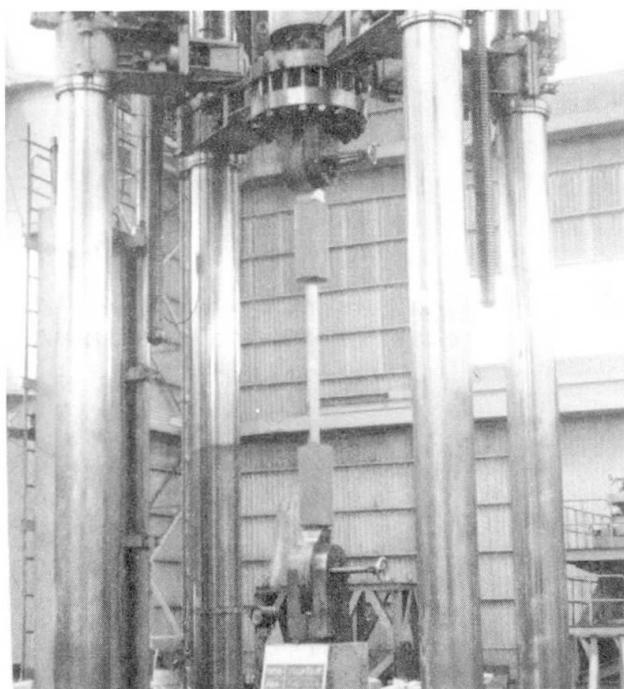
In view of the above, fatigue tests by axial tension and bending were conducted on specimens having the same thickness and anchorage structure as the cable system of an actual bridge, and the fatigue performances of various types of cable systems were investigated.

2. SPECIMENS

The specimens tested in the study are listed in Table 1. Both ends of cables of CFRC, LCR, and PWS types were anchored with sockets made of zinc-copper alloy (Zn 98%, Cu 2%). Wires of PWS, HiAm and NEW-PWS are 160kg/mm² class and wires of HT-PWS are 180kg/mm² class steels. High fatigue-strength sockets were attached to both ends of HiAm and NEW-PWS cables. These cables, HiAm 163 of non-grouted type (HiAm SWPC) and NEW-PWS 163 are planned to be used in Tatara Bridge to be the longest cable stayed bridge in the world.

3. METHOD OF TESTING

Tensile fatigue tests were conducted using the 400-ton fatigue testing machine shown in Fig. 1. Bending



type of test		cable system	cable length(mm)	number of specimen	remarks
Tension		CFRC-60	1990	9	$R=0.05-0.07$
		CFRC-85	1810	6	$R=0.3-0.4$
		LCR-100	2750	2	$R=0.39-0.49$
		PWS-169	1760	2	$R=0.59-0.66$
		HiAm-91	1930	4	$R=0.62-0.72$
		HiAm-127	1830	5	$R=0.45-0.58$
		HT-PWS-127	1750	4	$R=0.60-0.66$
Bending	Series I	PWS-127	4100	6	$d=+15\text{mm}$
		CFRC-85	4100	6	$d=+15\text{mm}$
		LCR-100	4100	2	$d=+15, 20\text{mm}$
	Series II	HiAm SPWS-163	10000	2	$\theta=+0.9$
		NEW PWS-163	10000	2	$\theta=+1.0$

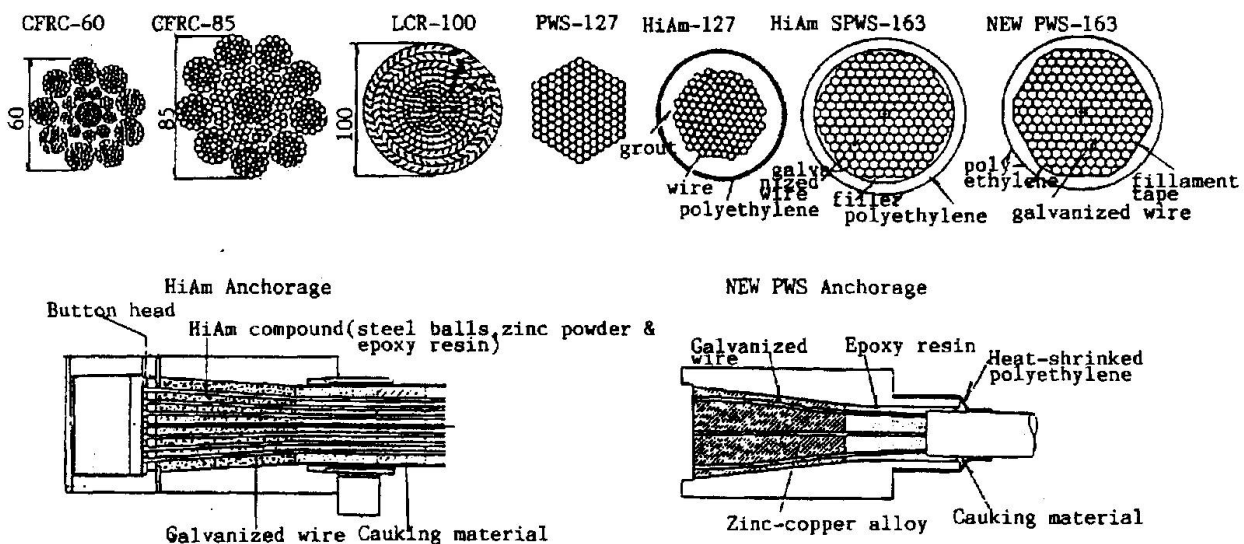


Table 1 Tested cable systems

fatigue tests were performed using the two bending fatigue testing machines shown in Fig. 2. Both testing machines had jacks for inducing tensile axial forces in cables, frames to sustain these forces, and devices to apply repetitive loads to the middle portions of cables. Loading, with the Type A testing machine for Series I, is by a system of applying forced displacement by motor drive, and with the Type B testing machine for Series II, is by a system of controlling displacement by an electro-hydraulic jack.



Series I had the purpose of investigating the bending fatigue strength of hanger ropes of suspension bridges, and similarly to attachment of hanger ropes in an actual bridge, a zinc collar of bell mouth shape at the front end is attached at the mouth of the socket so that the socket will not be directly bent. The drive section also has a collar with both ends rounded attached to the cable to prevent abrupt flexural deformation from occurring.

Series II had the objective of examining the bending fatigue strengths of anchorage portions of stay cables in cable stayed bridges, and therefore, the front ends of sockets were left in a manner that they could be directly bent.

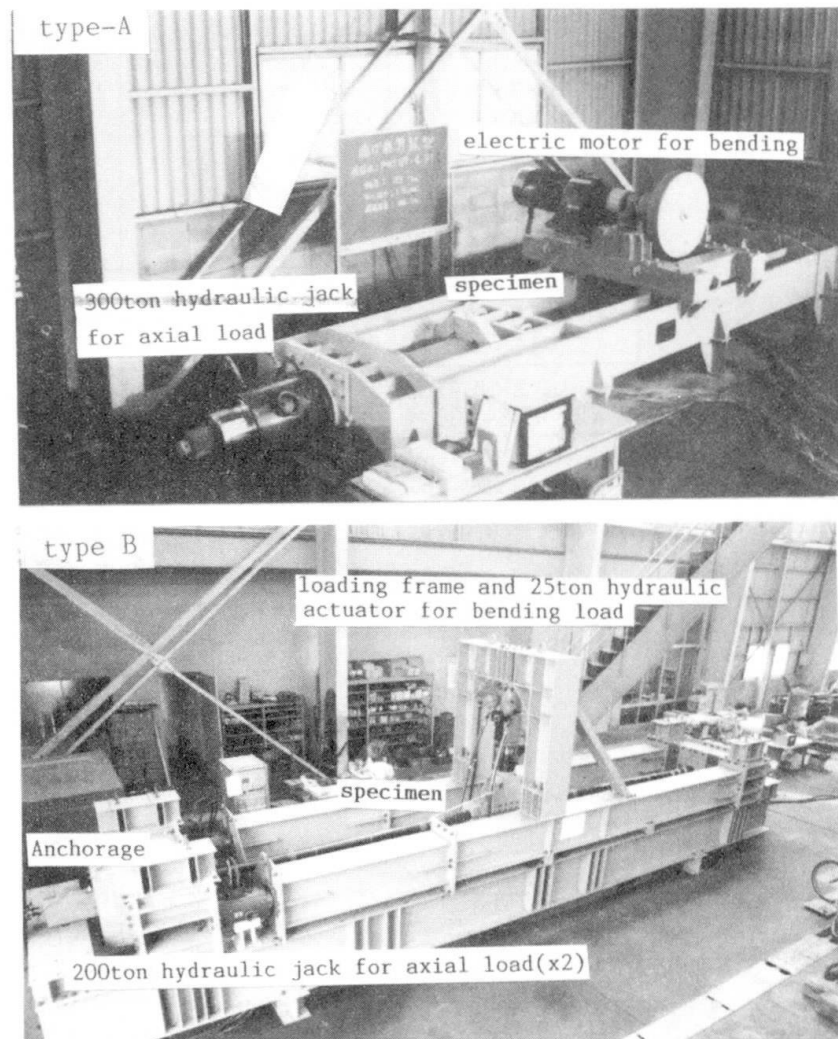


Fig. 2 Bending fatigue test systems

Detection of cable snapping during testing was accomplished by accelerometers fixed at both ends of specimens in tensile fatigue tests and in bending fatigue tests of Series I. In bending fatigue tests of Series II, detecting was done with a total of 6 AE sensors attached at the two ends of a socket and 4 locations at the middle part of the cable.

4. TENSILE FATIGUE TEST RESULTS

The state of progress in failure of element wires in CFRC rope is shown in Fig. 3. Breaking of wires progressed comparatively slowly from the first breakage up to 5 or 6 wires, after which it was gradually speeded up, and when the ratio of breakage exceeded the range of 10 to 20%, breakage began to occur consecutively.

The result of investigating the failure locations on taking apart the rope after tests indicates that with CFRC 60, breaking occurred in large number inside sockets, while with CFRC 85, breaking occurred more at general portions of rope. Cases of breaking at a multiple number of locations in a single wire were

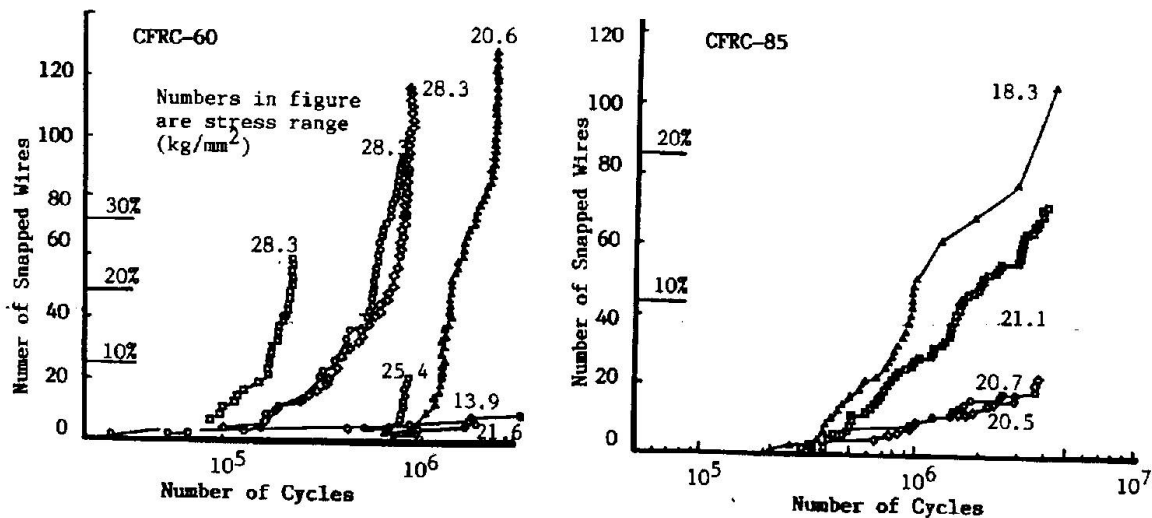


Fig. 3 The state of wire snapping of CFRC cable

more numerous with CFRC 85. It is considered that such trends of failure occurred due to differences in compositional structures and methods of winding of rope.

Fig. 4 shows the states of progress in breaking of element wires of PWS, HT-PWS, and HiAm, and all specimens indicate roughly linear relationships on semi-logarithmic axes.

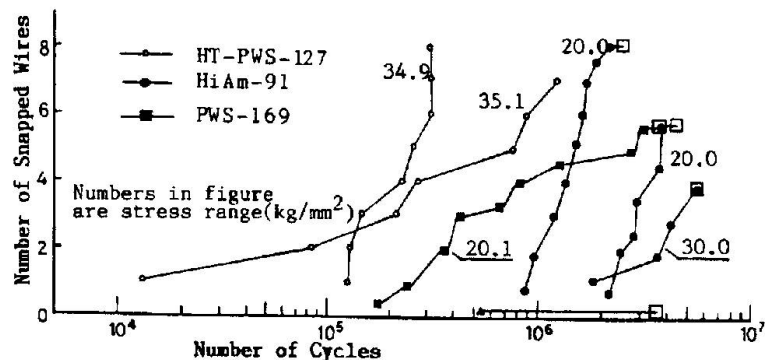


Fig. 4 The state of wire snapping

The results of investigations of wire breakage locations indicates that snapping occurred in a concentrated matter in wires at the outermost layers in the vicinities of socket mouths with PWS. With HT-PWS, snapping occurred in wires at the inner layers at locations 30 to 50 mm inside the sockets in case of specimens which had high fatigue strength. With HT-PWS and specimens that had fatigue strength which were comparatively low, snappings were concentrated at wires of the outermost layers at the socket mouth. These trends are thought to have been produced dependent on bending of element wires and condition of casting of zinc when attaching sockets.

The ratios of breakage locations of wires in the longitudinal direction of HiAm specimens are shown in Fig. 5. Snapping occurred only at anchorages in case of stresses being in a low range. Fig. 6 shows the locations inside cables of element wires which had broken, and it can be seen that almost all were wires of the outermost layer. That is, even though a socket of high fatigue strength, its fatigue strength was greatly affected by stress concentration produced accompanying anchoring, and it is thought breaking occurred from element wires at the outermost layer where the degree of stress concentration was highest.



The fatigue test results of CFRC 60, CFRC 85, and LCR in the relations with initial breakage, 2% breakage, and 5% breakage are shown in Fig. 7. With the time of 5% breakage as the reference, even though a correction is made for the difference with stress ratio, a tendency is seen for CFRC rope of 85 to be slightly lower in strength than CFRC 60. Also, it can be seen that the fatigue strength of LCR is slightly higher than that of CFRC.

The fatigue test results of PWS, HT-PWS, and HiAm are shown in Fig. 8. Many of the specimens were finished testing before their breakage ratios reached 5%, but from a comparison of PWS and HiAm, the effect of having made sockets to be of high fatigue strength is quite clear. Further, from the comparison of PWS and HT-PWS, it can be seen that fatigue strength is increased with increase in static tensile strength of element wires. However, the fatigue strengths of these cable systems are fairly low compared with the fatigue strengths of element wires, and it may be said that the influence of secondary stress due to the compositions and anchorage structures of cables is dominant in fatigue strengths of cable systems. Further, the life up to initial breakage becomes shorter

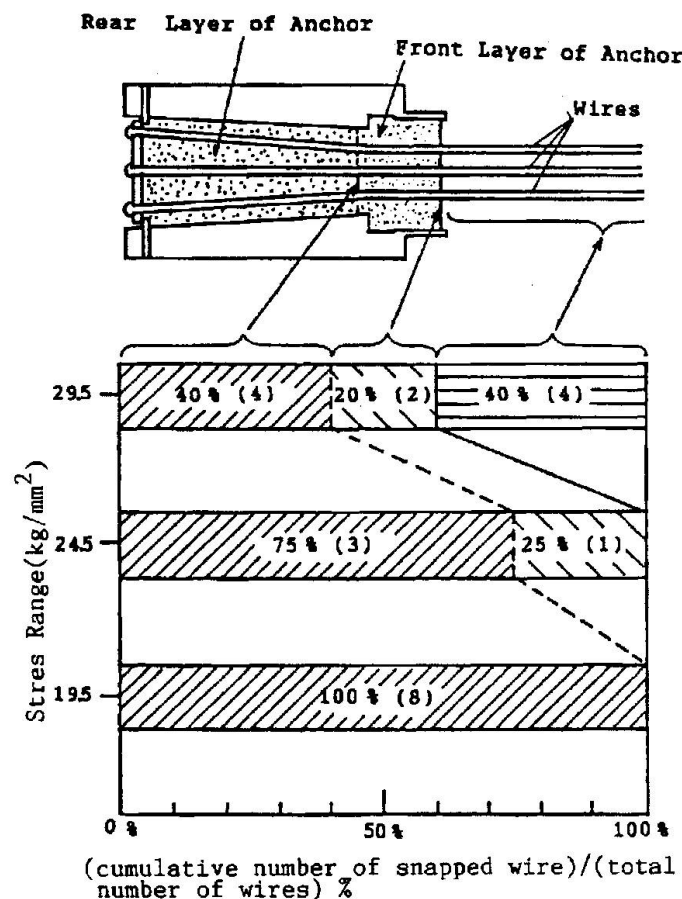


Fig. 5 Locations of wire breakage in HiAm cable systems

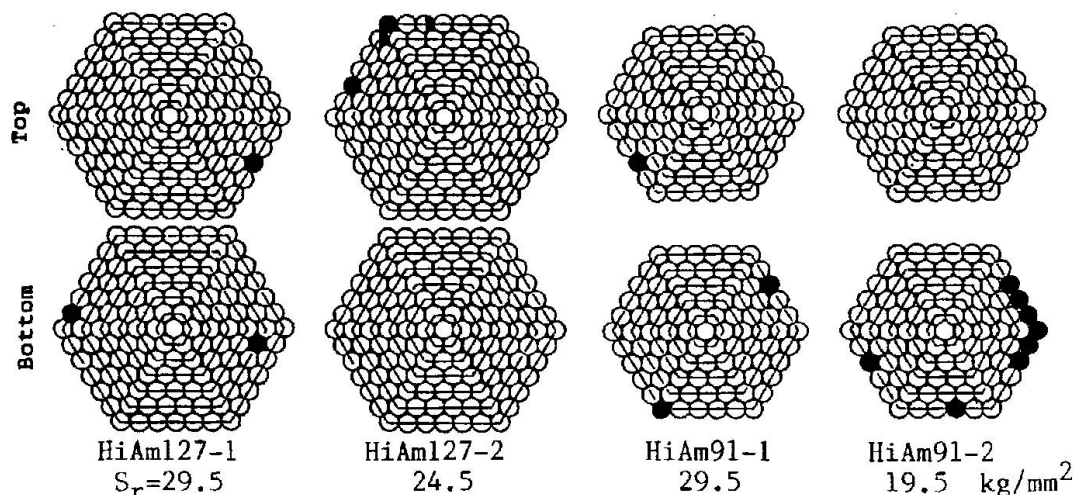


Fig. 6 Positions of snapped wire in HiAm cables

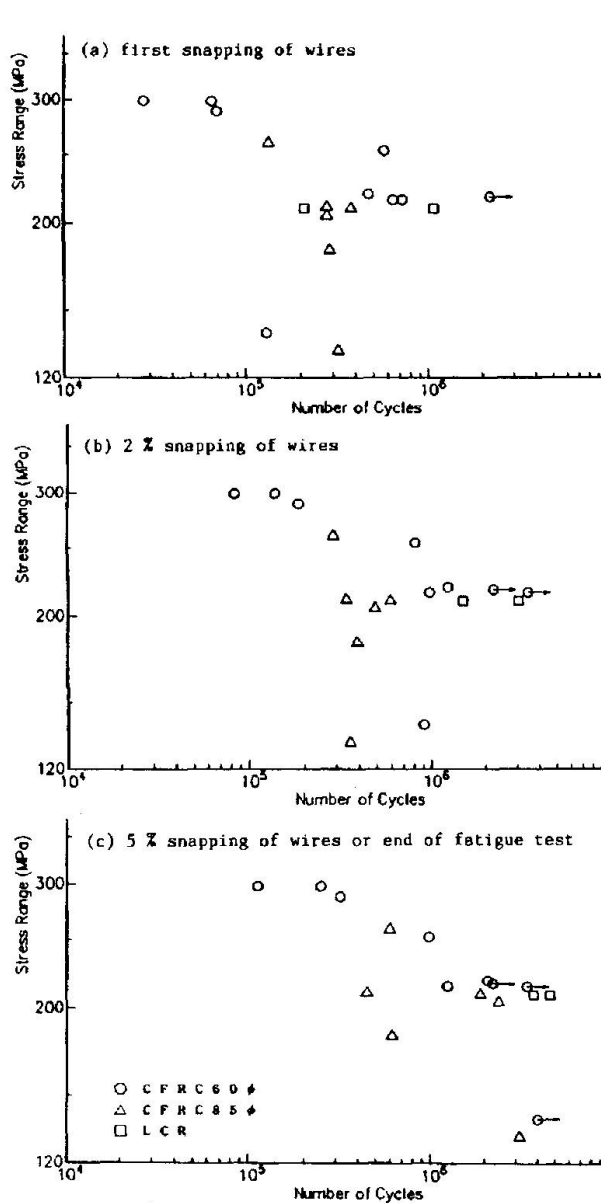


Fig. 7 S-N relationship of CFRC60, CFRC85 and LCR

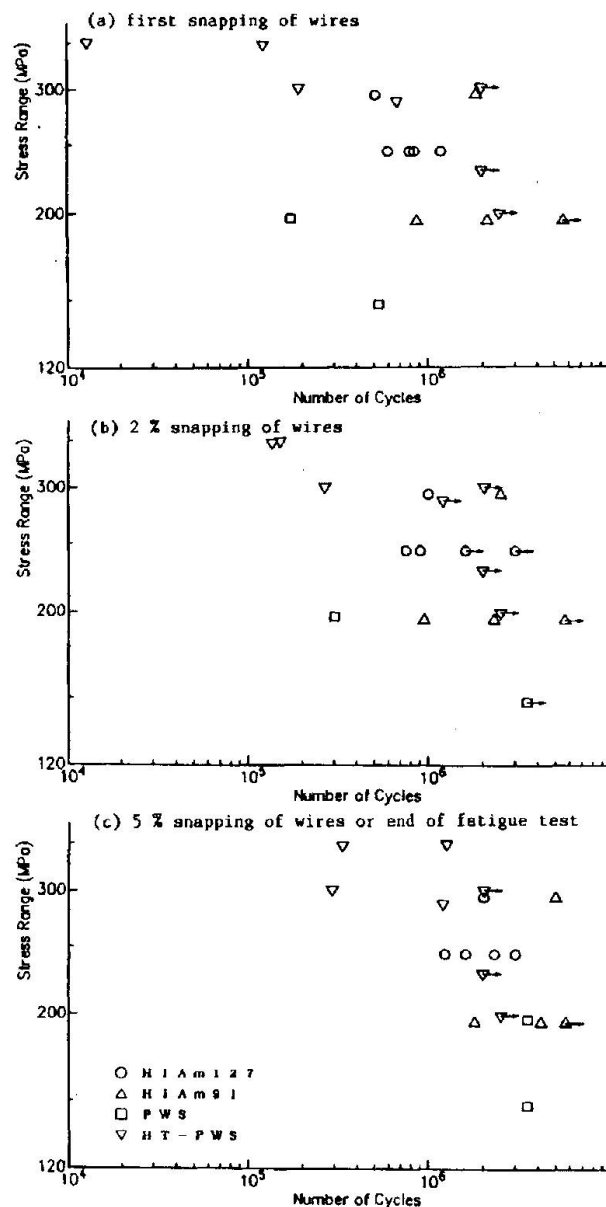


Fig. 8 S-N relationship of PWS, HT-PWS and HiAm

as diameter becomes larger, and it is shown that the degree of stress concentration becomes higher with increase in diameter.

5. BENDING FATIGUE TEST RESULTS

5.1 Series I:CFRC and LCR Cables

The stress occurring in the element wire is the combination of stress due to axial tension variation accompanying variation in cable length and stress due to bending deformation of the cable. Therefore, stress and fatigue behavior of a wire depends greatly on the composition and anchorage structure of the cable.



With CFRC specimens, two out of five specimens had axial tension of 200 tons and three had 150 tons induced. The stress occurring when axial tension was induced was 50 kg/mm^2 in calculated value and 48 kg/mm^2 in measured value for 200 tons, and 37 kg/mm^2 in calculated value and 35 kg/mm^2 in measured value for 150 tons. The forced displacement applied at the central drive section was 15 mm in all cases, corresponding to 0.57° in terms of angle. Fig. 9 shows the stress behavior of element wire due to bending of cable close to the collar at the fixed side of CFRC 85. It can be comprehended that rope which is an assemblage of element wires behave as a whole as a single elastic body possessing a certain bending rigidity.

Failures of element wires were concentrated at the collars at both ends and the drive section collar. The location of the wires broken are shown in Fig. 10, and wires that broke were all at location in contact with other strands. This is considered to have been because in the same strand element wires were wound laid parallel to each other and were in linear contact, whereas contact with a different strand was point contact, and contact pressure therefore became high. As shown in Fig. 11, fatigue cracks were all initiated from impressions occurring due to contact between element wires.

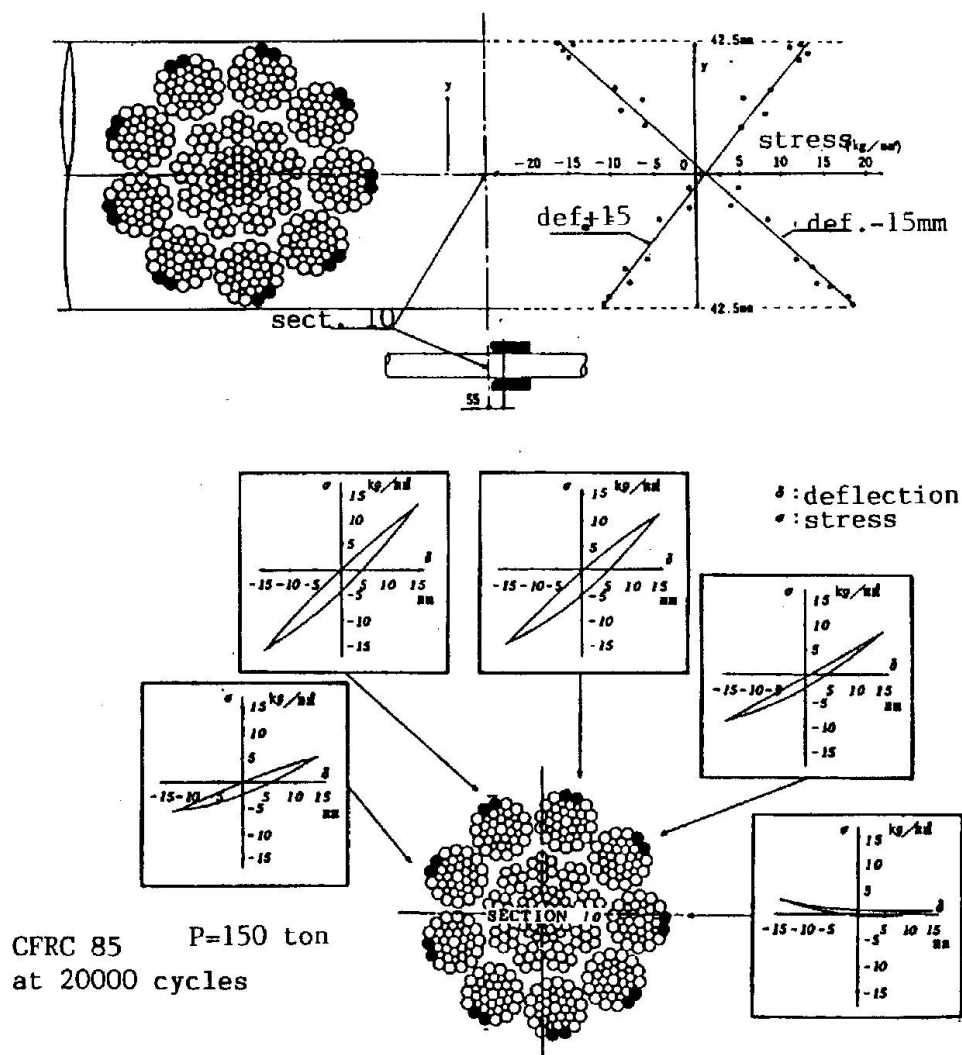
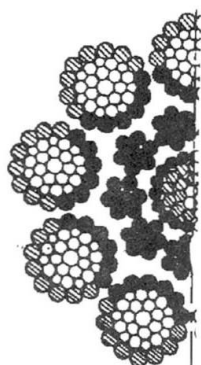


Fig. 9 Stress behavior due to bending



- many failures
- ◐ a few failures
- no failure

Fig. 10 Locations of the wires broken

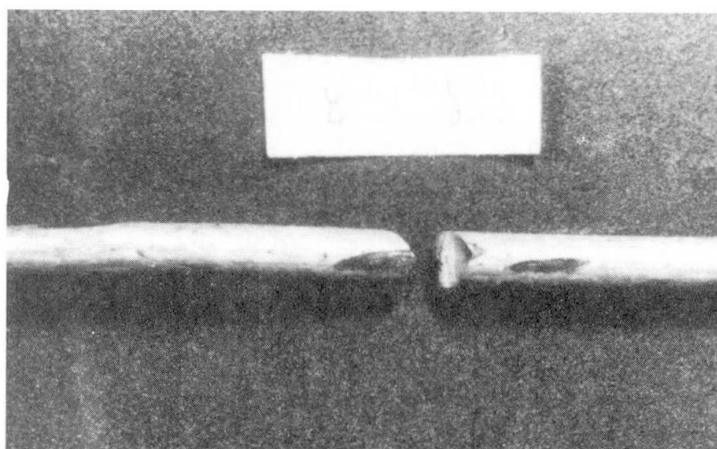


Fig. 11 Snapped wire

With LCR specimens, axial tension of 200 tons was induced. Stresses in an element wire at such time were 23kg/mm^2 in calculated value and 27kg/mm^2 in measured value. The forced displacements caused at middle parts were 20mm and 15mm, corresponding respectively with 0.76 deg and 0.57 deg in terms of bending angle. The stress behavior of an element wire in an LCR rope is similarly to CFRC rope, the rope behaved mechanically as single elastic body. Failures of wires were concentrated at collars having occurred mainly in the E3 and E2 layers which were the outermost and second layers.

Axial tension of 175 tons was induced in PWS specimens and fatigue tests were performed at forced displacement of 15mm (0.57 deg). Of the three specimens, two were flat top and one was pointed top. The calculated stress when 175 tons was induced was 70kg/mm^2 and the measured stress 72kg/mm^2 . Two PWS ropes were tested and breaking of element wires was only one wire at the parallel part and one wire at the middle of the drive collar part.

The bending fatigue tests in Series I are shown in relation to bending angle in Fig. 12. Of the three types, PWS possessed the highest fatigue strength.

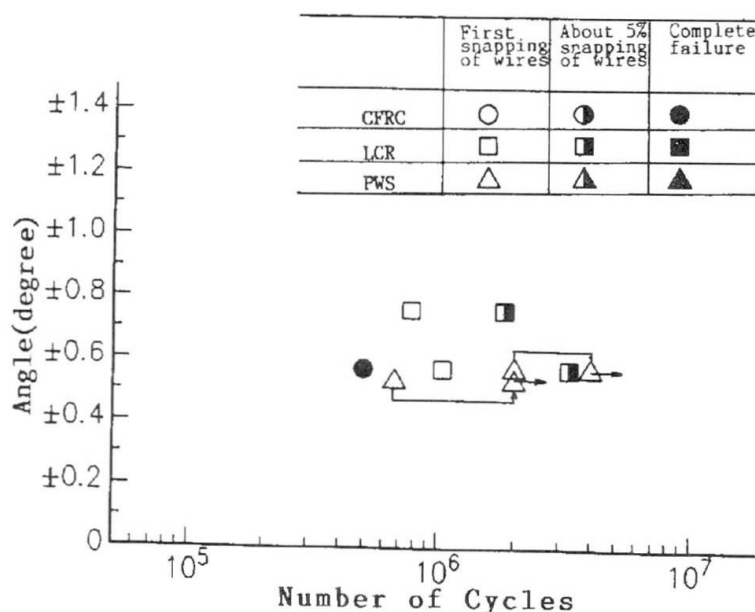


Fig. 12 Results of bending fatigue test (I)



5.2 Series II: NEW-PWS 163 and HiAm SWPC 163

Two each of NEW-PWS 163 and HiAm SWPC 163 which are PWS cables of non-grouted type for cable stayed bridges were tested. After inducing axial tension of 350 tons, displacement control fatigue tests were performed imparting the required forced displacements to the middle part. The relationships of bending angle and bending load with incremental stress in the axial direction are shown in Fig. 13. HiAm and NEW-PWS indicated similar behaviors.

The condition of bending stress occurrence is shown in Fig. 14. For all specimens, where bending stresses occurred were in the neighborhoods of the ends of sockets. From the results of measurements by stress concentration gauges attached connecting with sockets (Fig. 15), it is estimated that stresses of 20.0 kg/mm^2 occurred at bending angle of 0.9 deg at the socket end with NEW PWS, and 21.0 kg/mm^2 at bending angle of 1.0 deg with HiAm.

Two strain gauges were attached to a single element wire at the A and C cross section of HiAm cables with the purpose of investigating stress behaviors of individual element wires when flexure acts on a cable. As a cable was bent, bending stress acted on element wires also, but there were differences in stresses between locations in the vertical direction on the element wire and locations in the transverse direction. Fig. 16 shows the stresses measured at Cross Section A at 1.0 deg compiled according to offset from the middle of the cable. Stresses were not uniform even in the same element wire, and this indicates that all of the element wires in the cable were not deformed as one.

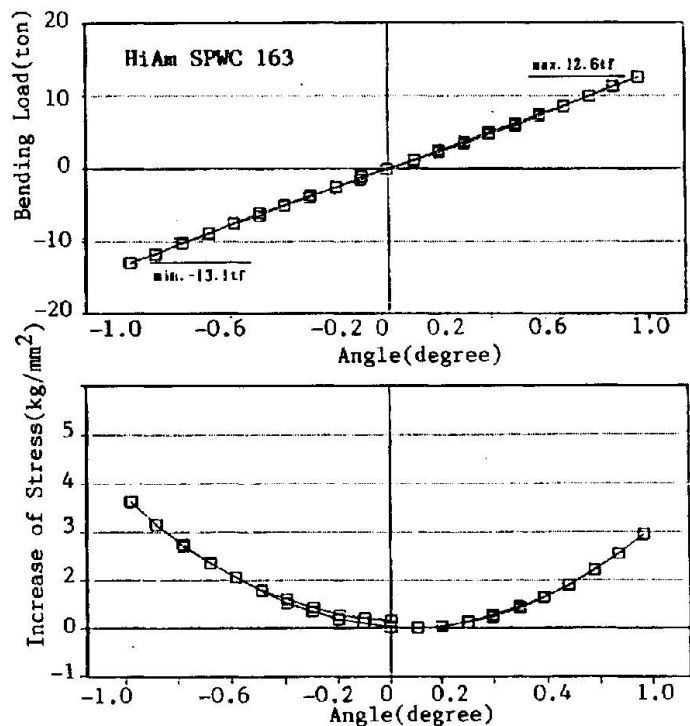


Fig. 13 Bending load, change of angle and increase of stress

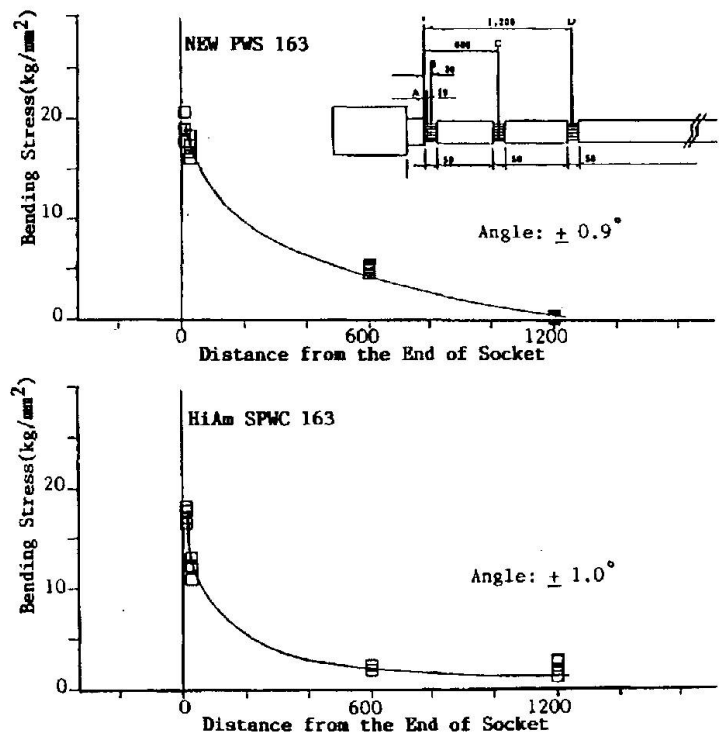


Fig. 14 Occurrence of bending stress

Repetitions of 0.9 deg for NEW-PWS were carried out for 10^7 cycles, but failure of element wires was not detected. The results of these experiments are shown in Fig. 17 together with results with NEW-PWS 139 tested under conditions close to those of these experiments. It can be seen that the two PWS cable systems used for these experiments possessed high fatigue strengths.

6. CONCLUSION

Fatigue tests of models with diameters of actual sizes were carried out on various cable systems for bridges. The results obtained may be summarized as follows:

(1) Extremely characteristic processes of fatigue failure process are indicated depending on the composition and method anchoring of the cable, and strength also differs greatly. Accordingly, scale effect on fatigue strength of a cable cannot be discussed ignoring the methods of composition and anchoring of the cable.

(2) The fatigue strength in the axial direction of cable system including the anchorage is much lower compared with that of an element wire. Even in a cable system having an anchorage structure considered to be high in fatigue strength, breaking of element wires is concentrated at the

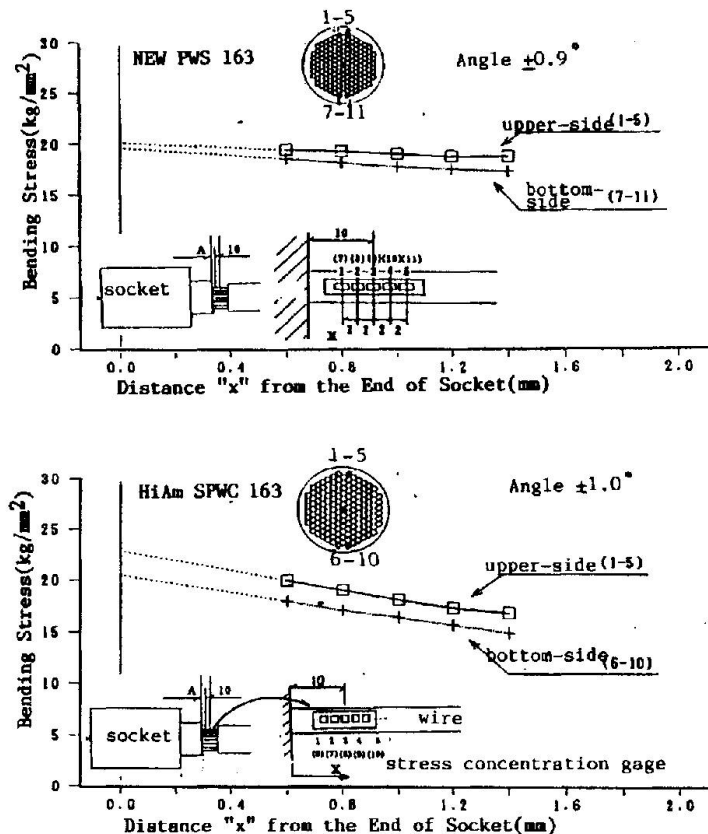


Fig. 15 Bending stress near socket mouth

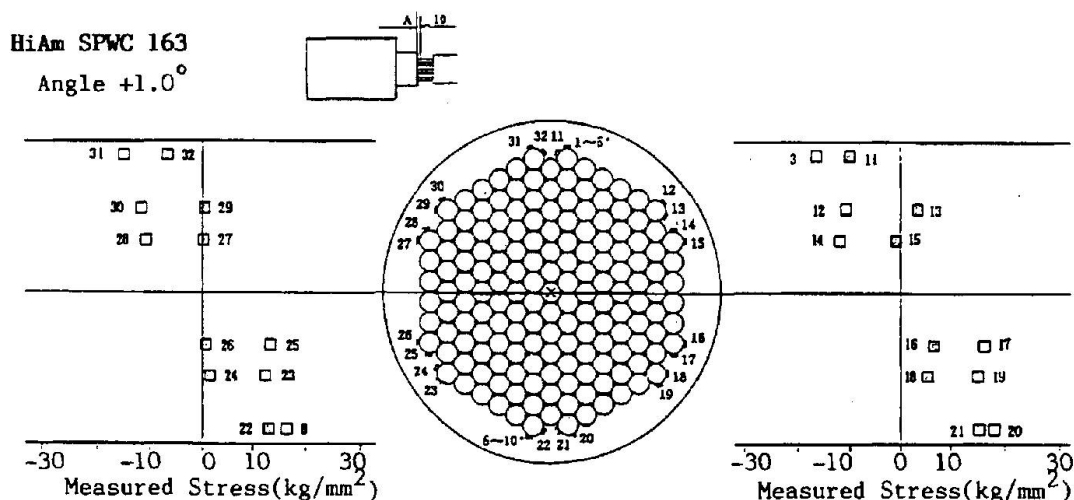


Fig. 16 Stress distributions in a cable



Fatigue Strength of Parallel Wire Strands in Anchorage

Résistance à la fatigue de câbles à fils parallèles à l'ancrage

Dauerfestigkeit von Paralleldrahtbündeln am Anker

Takehi MITAMURA

General Manager
Kobe Steel Ltd
Kobe, Japan

Kenichi SUGII

Manager
Kobe Steel Ltd
Kobe, Japan

Atsushi OKUKAWA

Site Gen. Mgr
Honshu-Shikoku Bridge Authority
Tokyo, Japan

Yoshito TANAKA

Director
Shinko Wire Co. Ltd
Amagasaki, Japan

SUMMARY

This paper concerns the fatigue strength of a parallel wire strand (PWS) which uses galvanized wires with a breaking strength of 1765 MPa and zinc-poured-sockets at both ends. It has been indicated the PWS fatigue strength declines at the zinc-poured-sockets. The causes of this are investigated through a fatigue test using a 37 wire PWS and FEM analysis. Furthermore, a method that can improve the fatigue strength without changing the structure of the present socket is proposed. The effectiveness of this method is also verified through a fatigue test using a 37 wire PWS.

RÉSUMÉ

Ce rapport traite de la résistance à la fatigue de câbles à fils parallèles utilisant des fils galvanisés à contrainte de rupture de 1765 MPa et des douilles scellées au zinc aux deux extrémités. La résistance à la fatigue de câbles à fils parallèles diminue aux douilles scellées au zinc. Les causes de ce phénomène sont étudiées par l'intermédiaire d'un essai de fatigue sur des câbles à fils parallèles à 37 fils et d'une analyse par éléments finis. Une méthode permettant d'améliorer la résistance à la fatigue, sans modifier la structure de la douille actuelle, est proposée. Son efficacité est également vérifiée par un essai de fatigue sur des câbles à fils parallèles à 37 fils.

ZUSAMMENFASSUNG

Die vorliegende Abhandlung befaßt sich mit der Dauerfestigkeit von Paralleldrahtbündeln unter der Verwendung von verzinktem Draht mit vergoßenen Zinksockeln and beiden Enden mit einer Bruchfestigkeit von 1765 MPa. Es gab Anzeichen dafür, daß die Dauerfestigkeit an den jeweiligen vergoßenen Zinksockeln abnimmt. Die Ursachen dafür wurden mit einem Dauertest mit 37-Draht-Bündeln und FEM-Analyse untersucht. Außerdem wird ein Verfahren vorgeschlagen, das die Dauerfestigkeit verbessert, ohne die Struktur der gegenwärtigen Sockel zu verändern. Die Wirksamkeit dieses Verfahrens wurde mit einem Dauertest unter Zuhilfenahme von 37-Draht-Bündeln bestätigt.



1. Introduction

It has been said that the endurance limit of PWS (prefabricated parallel wire strand) with zinc-poured-anchorage (including zinc-copper-alloy-poured anchorage) is about 150 MPa in terms of stress range when wires with a breaking strength of 1 569 MPa are used[1]. In the fatigue tests carried out so far, almost all wire-failure occurs inside the anchorage and hardly occurs at the free length. Because the wires with a breaking stress of 1 569 MPa itself possesses the endurance limit about 400 MPa in terms of stress range[2], the wire fatigue strength in the anchorage reduces by about 70%. Opinion to attribute the cause to heat effect at the time of zinc-pouring or wire fretting has been predominant, and in order to preclude these effects, a different anchorage system has been proposed[3]. However, the causes that lower the PWS fatigue limit in zinc-poured-anchorage have not yet been completely elucidated.

The purposes of our study are to find out causes reducing the PWS fatigue strength through fatigue tests and FEM analysis performed on the zinc-poured-anchorage of PWS as well as to improve the PWS fatigue strength without providing any significantly large structural change to the current anchorage.

In our study, PWS was first fabricated in accordance with the standard specifications which have been followed to date (hereinafter called the "standard PWS"), then fatigue tests were performed, and poured portions were taken into pieces to investigate the wire-failure condition in the anchorage. Samples used were PWS-37 (37 wire bundle) with 1.0-meter length between sockets which uses 5.0 mm- ϕ wires with a breaking strength of 1 765 MPa. The fatigue limit of 1 765 MPa wire itself is about 500 MPa in terms of stress range[2].

Then, FEM analysis was carried out on the anchorage and the stress condition of wires in anchorage was investigated. Based on the calculation results, the causes of wire-failure in anchorage were inferred and at the same time a method to improve the PWS fatigue strength was proposed.

Lastly, in order to verify the adequacy of these investigations, PWS with the proposed improved anchorage (hereinafter called the "improved PWS") was fabricated to carry out fatigue tests.

2. Fatigue Tests of Standard PWS

2.1. Standard PWS and specimen-size

Standard PWS is fabricated as follows:

- (1) Bundle and form wires in a hexagon.
- (2) After inserting the wire bundle into a socket, bend the wires and spray in a form of a broom.
- (3) As shown in Fig.1, set and fix wires in such a manner that the wire-spray-initiation-point coincides with the taper-initiation-point on the socket-inner-wall. (Note 1.)
- (4) Under pin-point temperature control, pour zinc.

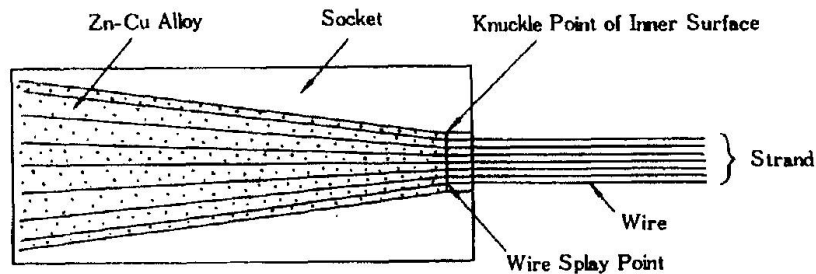


Fig.1 Rough sketch of standard PWS

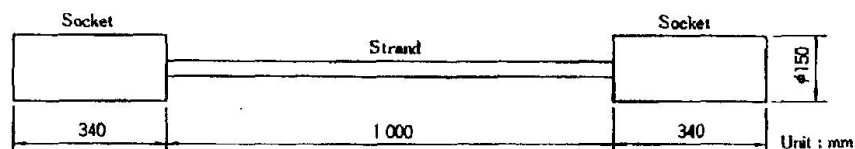


Fig.2 Dimension of specimen

(Note 1.) In order to complete the initial creep of poured metal, PWS has its poured-metal pressed from the rear side of the sockets, that is, so-called pre-compression is provided after pouring. It is the poured metal that is pressed and the wire is not pressed directly, but as a result, the wire bundle is pressed out several millimeters from the sockets. In strict sense, the setting referred to here is carried out with the displacement of wire bundle due to pre-compression taken into account so that the wire-spray-initiation-point coincides with the taper-initiation-point on the socket-inner-wall after pre-compression is achieved.

With the same procedure as specified above, eight pieces of test specimens (PWS-37) with the dimensions shown in Fig. 2 were newly prepared and fatigue tests were conducted. In preparing these specimens, special attention was given to the wire setting specified in Step (3) above. Zinc was poured in accordance with the Honshu-Shikoku Bridge Authority Standard, HBS G3503-1979 (zinc-copper-alloy instead of zinc: Zn 98%, Cu 2%; pouring temperature: 460 ± 10 °C).

In the fatigue tests, the maximum load was set to 579 kN for all the specimens and the minimum load was varied according to specimens to set the loading range. During the tests, so-called load control was performed to maintain this loading range constant. Consequently, with respect to the practical wire stress after the first wire failed, both maximum and minimum stresses varied and the stress range itself increased.



2.2. Test Results

Test results are shown in Table 1 and Fig. 3. The maximum and minimum stresses and stress range shown in Table 1 are values all calculated from the strand cross section before failure occurs. Fig. 3 arranges these values in terms of the number of cycles when the second wire-failure occurs and it corresponds to the 5% failure fatigue strength popularly referred.

The number of data is small but it is estimated that the fatigue limit of the standard PWS tested recently is about 150 MPa as well as the past test data used the 1 569 MPa wires. The test was characterized by appreciable scatter in the test results.

After the fatigue test, two of the standard PWS specimens (Specimen No.S-7 and S-8) were anatomized at the poured portion and wire-failure condition was investigated. All wire-failure occurred in the socket and primarily at the area 10 mm inside from the taper-initiation-point on the socket-inner-wall as shown in Table 2. The wire-fracture surface is divided into two sections as shown in Fig. 4, a fatigue fracture surface cracked at about 45° to the wire axis and a final fracture surface nearly normal to the wire axis.

Specimen	Maximum Stress (MPa)	Minimum Stress (MPa)	Stress Range (MPa)	Frequency (Hz)	Number of Cycles (x 10 ⁴)		
					First Wire Failure	Second Wire Failure	Test Stop
S-1	796	649	147	4	No Failure		200.0
S-2	796	600	196	4	61.8	64.8	64.8
S-3	796	600	196	4	112.0	130.0	130.0
S-4	796	600	196	4	58.0	78.8	78.8
S-5	796	600	196	4	81.0	92.0	92.0
S-6	796	550	246	4	48.5	50.9	50.9
S-7	796	550	246	4	19.5	29.8	29.8
S-8	796	550	246	4	22.5	23.4	23.4

Table 1 Fatigue test result of standard PWS

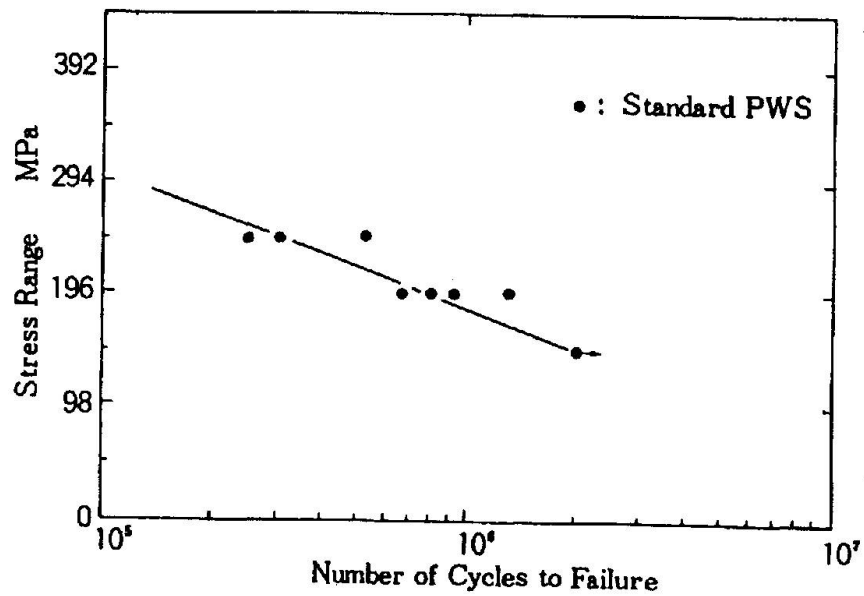


Fig.3 Fatigue test result of standard PWS

Specimen	Number of Broken Wires	Broken Wire	X mm
S-7	2	(2)	-8
		(14)	-5
S-8	2	(1)	-9
		(7)	-7

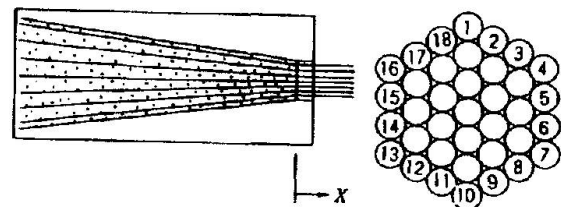


Table 2 Wire-failure location of standard PWS

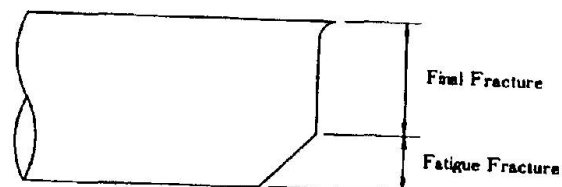


Fig.4 Rough sketch of wire fracture surface



3. FEM Analysis of Standard PWS Anchorage

In an attempt to attain relevance to the above fatigue tests, the model for anchorage of PWS-37 is assumed as shown later to carry out FEM analysis. The model used was a plane axisymmetric model, on which elastic analysis was conducted. The elastic modulus of socket, wire, and poured metal were 206 GPa, 196 GPa, and 20 GPa, respectively, and the Poisson's ratio was all designated to 0.3. The slips between respective elements were not taken into account. In dividing meshes, the outermost-layer-wire was divided into four in the wire radial direction so that the stress distribution of the wire surface can be observed, and the inner-layer-wires were divided into two.

Fig. 5 shows the mesh divisions together with calculation results. For analysis, a general-purpose program PLASTO was used.

The calculation results shown in Fig. 5 represent the distribution of stress on the outermost-layer-wire surface, which is shown as a stress ratio when the principal stress of the free length is designated as 1.0. As clear from Fig. 5, the vicinity of the taper-initiation-point on the socket-inner-wall serves as a stress concentration area for the outermost-layer-wire surface. The principal stress shows the peak nearly at the taper-initiation-point on the socket-inner-wall and is about 40% greater than that at the general strand portion in terms of numerical value. On the other hand, the maximum shear stress shows the peak at about 5 mm inside from the taper-initiation-point on the socket-inner-wall and this is also 40% greater than that of the free length. As compared with the principal stress which shows the peak collectively at one point, the maximum shear stress shows comparatively smooth peak development. It is assumed that these stress concentrations are primarily attributed to the wedge effect of poured metal due to the taper provided on the socket-inner-wall.

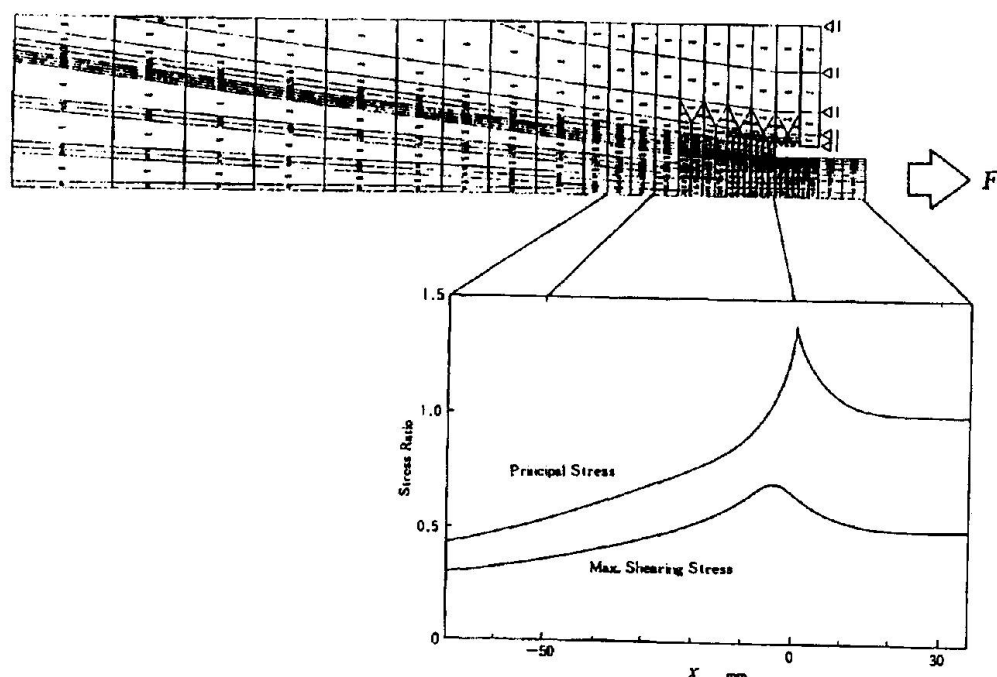


Fig.5 Structural model and stress distribution of outermost-layer-wire surface



4. Estimation of Causes Reducing Fatigue Strength of Standard PWS and Investigation on its Improvement

4.1. Estimation of Causes Reducing Fatigue Strength

The results of fatigue tests and FEM analysis can be summarized as follows:

- (1) The area about 20 mm inside from the taper-initiation-point on the socket-inner-wall serves as a stress concentration area for the outermost-layer-wire surface, and the peak values of both principal stress and maximum shear stress are increased by about 40% as compared with those of the free length.
- (2) The wire-failure position is located at the area 10 mm inside from the taper-initiation-point on the socket-inner-wall and corresponds to the wire-bending affected zone.
- (3) The fatigue crack of the failed wire initiates at about 45° with respect to the wire axis.

Putting these together, the causes reducing the fatigue strength of the standard PWS in anchorage can be inferred as follows. That is, the problem lies in the fact that the wire-spray-initiation-point subjected to the wire-bending effect was aligned to the taper-initiation-point on the socket-inner-wall, which is likely to become the stress concentration area. It is also estimated that the maximum shear stress is greatly responsible for fatigue initiation and propagation.

On the other hand, the appreciable scatter in fatigue test results of the standard PWS might be attributed to interactions between the following factors.

- (1) Depending on the individual difference of workers' skill, scatter occurs in wire-bending degree and range.
- (2) The relative position of wire-bending affected zone and stress concentration point subtly deviate according to specimens.

4.2. Investigation of Improvement in Anchorage

If the above inference is correct, the following can be suggested as the improvements of anchorage.

- (1) Provide a gentle taper angle on the socket inner wall to reduce wire stress concentration.
- (2) Avoid wire-bending.
- (3) Displace the wire-spray-initiation-point from the stress concentration area.

Among them, in Suggestion (1) above, the setting rate of poured metal due to strand tension after installation becomes great, increasing the apparent creep as a cable unit. Suggestion (2) requires newly a device to elastically spray the wires during pouring and hold the wires until poured alloy solidifies; this creates another problem of disposing of wire terminals before the subsequent pre-compression.

The simplest improvement is Suggestion (3), and, in concrete, it can be achieved as follows. That is, the wire-spray-initiation-point is moved scores of millimeters toward the socket inside, displacing the wire-bending affected zone from the stress concentration area.

In the recent investigation, the wire-spray-initiation-point was moved by 50



millimeters toward the socket inside and located as shown in Fig. 6.

5. Fatigue Test of Improved PWS

Ten specimens of improved PWS were prepared and fatigue tests were performed. The specimens were prepared in the same size, by the same method, and by the same personnel as the specimens of the standard PWS, except that the wire-spray-initiation-point was shifted 50 millimeters backward.

Test results are shown in Table 3, and Fig. 7. Fig. 7 also shows the test results of the standard PWS. Judging from Fig. 7, the endurance limit of the improved PWS could be estimated to be about 340 MPa. Because the endurance limit of the 1765 MPa wire itself is about 490 MPa, the fatigue reduction rate in the improved anchorage has been suppressed to about 30%. [The fatigue reduction rate was 70% in the case of the standard PWS.]

Two of the improved PWS specimens (Specimen No. I-1 and I-2) were anatomized at the poured portion and investigation was made on the wire-failure condition as done for the standard PWS specimens. The wire failure positions were 2 millimeters and 15 millimeters inside, respectively, from taper-initiation-point on the socket-inner-wall. Same as the standard PWS, the fracture surface consisted of two sections: fatigue fracture surface cracked at about 45° to the wire axis and final fracture surface nearly normal to the wire axis.

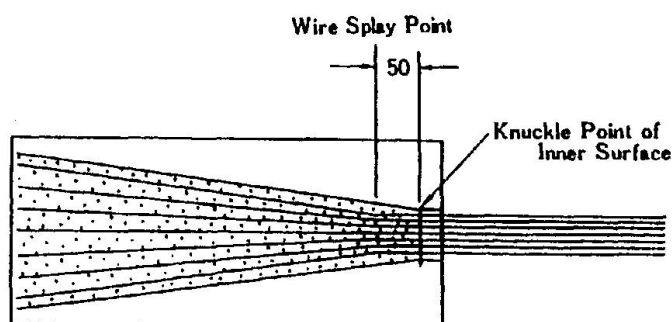


Fig.6 Rough sketch of improved PWS

Specimen	Number of Broken Wires	Broken Wire	x (mm)
I-1	1	(14)	- 2
I-2	1	(9)	-15

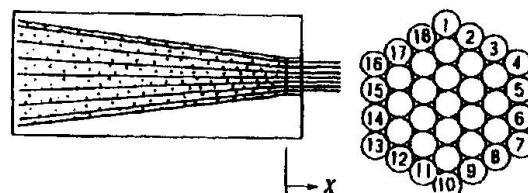


Table 4 Wire-failure location of improved PWS

Specimen	Maximum Stress (MPa)	Minimum Stress (MPa)	Stress Range (MPa)	Frequency (Hz)	Number of Cycles (x 10 ⁴)		
					First Wire Failure	Second Wire Failure	Test Stop
I-1	796	550	246	4	174.0	No Failure	200.0
I-2	796	499	297	3	139.0	No Failure	200.0
I-3	796	452	344	3	No Failure		200.0
I-4	796	428	368	3	68.5	No Failure	200.0
I-5	796	418	378	3	62.3	64.8	64.8
I-6	796	404	392	3	40.6	56.2	56.2
I-7	796	379	417	3	50.5	52.0	52.0
I-8	796	355	441	3	26.2	29.8	29.8
I-9	796	306	490	3	23.9	28.5	28.5
I-10	796	282	514	3	11.8	14.1	14.1

Table 3 Fatigue test result of improved PWS

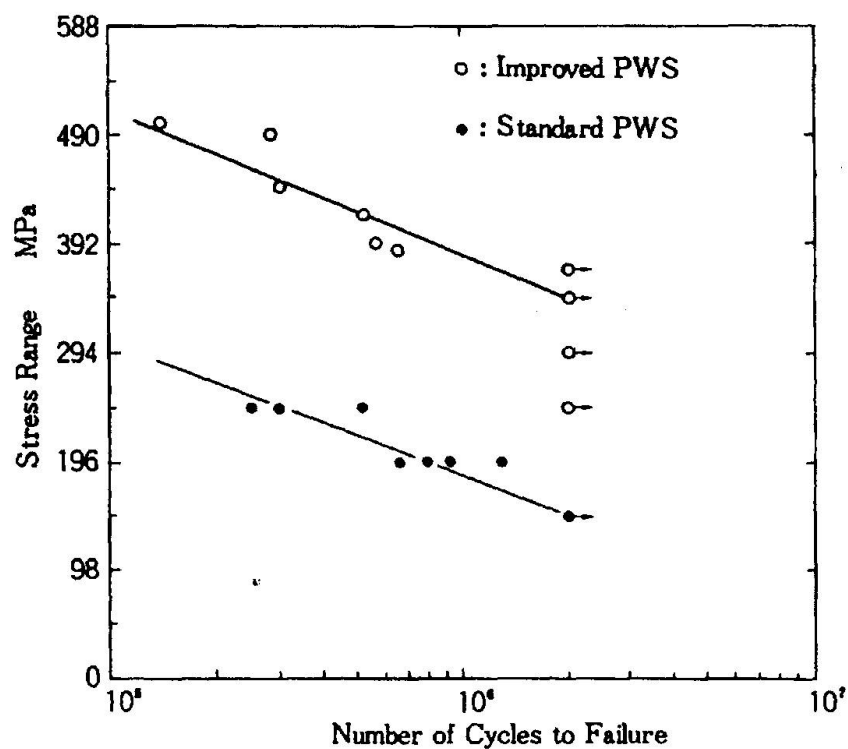


Fig.7 Fatigue test result of improved PWS



6. Discussion

With the foregoing description, it has been evidenced that the improved PWS in which the wire-spray-initiation-point is shifted only by 50 millimeters toward the socket inside as compared to that of the standard PWS has a great possibility to remarkably improve the fatigue strength of PWS with zinc-poured-anchorage.

Shinke et al. have already pointed out that slightly changing the anchorage fabrication method can generate a difference in fatigue strength of PWS with zinc-poured anchorage[4]. Shinke et al. fabricated PWS specimens with zinc-poured-anchorage using 1 569 MPa wire of the following two types:

(Type A) Wire spray was performed in the most popular conventional method like the the standard PWS in this paper.

(Type B) Wire-bending curvature of the wire spray portion is made slightly gentle.

and conducted fatigue tests. They further compared the fatigue test results with those[5] of single wire specimens with zinc-poured-anchorage (Type C) and summarized as follows:

(a) Fatigue limit at 2 million cycles of Type A and Type B is about 200 MPa and 250 MPa, respectively.

(b) That of Type C is about 340 MPa.

With these data taken into account, the recent investigation and test results are discussed as follows:

(1) The wire fatigue strength reduces in the zinc-poured-anchorage, and the reduction rate increases in order of single wire not subjected to bending, PWS with slightly smaller bending rate than that in current fabrication specifications, and PWS wire-sprayed in accordance with the current fabrication standard.

(2) In the zinc-poured-anchorage, even wire free from bending reduces fatigue strength. One of the principal causes could be attributed to the stress concentrated on the wire surface in the vicinity of the taper-initiation-point on the socket-inner-wall. According to the investigation results of the wire fracture surface, the maximum shearing stress arising from the wedge effect of poured metal seems to be greatly responsible for the initiation of fatigue crack.

(3) It would be appropriate to estimate that the bending magnitude of the wire spray portion is also responsible for the reduced fatigue strength in the regular PWS anchorage, to which wire spray is performed and zinc is poured. That is, the portion which is more greatly subjected to wire-bending and acts as a weak point with respect to the initiation of fatigue crack seems to be more likely to fail earlier due to fatigue.

(4) Same as the stress on the wire surface which is distributed in a certain area, the susceptibility of bent wire to fatigue crack would be also distributed in a certain area, and fatigue strength seems to vary according to the correlationship between respective distributions. For example, the wire is most likely to fail due to fatigue when the stress concentration peak coincides with the weakest point of the wire, and when these deviate each other, either factor becomes critical and possibly causes fatigue failure.

Difference of wire bending technique of each individual worker or subtle difference in wire bundle extrusion rate due to pre-compression may tend to cause the correlationship between these distributions to vary in a unit of millimeter. It is estimated that appreciable scatter in fatigue test results generated in the standard PWS may be caused by the minor deviation of stress



concentration area and wire weak point.

(5) From the above estimation of causes, following improvements are proposed.

(a) The socket shape will be changed to the extent that would not cause any detrimental effect on the setting rate of poured alloy in order to alleviate stress concentration on the surface.

(b) The PWS fatigue limit can be improved by either relaxing the bending magnitude of the wire located at the stress concentration area or designing a method that does not need any bending at all. The method proposed in this paper is to locate the wire free from bending at the stress concentration point.

7. Conclusion and Future Subjects

In this study, fatigue tests and FEM analysis were carried out on zinc-poured PWS-37 used the wires with a breaking strength of 1 765 MPa and causes reducing fatigue strength of conventional standard PWS were estimated and improvements of anchorage were investigated. Our conclusions are summarized as follows:

(1) 5% failure fatigue strength of standard PWS is about 150 MPa in terms of stress range in the recent experiment using 1 765 MPa wire and appreciable scatter was found in experiment results.

(2) From the observation of wire fracture surface and FEM analysis results of anchorage, it was inferred that the fatigue failure in anchorage is attributed to the locational coincidence of the stress concentration area of the wire surface near the taper-initiation-point on the socket-inner-wall with the wire-bending affected zone.

(3) To improve the fatigue strength of PWS with-zinc-poured-anchorage, proposal was made to remove the wire bent portion from the stress concentration area and verification experiments were carried out. As a result, it has been confirmed that 5% failure fatigue strength of PWS using the 1 765 MPa wire can be increased from about 150 MPa before improvement to about 350 MPa in terms of stress range.

(4) Following items remain as future subjects:

- Increase the number of data to complete the S-N curve.
- Carry out fatigue tests with PWS of greater size.

REFERENCES

- [1] DIN 1073 Stahlerne Strassenbrucken - Berechnungsgrundlagen, Jul.1974
- [2] Ishioka, Ikeda, Oki, Yamaoka : Steel in Honshu-Shikoku Bridge Project, R&D, Kobe Steel Engineering Reports (in Japanese), Vol.38, No.1, pp.63-66, Jan.1988
- [3] Birkenmaier : Fatigue Resistant Tendons for Cable-Stayed Construction, IABSE Proceedings, P-30/80, pp.65-79, 1980
- [4] Shinke, Hironaka, Oishi : Fatigue Strength of PWS, R&D, Kobe Steel Engineering Reports (in Japanese), Vol.28, No.2, pp.52-54, Apr.1978
- [5] Yamamoto, Moriwaki, Sakakibara : Fatigue and Creep Properties on Cable Wire for Long-Span Bridge, Proceedings of JSCE Annual Meeting, I-169, p.469, 1969

Leere Seite
Blank page
Page vide

Fatigue Testing and Force Distribution in Steel Wire Ropes

Essais de fatigue et distribution des forces dans les câbles en acier

Ermüdungsversuche und Kraftverteilung in Stahldrahtseilen

Lourus WIEK

Delft Univ. of Technology
Delft, The Netherlands

Lourus Wiek, born in 1932, has worked as mechanical engineer since 1953. He has performed wire rope research at Lab. of Materials Handling TUD since 1963, graduated in Mech. Eng. from TU Delft in 1974, received his doctorate at TU Delft in 1986. He is Lecturer at the TU Delft. President of OIPEEC since 1991.

SUMMARY

Wire ropes and strands under tension are subjected to attendant stress, which influences their endurance. A description of the stress measurements on wire ropes in regular lay and strands leads to the suggestion: Five wire rope lays or fourteen wire lays may meet the independence assumption in statistical theories. This is equivalent to 30 times the rope diameter, or fourteen wire lays for strands. The minimum length of a fatigue test sample must be taken as two layer longer to cover influences of the rope terminals.

RÉSUMÉ

Des câbles en acier et des torons sont soumis à des tensions additionnelles, lesquelles ont une influence sur l'endurance. Une description des mesures de tension sur un câble croisé et un toron conduit à la suggestion: 5 fois le pas de câblage ou 14 fois le pas de toronnage correspondrait à l'indépendance admise dans les théories statistiques. Ceci correspond à une longueur de 30 fois le diamètre du câble, ou 100 le diamètre d'un toron. La longueur minimale de l'éprouvette doit être augmentée de 2 pas de câblage ou de toronnage au moins pour prévenir les influences des attaches du câble.

ZUSAMMENFASSUNG

Zugbeanspruchte Drahtseile und Litzen sind Nebenspannungen unterworfen, die die Ermüdung beeinflussen. Aus Spannungsmessungen an Kreuzschlagseilen und Litzen wird abgeleitet, daß 5 Schlaglängen eines Seiles oder 14 Schlaglängen einer Litze nötig sind, um die Voraussetzung statistischer Unabhängigkeit zu erfüllen. Das ist äquivalent zu 30 Seildurchmessern oder 100 Litzendurchmessern. Die Mindestlänge eines Probestücks muß mindestens zwei Schlaglängen zusätzlich umfassen, um einen Einfluß der Seilverankerungen auszuschalten.



1 INTRODUCTION.

Taking into the account what has been published on the theory [1] and the experimental experience [2] [3], there is little doubt of the existence of a length effect on fatigue failures of steel wire ropes and strands. In the case of wire ropes and strands, however, the backgrounds of this effect may give rise to further discussions.

Research on steel wire ropes in the Laboratory of Materials Handling at Delft was mainly focused at repeated bending over sheaves of ropes under tension. The reason was, that the wire rope endurance with this type of dynamic load appeared to be much shorter than with pulsating loads on straight wire ropes and further that bending over sheaves happens in most transport equipment. Still, certain measuring results give indications with regard to some aspects of the length effect on fatigue testing of steel wire ropes and strands.

It should also be observed, that in the case of some applications like in mooring ropes, hoisting ropes and boom ropes of heavy duty cranes, which some times have a length of more than 1 km, it may be wise to take into account the length effect.

Theoretical as well as experimental reflexions on tensile fatigue testing of drawn steel wires mostly mention the distribution of initial micro-cracks or flaws as the main cause of fatigue failures. If applications of steel wire ropes or strands are involved, however, more influences should be mentioned. In those cases next to the influence on the endurance of the notorious fretting process other factors play a role. These can be divided into influences on the load capacity and influences on the strength.

The tensile load capacity is influenced by:

- The distribution of the load among the wires of the wire rope or strand.
- Attendant stresses due to the geometry of the rope or strand.
- The response of the rope or strand on the dynamic load.
- Local influences of the rope terminations on the state of stress.

The influence of the response and of the rope terminations can be large. Still these will not be considered here, because they strongly depend on the application or construction and give little general information on the length effect.

The strength of the rope or strand will be influenced by:

- The re-establishing property of wires in the wire rope or strand.
- The variation of the material strength of the composing wires.
- The distribution of the damage over the length of the rope.

The distribution of the damage mainly depends on the application, while the distribution of the material strength depends on the quality of the wire. As far as the rope strength is concerned, this paper will be restricted to the re-establishing property of a wire rope or strand.

2. LOAD DISTRIBUTION IN WIRE ROPES.

Different from individual reinforcing bars or prestressing wires, many attendant stresses appear in steel wires of stranded wire ropes, if they are subjected to a tensile force. Even in case such wire ropes are not bent over sheaves and remain in a straight position, attendant stresses such as contact pressure and bending stress, will reduce the endurance of the individual wires. Direct measurements of the contact pressure between wires and strands are not possible without influencing the rope mechanism.

Because of this reason it is difficult to draw up a well verified model of the distribution. Still the contact pressure is interesting, as it can be a factor of a fretting process. It can also be considered, that the contact pressure is caused by components of the tensile forces in the curved wires and strands. These components have the direction of the principal normal and keep the strands and the rope firmly in their circular shape. Further, contact pressure appears to have at least a relation with the tensile stress in the wires and the tensile force in the strands. So for more than one reason measurements of normal stresses in the wires can be useful, because the results also tells something of the contact pressure.

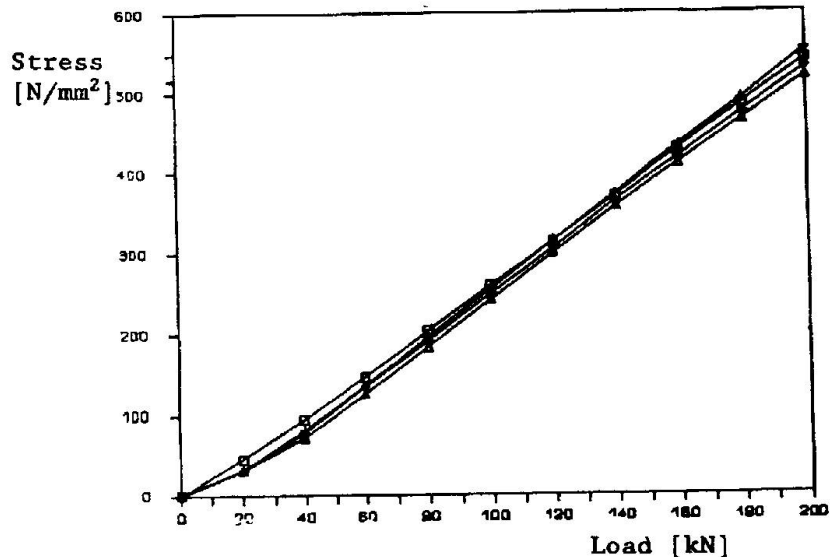


Fig.1 Mean value of normal stress of four tensile tests.

keep the strands and the rope firmly in their circular shape. Further, contact pressure appears to have at least a relation with the tensile stress in the wires and the tensile force in the strands. So for more than one reason measurements of normal stresses in the wires can be useful, because the results also tells something of the contact pressure.

2.1 Stress measurements.

Measurements of normal stresses can be performed by using very small strain gauges with a measuring gridd of about 1 mm times .6 mm. If sufficient strain gauges are cemented more or less random, each at the outer surface of its own wire crown and in the direction of the wire axis, considerable differences in normal stresses will be found.

At Delft these stress measurements were carried out for many years. The tests were performed with about twenty strain gauges, cemented within a distance of two times the lay length of the test rope. From the results the following interesting conclusions can be drawn:

- Apart from the lower loads, the mean value of the normal stresses approximates a linear function of the tensile load.
- As could be expected because of the lower tensile stiffness, the mean value of the normal stress at the outerwires is 5 to 20 % lower than the calculated mean tensile stress of the rope. The difference depends on



the type of wire rope.

- The differences in normal stress at outerwires can be characterised by the standard deviation of the normal distribution.
- A new rope, which is not yet exposed to a dynamic load, can under normal load conditions show very large relative standard deviations. In the past even values of 90 % of the mean value were measured.
- After running in with 10,000 load cycles of moderate load amplitudes, the standard deviation decreased to a lower value.

Before fifteen years this value was not less than 50 % of the mean value, measured under a tensile load of 25 % of the ultimate breaking load.

When nowadays ropes are tested under such conditions, standard deviations are found of 30 up to 35 %. This improvement of the quality must be attributed to the quality assurance systems, which many ropemakers have introduced.

2.2 Measuring results.

As an example figures 1, 2 and 3 show the results of stress measurements performed on a 6x25 Filler wire rope with an independent wire rope core. This rope with a diameter of 26 mm was laid in ordinary lay with a lay-length of 167 mm. The ultimate breaking load (U.B.L.) was 434 kN, while the actual breaking load was 485 kN.

Stress
[N/mm²]

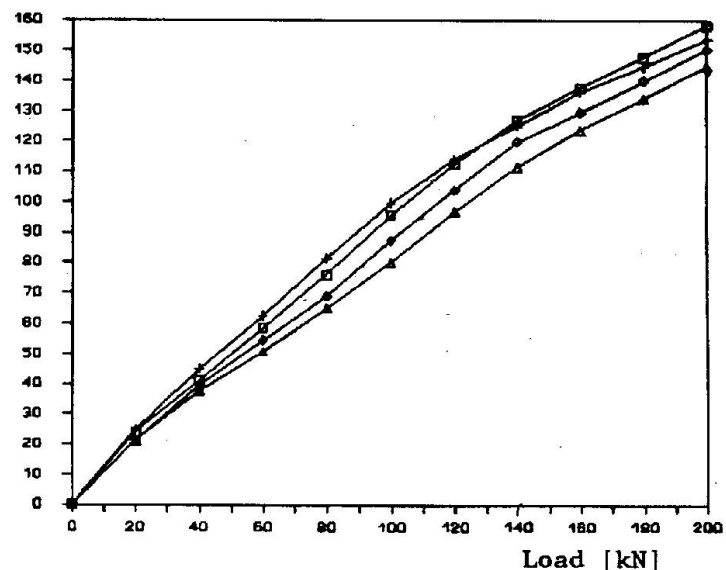


Fig. 2 Standard deviation of four tensile tests.

Within a length of two times the lay-length of the rope (335 mm) 20 strain gauges were cemented. All gauges were distributed among four strands and four gauges on the same wire.

After preparation the sample was subjected to a tensile test in steps of 50 kN up till a maximum of 200 kN, which means up to 40 % of the actual king load. At each load step the train of the 20 gauges was measured by a fast automatic data logger, which put the results into a personal computer, where these were transformed into stresses and stored in a data base. The data base was connected with a spread sheet programme to produce the graphs in the desired shape. These instruments reduced the risk of measuring errors due to changes in tensile load, mistakes in the calculations and the graphs.

After the static tensile test, the sample was subjected to a pulsating test. The upper bound of the load was 200 kN and the lower bound was 20 kN. The test frequency was 2.5 Hz. After 5000

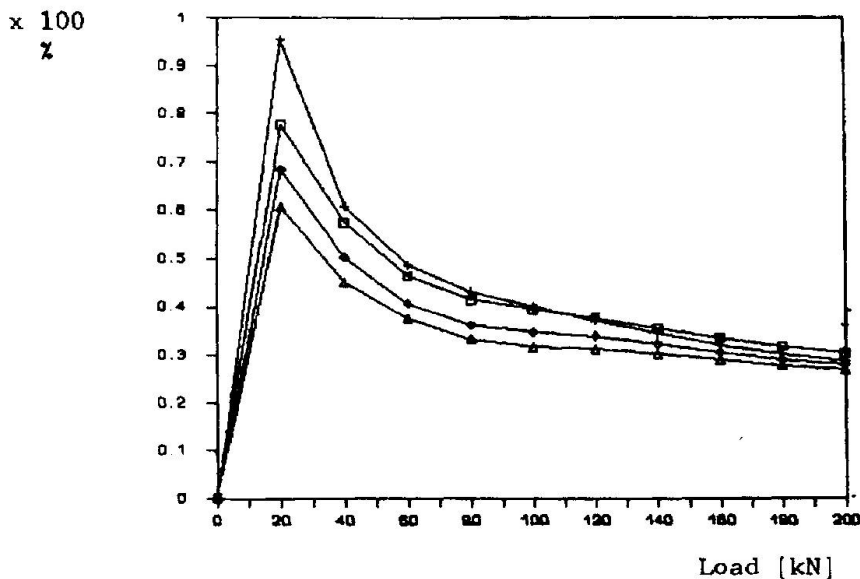


Fig. 3 The relative standard deviation of four tensile

load cycles the pulsation test was interrupted to repeat the tensile test with stress measurements. After two periods of 5000 cycles followed by a static tensile test, the wire with four strain gauges was slit with a small grinding machine. This artificial wire fracture was made in the wire with the strain gauges nr.2 and nr.4. The distance up to the gauge nr. 4 was 7 lays of the wire in

the strand, while the gauge nr. 2 was at 12 layst from the fracture. After a second tensile test in order to look after the influence of the fracture, the pulsating test with interruptions was continued. The experiment was ended with a rope fracture at one of the rope terminations after 35260 cycles. This termination was a clamp of the wedge type.

As shown in figure 1, the character of the average stress did not change due to the pulsating load. The value of the average stress under a tensile load of 200 kN tended to decrease by 3,5 % of the maximum stress of 550 N/mm².

Also the standard deviation decreased by 13 % of the maximum value after the periods of the dynamic tensile load. See figure 2. Apart from the load of 20 kN the standard deviation increased rather linearly with the tensile load up to 140 kN, which means 30 % of the ultimated breaking load. At a further increase of the load, the deviation tends to stay behind.

The relative standard deviation (fig. 3) has a tendency to approach asytmotically to a value of 31 % before and 28 % after the dynamic load cycles.

2.3 Stress measurements inside the strand.

The stresses of the measurements described above were normal stresses and even though the sum of the bending stress and the tensile stress will influence the development of fatigue cracks, it w ould be interesting to separate them. The separation of the tensile stress can provide more certainty about the tensile load distribution.

Therefore, in a new experiment a second strain gauge was cemented in the same wire cross section but just opposite to a gauge on the crown of an outerwire. To ensure that a wire could be taken out of

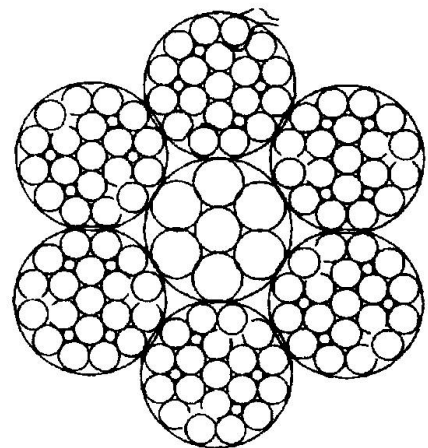


Fig. 4 Strain gauges in and outside the strand.

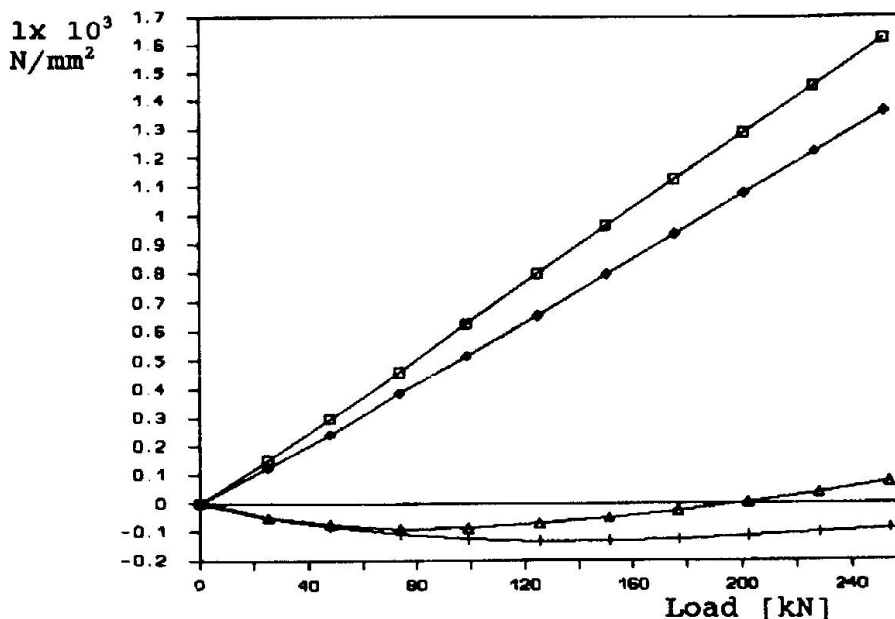


Fig. 5 Measured stresses at a wire in and outside the strand.

a strand in order to cement the gauge inside the strand, a strand had to be taken out of the rope first. The wires around the measuring wire had to be carefully treated in such a way, that the gauge inside the strand would stay free and that the electrical lead wires of the gauge could be guided outside, without running the risk to be cut off during the measurements. The

following step was to carefully replace the wire into the strand and to replace the strand into the rope. The last mentioned action caused a difficult problem, because we could not get the strand back exactly at the same position as before the treatment. It did not lie tight enough around the steel core and, therefore, it was less stiff than the other strands.

Still the measuring results of that experiment are sufficiently interesting to show some of them here. The test procedure of this experiment was more or less equal to the procedure of the described experiment where only gauges at the outside of the rope were used. Figure 5 shows the measured stresses of two pairs of strain gauges, which are very high at the inner side (an average of 1460 N/mm² under a load of 50 % of the U.B.L.) and very low at the outer side (an average of 0 N/mm² under the same tensile load). How the normal stress appeared to be divided in tensile stress and bending stress, is demonstrated in figure 6 and figure 7.

In this case the tensile stress was of the same order as the bending stress.

The results are compared with the normal stresses of gauges at the crowns of wires of other strands

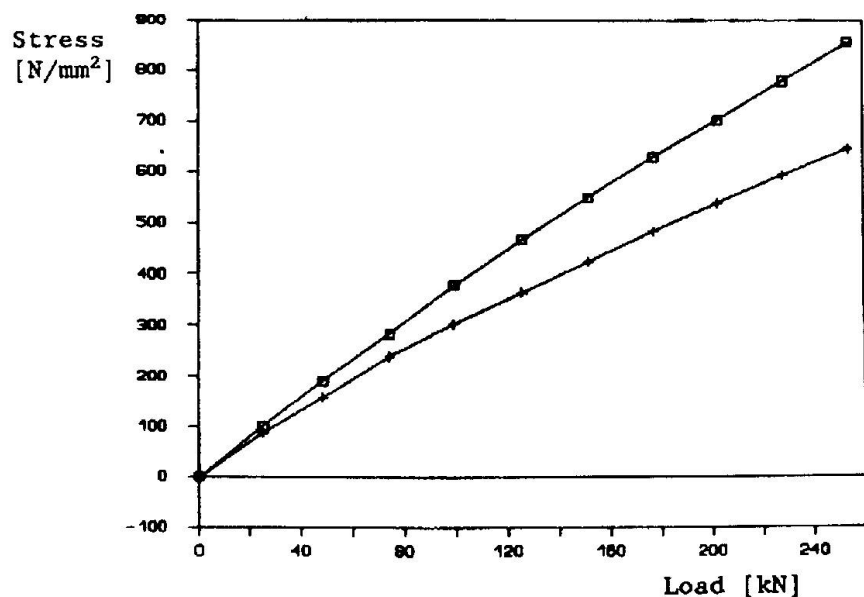


Fig. 6 Tensile stress.

than the one with gauges inside. These stresses were measured at the same time as those in figure 5. The results - a maximum average normal stress of 760 N/mm² does not give rise to serious objections against the maximum average tensile stress of figure 6 (740 N/mm²). The maximum of the average bending stress of figure 7 (740 N/mm²), however, is much too high, due to the change in the position of the treated strand already mentioned.

The results of this experiment indicate that one can assume, that the variation of the normal stress is mainly caused by attendant bending stresses and that the distribution of the tension load among strands and wires is more even than the deviation of the bending stress.

2.4 The re-establishing length of a wire fracture.

When describing the first experiment, the make of an artificial wire fracture is mentioned. The intention of that fracture was to verify the earlier found relation [4] between the full re-establishment of the wire function after a fracture and the number of lays of the wire in the strand. The

relation was, that 7 lays of a wire in a strand after a wire fracture, the wire will bear its full part of the load again.

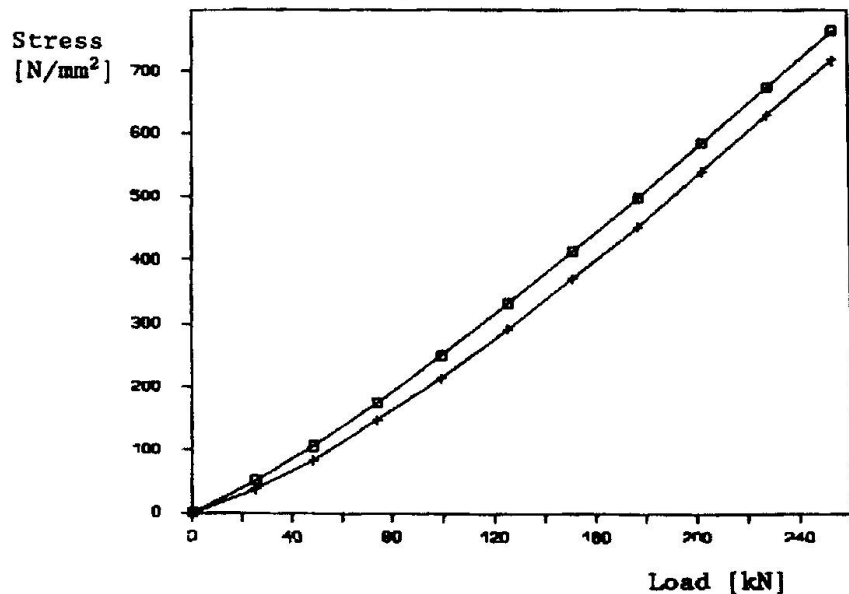


Fig.7 Bending stress in an outerwire.

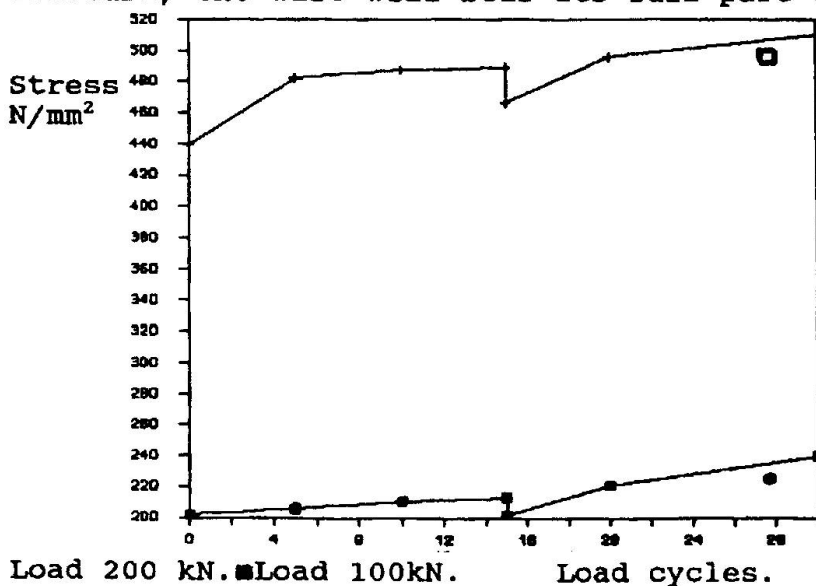


Fig.8 Stress gauge nr.4 as a function of the endured load cycles.

Figure 8 gives the measured stresses of the strain gauge nr.4 at a tensile load of 200 kN as well as at a tensile load of 100 kN as a function of the endured periods of load cycles. The gauge nr.4 was situated at a distance of 7 lays of the wire from the fracture, which was made after three period of 5000 load cycles. Before and after cutting of the wire also the stress was measured. From

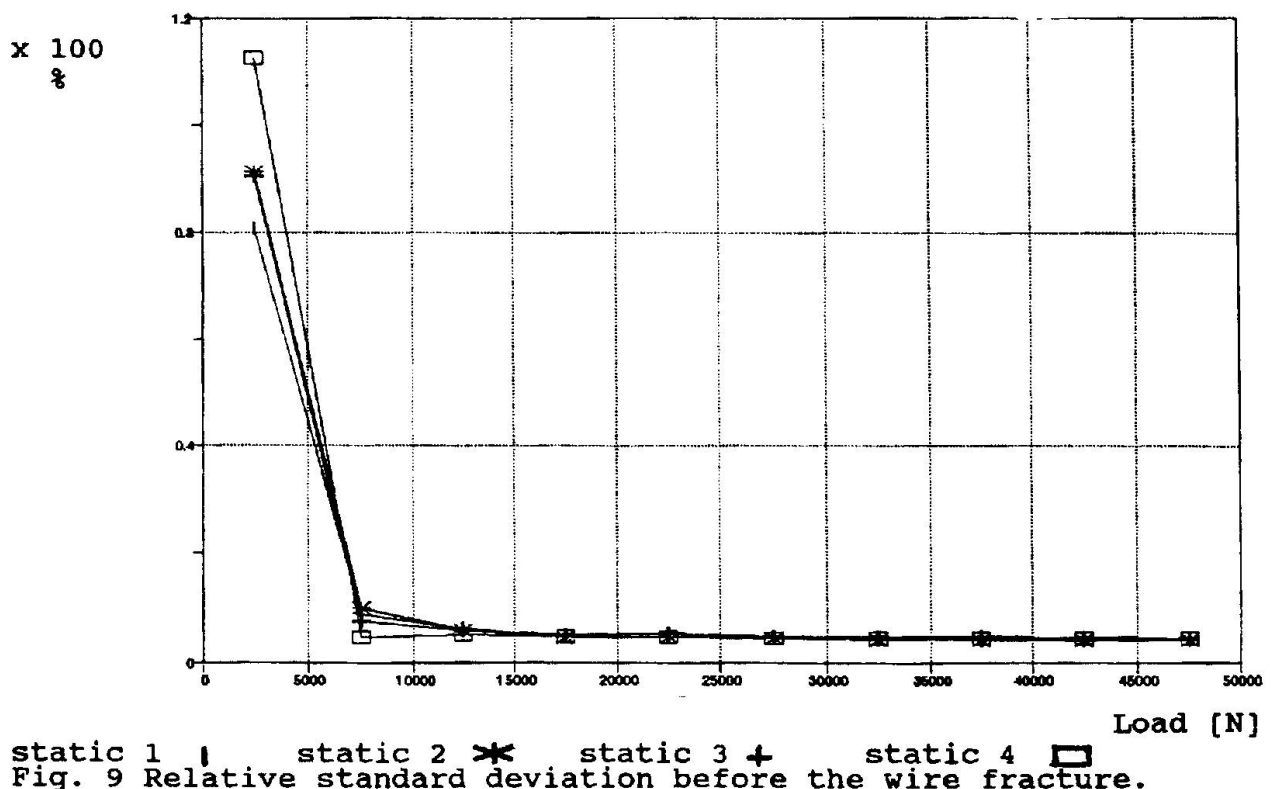


figure 8 can be observed that the re-establishing length still consist of at least 7 lays of a wire in a strand. This distance corresponds with two to two and a half times the lay length of a rope. The latter is also used as half the inspection length in the discard criteria of ISO [5], because the mentioned distance of 30 times the rope diameter corresponds with two times two and a half lays, which lie at each side of a fictive rope cross section. Besides the inspection length, wire fractures and other damage will not influence the strength of that part of the rope. So, if one looks for a wire rope length that meets the independance assumption for the calculation of the length effect [1], one could consider the inspection length of 30 times the rope diameter could. If e.g. 2 to 3 times the lay length is added to this in order to cover the influence of the rope terminations, a length of about 50 times the rope diameter is found, which is suitable as a minimum length of a wire rope sample for a fatigue test.

3. LOAD DISTRIBUTION IN STRANDS.

The geometry of stranded wire ropes and single strand wire ropes are quite different and therefore their behaviour under static loads as well as under dynamic loads might also be quite different.

Next to the measurements on stranded ropes also stresses of the



outerwires in a 36 WS strand of 114 mm in diameter are measured. The procedure of these measurements was the same as described in item 2.1. Only the number of straingauges was diminished by 10, because of the lower number of outerwires. Therefore, the attention can be focused on the measuring results. The mean value

of the normal stresses due to the stepped tensile tests were up to 48 kN nearly linear to the tensile load and reached a maximum value of 500 N/mm².

Also in this case a period of 5000 cycles of the pulsating test (upper load 49 kN, lower load 22 kN) caused a small decrease by the mean stress value. After the artificial wire fracture was made, the maximum of the mean value was stabilized at 450 kN. Before the wire fracture the relative standard deviation of the stresses (Fig. 9) showed a very fast approach to a stable value of 4.5 %. After the fracture the relation between the relative standard deviation got a characteristic course (Fig.10). Under moderate loads the maximum standard deviation was 38 %.

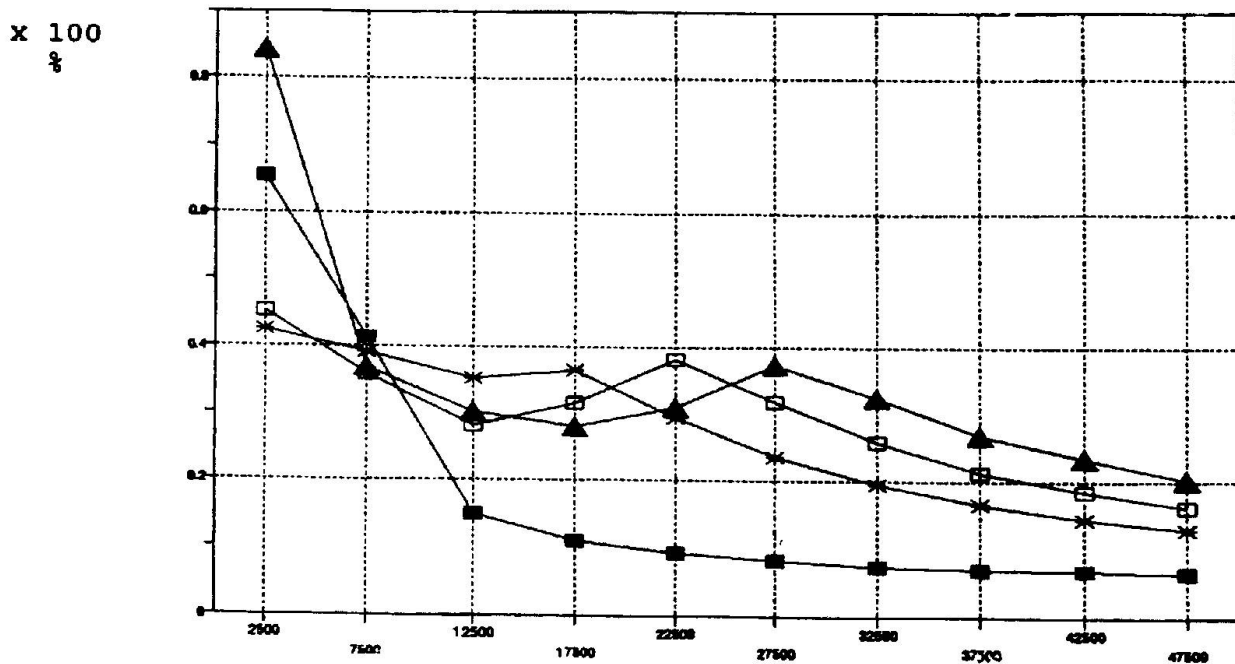


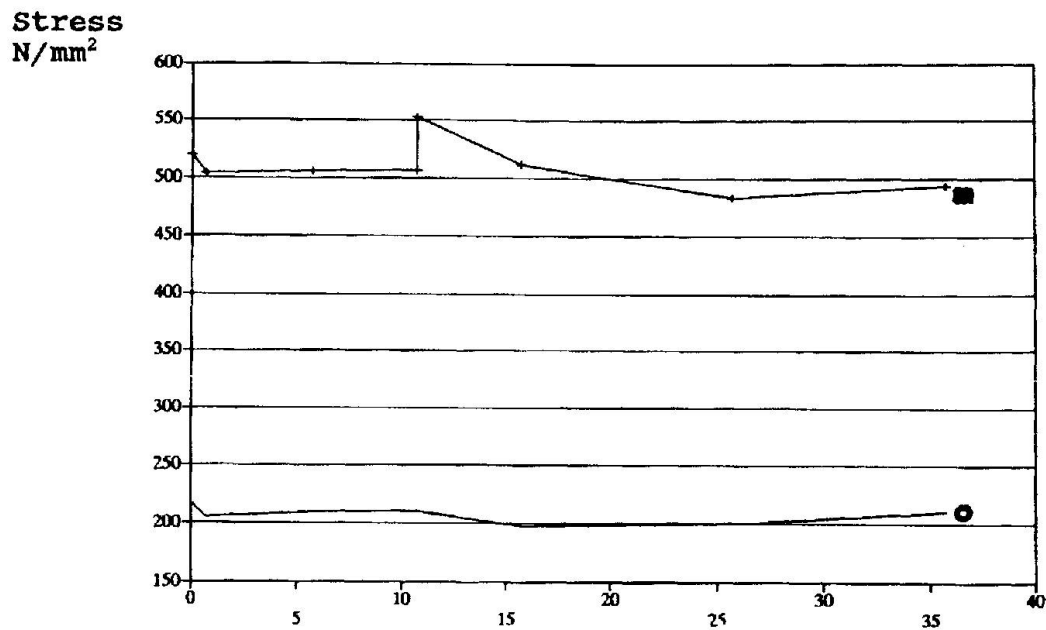
Fig. 10 Relative standard deviation after the wire fracture Load [N]
static 5 ■ static 6 × static 7 □ static 8 ▲

while under the maximum load it tended to approach 18 %.

3.1 The re-establishing length.

After four tensile tests alternated with three periods of 5000 cycles of the pulsation test, a wire fracture was simulated by grinding off the wire at a distance of 7 lays from strain gauge nr.8. The figure nr. shows an increase of the stress by 10 %. After the next 5000 cycles of the pulsating test the stress returned to its original value.

The last figure indicated that a re-establishing length of a wire in a single strand could be a length of 7 lays. With a lay length of about 7 times the strand diameter and one re-establishing length at each side of an imaginary strand cross section the length which meets the independent assumption can be taken 100 times the strand diameter. If the lay length is much more than seven times the strand diameter, however, the validity must be verified. In this case, however, the wire was not turned out of the rope and that must be taken as a condition.



x 1000 Load cycles

Load 24 kN ○

Load 48 kN ■

Fig. 11 Mean stress of gauge nr.8 after periods of dynamic load.

REFERENCES.

1. Castillo E., Fernandez-Canteli A., Statistical models for fatigue analysis of long elements. Introductory Lectures workshop IABSE pages 17 and 18, 1992.
2. Esslinger V., Fatigue testing of wires and strands. Test procedures and experimental studies. Introductory Lectures workshop IABSE pages 35 and 36, 1992.
3. Gabriel K., Nürnberger U., Failure Mechanisms in fatigue. Introductory Lectures workshop IABSE pages 55/58, 1992.
4. Wiek L., The influence of broken wires on wire rope strength and discarding.
Round Table of OIPEEC. Luxembourg October 1977.
5. ISO 4309, Wire rope for lifting appliances. Code of practice for examination and discard. UDC 621.86.065.3 page 4, 1981.

Tensile Fatigue of Very Short Samples of Stranded Wire Rope

Fatigue à la traction de courts échantillons de câbles toronnés

Zugermüdung sehr kurzer Proben von Drahtlitzenseilen

Richard CHAPLIN
Senior Lecturer
University of Reading
Reading, UK



Richard Chaplin graduated from Cambridge University in 1966 in Mechanical Sciences followed by a PhD on composite materials. He has worked in a structural consultants office and in an aircraft design office. His current preoccupation is with the endurance of ropes.

SUMMARY

This paper describes the outcome of a series of tension-tension fatigue tests on samples of six strand wire rope with lengths from one to four rope lay lengths. Despite expectations to the contrary, it is found that following good practice in the preparation of terminations, and with an initial overload at the start of each test, consistent high fatigue lives can be obtained with no length effect apparent.

RÉSUMÉ

L'auteur fournit les résultats d'une série d'essais à la fatigue, sous sollicitation pulsatoire de traction, effectués sur des échantillons de câbles comportant six torons, et dont la longueur variait de un à quatre pas de torsade. Contrairement à toute attente, l'expérience a montré que, dans le cas d'une bonne préparation des extrémités et d'une surcharge initiale au début de chaque essai, il était possible d'atteindre des valeurs de durée de vie élevées sans entraîner des effets apparents sur la longueur des échantillons.

ZUSAMMENFASSUNG

Der Beitrag beschreibt die Ergebnisse einer Versuchsserie mit Zugschwellbelastung an Proben von Seilen aus sechs Litzen, deren Länge von einer bis zu vier Seilschlaglängen variiert wurde. Trotz gegenteiliger Erwartung wurde beobachtet, daß bei sorgfältiger Bearbeitung der Enden und Anfangsvorbelastung zu Versuchsbeginn durchgängig hohe Ermüdungsstandzeiten ohne auffälligen Längeneinfluß erreicht werden können.



1 INTRODUCTION

In response to an invitation to participate in the IABSE Workshop on Length Effects on Fatigue of Wires and Strands, since the author's main area of interest has been stranded ropes, a short investigation has been made of the influence of sample length on the tensile fatigue endurance of such a construction. The investigation has not been intensive and only a limited set of results has been obtained within the time available, but these are never the less considered to be worth reporting.

Over recent years there has been considerable interest in the tensile fatigue of wire ropes for use in offshore applications, especially as components in mooring systems for oil exploration, production, and accommodation platforms [1]. This interest has stimulated numerous investigations at different levels, on various different issues, but the question of length has not been addressed specifically. For the majority of these investigations there has been a tacit acceptance that, provided samples tested have lengths of at least six lay lengths, but preferably more than ten lay lengths, then results will be representative of the very much longer ropes employed in service. The unstated basis for this acceptance is that while service lengths of rope (which may be as much as 2 km long) are different in statistical terms, any increased probability of failure at a given level of loading associated with high length, is counterbalanced by additional loading components (bending near terminations, imbalance etc.) that are exacerbated by shortness.

The guideline for sample length based upon "lay length" translates for a typical six strand rope to 40 diameters as an absolute minimum or 60 diameters as a preferred length. These translations into lengths defined as diameters have then been taken as more generally applicable to other constructions. Whilst this may seem reasonable for fairly conventional spiral strands or multi-strand ropes, real problems are likely to arise with some of the more specialised constructions now being considered for taut vertical mooring systems which have very long lays.

Therefore having resolved some of the more basic issues affecting fatigue, the length effect issue is one which is likely to become of greater significance to offshore applications, and in this context the IABSE initiative is most timely.

2 BACKGROUND

2.1 Stranded Rope Constructions

The essentially helical construction of a traditional rope provides the mechanism that gives the rope its essential quality of bending flexibility under high tensile load. This flexibility is achieved in practice by a geometry that permits the wires to slide in relation to one another, as described by Gibson [2] and quantified by Nabijou [3], to equalise the strains otherwise associated with distance from the rope axis when bent. But, when the rope is clamped in a way which locally prevents any relative sliding, the capacity to escape these bending strains is restricted in a way recently described in detail by Andorfer [4].

Such problems can be especially acute when there are two effective clamps close to each other. In this context clamping can be achieved by an attachment, such as a pendant chair on an aerial ropeway, or clearly by a termination, but also, to a degree, by the transverse loading associated with the rope running onto a sheave or a drum. As

discussed by Andorfer, the effect on bending behaviour of such clamps will be influenced by proximity in a nonlinear way that reflects the amplitudes of the helical features of the construction. So that, assuming that strand lay (i.e. the pitch of a wire in a strand) is comparatively low, then clamps effectively located at exactly one rope lay length will not reduce bending compliance from that of the unclamped rope. However clamping at say a half lay length, but also at one and a half lay lengths, will lead to appreciable reductions in compliance.

By a similar argument it will be apparent that different spacings between clamps put on a rope in a bent state, will have different consequences for mean axial wire stresses when the rope is pulled straight. Clamps spaced at integral numbers of lay lengths should have no effect, and the worst effects must be expected for intermediate spacings. But the greater the distance between clamps the greater the length for redistributing the imbalances associated with clamping at lengths which are not integral numbers of lays, and so the less the effect.

The magnitude of the wire length inequalities associated with straightening a bent rope is dependent on the non integral part (the residue after subtracting the integral part) of the number of lay lengths between clamps. The magnitude of the resulting strains and stresses will fall with increase in the length over which the inequalities are redistributed.

These observations clearly have relevance for bending fatigue of ropes running on and off sheaves or drums: there are also evident implications for tensile fatigue.

2.2 Geometrical influences on rope endurance in bending

The "bending over sheaves" fatigue testing of ropes (BOS fatigue) has been the subject of considerable investigation starting with Albert in 1828 [5] but really only being put on a scientific basis by Scoble in 1920 [6]. Various investigators have considered rope length effects in the context of BOS fatigue. There are two length parameters which profoundly influence endurance:

- (i) bending length [2, 5, 6, 7] (the amplitude of rope movements on and off the test sheave);
- (ii) contact arc length [2, 5, 6] (the length of rope in contact with the test sheave).

In broad terms the effects of both these parameters are that endurance at constant load tends towards infinity as either length tends to zero, but the effects have been found to correspond in terms of the lay length of the rope. This is especially apparent with the effect of contact arc length, where endurance falls to a minimum at about one half a lay length [5, 6], but is approximately constant for lengths greater than one lay length, though there is a suggestion in Muller's results [6] of a periodic fluctuation in phase with lay length.

2.3 Parameters influencing fatigue endurance in tension

In fatigue testing of wire ropes under a tensile load which fluctuates at constant amplitude, a significant number of parameters in addition to the mean and range of the load can influence the result. These include:



- (i) overall class of construction e.g. six strand with IWRC, spiral strand, multi strand, etc.
- (ii) details of construction, e.g. 6×36 or 6×19, 1×147 or 1×292, 35×7 or 57×7, but also including the lay angles and details of wire diameters;
- (iii) quality of manufacture, i.e. the dimensional consistency and balance between similar elements;
- (iv) wire grade, essentially the minimum strength;
- (v) wire quality, including ductility, residual stress distribution and surface finish;
- (vi) lubrication;
- (vii) diameter scale effects (though these are largely encompassed effectively by other parameters);
- (viii) definition of what constitutes failure (ranging from say the detection of five broken wires to total destruction);
- (ix) sample preload;
- (x) type and quality of termination;
- (xi) test length.

Of these eleven parameters, the first eight are a function of the rope itself, (viii) is an arbitrary decision depending on the way in which the data are intended to be used, but the last three are likely to contribute to "scatter" in the results for a given rope.

A fact to emerge very clearly from a detailed examination of published research in this area [1] is that carefully conducted tests on samples taken from the same length of rope perform with a high degree of consistency, and results can be expected which fall within a very narrow band of scatter, generally conforming to a simple single power "s-N" equation. The implications of this observation are that, from the designer's point of view the problem is much more that of allowing for variation between ropes, even those that are nominally the same, than variation in fatigue performance of any given rope; but there is also the problem of defining what constitutes a "carefully conducted" test.

This last point has special significance in relation to the last three parameters listed above. Length is the main topic under discussion here, but usually any one set of tests is likely to have been performed on samples of equal length. Preloading is significant in that it has been shown to enhance endurance significantly [8], but reportedly only when the overload is applied to the sample as terminated for test, and only with loads in excess of 60% of rope strength. The implication of this is that the function of the preload has more to do with the termination than any other possible effects although the potential for such a procedure to improve unequal load sharing induced by geometrical imbalance will be discussed below.

The influence of the terminations is of course well known as the greatest source of problems when trying to characterise the tensile fatigue behaviour of a rope. One of the reasons for this being such a problem is that the great majority of conventional stranded ropes are employed in applications where there is always some feature

associated with the manner of use, most commonly bending over sheaves, that concentrates the degradation mechanisms away from the ends: the ends of the rope and therefore the terminations are not seen as being critical in determining life. When tension fatigue is significant, that is no longer true, but, in the author's experience, a resistance to following precise specifications for termination procedures is encountered in the industry. Such difficulties are becoming significantly less common, and much better procedures with better control of quality seem to be in use, especially for the larger specialised ropes.

When assessing tensile fatigue data for a given rope, significant scatter is usually a sign of termination problems. Any characterisation of the fatigue behaviour of the rope must employ termination procedures that eliminate end effects, and in these terms rejection of data points associated with end failures is justified. But the use of the resulting characteristic in relation to establishing safe service life for ropes in service, must only be on the basis that actions are taken to ensure that the ropes in service will not suffer end effects.

3 EXPERIMENTAL PROCEDURE

3.1 Objective

The objective of the experimental work was to investigate the effect on the endurance of a stranded rope in tensile fatigue of very short test lengths. The particular area of interest was from one to about four lay lengths.

3.2 Sample Preparation

The rope selected for the tests was a six strand rope with independent wire rope core that had already been the subject of extensive testing in a programme of work [9,10] investigating "bending-tension" fatigue (small amplitude bending in phase with fluctuating tension). A detailed specification for the rope is given in Table 1.

Rope Construction:	13 NAT 6(12 + 6F + 6 + 1) + IWR(6(6 + 1) + IWS(6 + 1)) 1770 ZS 111 67.3 6x19 filler IWR
Actual Rope Diameter d :	13 mm
Actual Cross Section A_m :	85.7 mm ²
Nominal Wire Grade:	1770 N/mm ²
Nom. Tensile Strength R_o :	111 kN
Actual Breaking Load F_m :	122.55 kN
Lubrication:	Bri-Lube 60 ®

Table 1: Specification of test rope.

One of the reasons for selecting this rope was that its fatigue behaviour had already been assessed from tests on samples of 750 mm length, without overload [10]. The resulting equation, at a mean of 20% (F_m), was: $N = (113 / range\%)^{9.63}$



The procedure used for terminating the samples is one that has been developed over an extended period of investigations. A filled polyester resin cone is cast over the wire brush using a split mould. The sample when removed from the mould and associated supporting fixture is assembled into a conical collet with split conical spacers, on the test frame. The significant features of the moulding system are a clamp which supports the sample over the full length between terminations, and a mould which permits injection of the resin from the base of the cone, as shown in Figure 1. This arrangement ensures that as the resin rises around the wires all air is effectively excluded, and injection ceases when the resin reaches the neck. The clamping fixture ensures that the rope is located axially and concentrically.

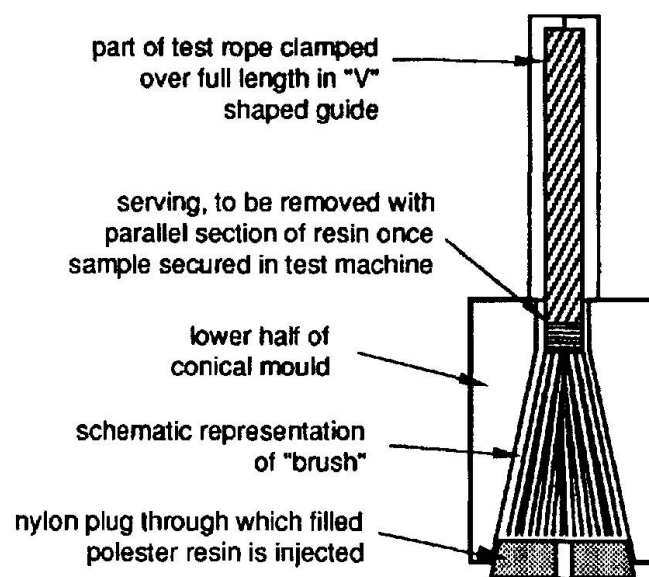


Figure 1: Arrangement employed for moulding conical ends of test samples, injecting resin vertically upwards into the mould.

3.3 Testing

Testing was performed using a 100 kN servo-hydraulic testing system under closed loop load control at a frequency of 1 Hz, ensuring that rope temperature was maintained below 35° throughout all tests.

A decision was made at the start of the programme that in order to minimise the influence of termination inaccuracies, an overload would be applied to every sample at the start of the fatigue test. The magnitude selected for this load was 50% of the actual ultimate breaking load, F_m . This was considered as sufficiently high in relation to the maximum load to be beneficial, but not so high as have too much influence on life [8].

The mean load for the tests was chosen as 20% F_m , since that was the same as used in the earlier tests. The range was initially set at 34% (i.e. $20 \pm 17\%$) because on the basis of the previous results that should give a life of about 10^5 which would be convenient for testing. The first test at this level resulted in a life which was a factor of five

greater than the estimate, so the load range was increased to 36% F_m to reduce the endurance to a more convenient level.

4 RESULTS

4.1 Test data

Table 2 lists details of all the tests performed.

Test No.	Sample Length mm	Length rope lays	Cycles to Failure	Comment
1	304	3.58	567683	discounted - load range 34%
2	334	3.93	136892	OK
3	262	3.08	144457	OK
4	234	2.75	168304	OK
5	200	2.35	122530	OK
6	164	1.93	132384	OK
7	133	1.56	151904	OK
8	370	4.35	102060	discounted - end failure *
9	93	1.09	199945	discounted - initial overload 64%
10	136	1.60	50114	discounted - end failure *
11	148	1.74	113766	discounted - end failure *
12	163	1.92	174701	OK
13	96	1.13	188686	OK
14	238	2.80	231085	OK
15	202	2.38	204716	OK
16	269	3.16	182695	OK

Table 2: Test results. Note all tests, except No. 1, conducted at $20 \pm 18\% F_m$, with a single initial overload to $50\% F_m$. Test samples 8, 9, 10 & 11 were incorrectly terminated with the "brush" positioned outside the cone.

The first test, as mentioned above was at a different load range from those which followed, and should not be considered as part of the set. Test numbers 8, 9, 10 & 11 were incorrectly terminated with the "brush" positioned outside the cone to varying degrees, and should also be discounted. Of these four test 9 also received an additional accidental overload to a level of $64\% F_m$.

4.2 Distribution of results

Figure 2 shows the selected set of endurances ("OK" in Table 2) plotted as a function of the sample length, measured between the socket faces after initial overload, but before commencing fatigue.

In an effort to uncover some indication of a trend in the data, and following the argument in Section 2.1 relating to the straightening a curved rope, the results have also been plotted as a function of the "residual" length, defined as the remainder after subtracting the integral part of the sample length (in rope lay lengths) from the full length (also in rope lays).

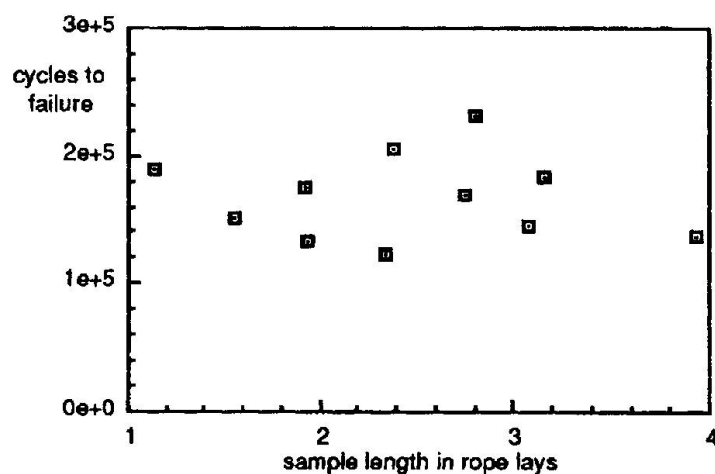


Figure 2: Valid test results plotted in terms of length between socket faces, in rope lay lengths.

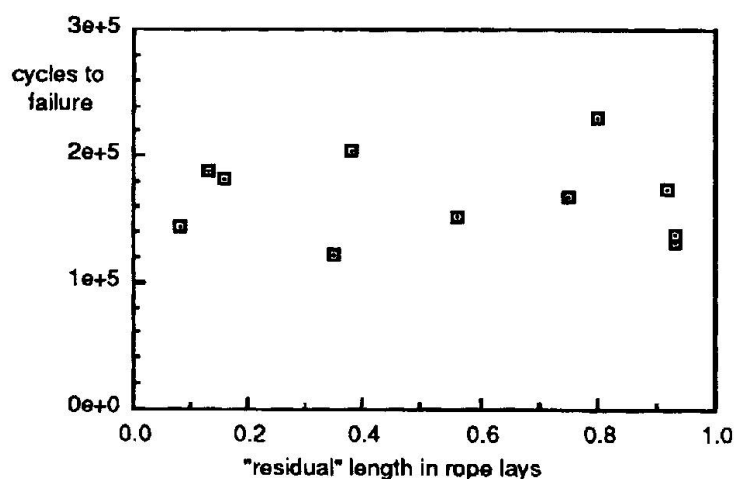


Figure 3: Valid test results plotted in terms of "residual" length, defined as the remainder of length between socket faces, in rope lay lengths, after subtracting the integral part of the length.

5 DISCUSSION

There are two worthwhile observations that can be made from these results, the first of which concerns the effect of preload on the endurance measured. The initial overload to 50% of the rope breaking load has dramatically improved the performance from what had been measured previously, at the same load levels, for the same rope. The previous analysis of fatigue performance was based on exactly the same procedures for preparation (with minor modifications to accommodate length differences), gripping and testing, and the analysis was based on data that excluded any termination failures with the results very closely spaced about the mean line

Data for the previous tests performed without pre-load have been plotted together with the new data in Figure 4. The clear distinction between the two sets can be seen. It can also be noted that one test result in the previous series, on a rope that had

received an accidental overload of unknown magnitude prior to test exhibited an even greater life enhancement than indicated here. This tends to suggest that the difference between the two sets of results cannot be associated with length, but attributed to the overload.

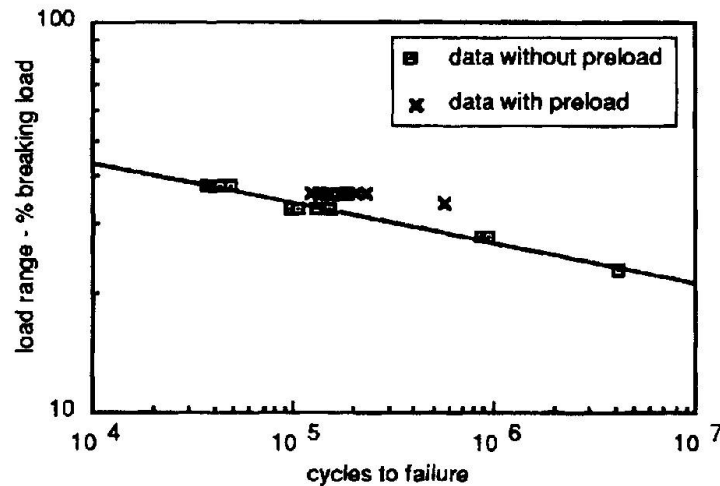


Figure 4: Comparison of test results obtained both with and without pre-load (data for no pre-load obtained from ref. [10])

The results for the tests on samples of different lengths, plotted in Figures 2 & 3 show no sign of any length effect, whether absolute or residual, at all. To seek further explanation results have been replotted in Figure 5 in the order in which the ropes were tested. Some suggestion, though not at a high level of significance, is present that there is a progressive improvement. This could possibly be associated with a learning process for terminating unfamiliar length samples.

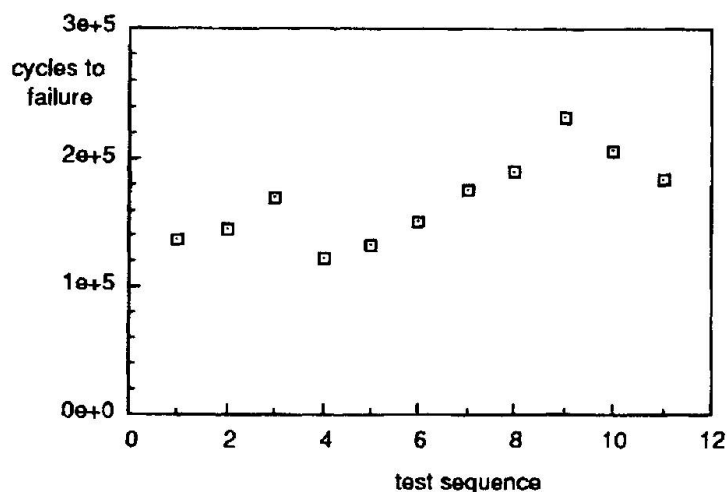


Figure 5: Valid test results plotted in terms of the order in which they were performed, which corresponds to the sequence of preparation.



6 CONCLUSIONS

- 1 Length effects in tensile fatigue of very short test ropes have not been found.
- 2 The beneficial influence of an initial overload in significantly extending the endurance of a stranded rope in tensile fatigue has been demonstrated to be applicable to very short samples.
- 3 The benefits of preload are most probably due to eliminating geometrical imbalances, whether associated with rope manufacture or termination, and as such could be responsible for the observed absence of the expected adverse length effects in very short samples.
- 4 Further work is clearly needed to clarify these issues, investigating:
 - (i) the effects of similar preloads on longer samples;
 - (ii) the influence of preload magnitude;
 - (iii) the length effects on short samples without preload (not easy).

7 REFERENCES

- 1 Chaplin, C. R. & Potts, A. E. *Wire Rope Offshore – a Critical Review of Wire Rope Endurance Research Affecting Offshore Applications* University of Reading Research Report for Dept. of Energy, HMSO Publication OTH 91 341, 1991.
- 2 Gibson, P. T. *Wire Rope Behaviour in Tension and Bending* Proc. First Annual Wire Rope Symposium. Pub. by Engineering Extension Service, Washington State University, Pullman, Washington, March, 1980.
- 3 Nabijou, S. *Frictional Behaviour and Fatigue Performance of Wire Ropes over Small Sheaves* PhD Thesis, Imperial College of Science, Technology and Medicine, University of London, 1990.
- 4 Andorfer, K. *The influence of short grips on the wire and strand mobility in round strand ropes running over sheaves* OIPEEC Bulletin No. 63, June, 1992.
- 5 Muller, H. *The Properties of Wire Rope under Alternating Stresses* Wire World International, Vol. 3, No. 5, October, 1961.
- 6 Scoble, W. A. *Fourth Report of the Wire Ropes Research Committee* Proc. IMech.E., May, 1930.
- 7 Feyrer, K. *Effect of Bending Length on Endurance of Wire Ropes* Wire World International, Vol. 23, July/August, 1981.
- 8 Stonesifer, R. & Smith, H. L. *Tensile Fatigue in Wire Rope* Proceedings of 11th Annual Offshore Technology Conference, Paper No. OTC 3419, May, 1979.
- 9 Ridge, I. M. L., & Chaplin, C. R. *Bending-tension fatigue – the influence of fluctuating load on the safety of ropes in bending* OIPEEC Bulletin No. 62, December, 1991.
- 10 Ridge, I. M. L. *Bending-Tension Fatigue of Wire Rope* PhD Thesis, University of Reading, June, 1992.

8 POSTSCRIPT

Following the discussion of this paper it is apparent that there are some important points which are not really given enough emphasis:

- (i) tension-tension fatigue data for any given stranded wire rope or spiral strand, provided tests are conducted with adequate care on samples of reasonable proportions, are invariably tightly grouped with remarkably little scatter;
- (ii) short samples have a greater tendency to premature termination failures, and, largely as a consequence, show more scatter and a lower mean life;
- (iii) the fatigue performance of a given rope can be radically modified, for example by initial over-load;
- (iv) nominally similar ropes from different manufacturers, or even from the same manufacturers, can have a radically different fatigue performance.

"Reasonable proportions" in this context would be a test length which is at least forty diameters (six lay lengths of a typical stranded rope), but sixty diameters would be preferred. Any test piece with a length of less than forty diameters must be considered too short. However the implications of the work described here are that the problems of a short rope can be overcome by preload, but the inturn is likely to distort the behaviour.

In translating from laboratory test data to the endurance prediction of ropes in service, it is first necessary to eliminate the adverse effects of poor termination and short samples by adoption of good practice. Then the important point to conclude from the above observations is that the distribution of endurances obtained for any one rope, compared with the distribution of mean endurances obtained for different ropes, is such that the statistical modelling of the influence of service length is likely to be of minimal significance compared with the problem of modelling the differences between ropes.

This conclusion implies that "length effects" are not really an issue. The issue that must be resolved however is that of statistically modelling the differences between ropes, acknowledging that the fatigue results for a rope at the lower end of that distribution will *all* tend to be low.

Leere Seite
Blank page
Page vide

Fatigue Life of Coupling Joints of Prestressing Tendons

Comportement à la fatigue des ancrages de câbles

Ermüdungsfestigkeit von Spanngliedkopplungen

Gert KÖNIG

Prof. Dr.
T H Darmstadt
Darmstadt, Germany



Gert König, born 1934, received degrees engineering 1960, and PhD in 1966. For nearly 20 years working at the Institut für Massivbau of TH Darmstadt.

Ireneusz DANIELEWICZ

Dipl.- Ing.
T H Darmstadt
Darmstadt, Germany



Ireneusz Danielewicz, born 1959, received degrees in civil engineering in 1986. For four years he worked as a structural engineer at the Hochtief AG. At present, he is involved in research on fatigue behaviour of splice devices of prestressing tendons at the TH Darmstadt.

SUMMARY

In the case of post-tensioned members, mainly the splice devices of the tendons are endangered by fatigue. The fatigue resistance of the coupler is considerably lower than that of the prestressing steel outside the coupling joint. Experimental work to study the fatigue behaviour of couplers embedded in concrete of two different post-tensioning systems has been carried out. This paper presents the experimental results, and a simple method to calculate the stresses in the tendons and in the reinforcing steel considering the realistic bond behaviour of the prestressing steel and the reinforcing steel.

RÉSUMÉ

Dans le cas de structures précontraintes, les ancrages des câbles sont les principaux points menacés par la fatigue. La résistance à la fatigue de l'ensemble est considérablement moindre que celle de l'acier prétendu. On a fait des études expérimentales pour déterminer le comportement de l'ancrage à la fatigue sur deux systèmes de précontrainte différents. Cet article présente les résultats expérimentaux ainsi qu'une méthode simple pour calculer les tensions des câbles et de l'armature renforcée, en considérant la relation entre le comportement de l'acier prétendu et celui de l'acier renforcé.

ZUSAMMENFASSUNG

In Spannbetragwerken sind die Spanngliedkopplungen meist ermüdungsgefährdete Bauteile, da ihre Ermüdungsfestigkeit wesentlich niedriger ist als die des Spannstahls außerhalb des Kopplungsbereichs. Es wurden experimentelle Untersuchungen zur Erforschung des Ermüdungsverhaltens der Kopplungen eingeleitet. Dieser Artikel berichtet über die Ergebnisse der durchgeführten Versuche an Kopplungen zweier unterschiedlicher Spannsysteme und zeigt eine einfache Methode zur Berechnung von Spannungen des Betonstahls und des Spannstahls in Querschnitten mit gemischter Bewehrung.



1. INTRODUCTION

In addition to the simple method for the fatigue design, in which the highest calculated stress range should not exceed the nominal value of the endurance limit, more detailed design methods are presented in EC-2 and Model Code 90. These methods require realistic S-N curves of the materials used, as well as precise descriptions of the actual fatigue loading.

Investigations at the Otto-Graf Institute at Stuttgart [1] have shown that the fatigue failure is primarily caused by fretting corrosion between the coupling elements. These tests have been carried out with free straight tendons, but an additional fretting effect might occur, reducing the fatigue strength if a spliced tendon is embedded in concrete.

Different systems of spliced tendons embedded in concrete have been tested by Kordina and Günther [2]. As a result of these tests the fatigue limit for 2 million cycles is significantly lower than when tested in air. But these tests were performed without any additional ordinary reinforcement crossing the joint.

A safe fatigue design also requires a realistic calculation of steel stresses. Due to different bond behaviour of reinforcing and prestressing steel, the real stresses differ from the results of a common cracked stage calculation. The effect of this stress redistribution in the case of a coupling joint is not known until now.

In the following experimental work concerning the fatigue behaviour of embedded couplers under realistic conditions and the redistribution of the steel stresses is described, in addition a simple method to calculate the stresses in tendon and in reinforcing steel considering the different bond behaviour of tendons and reinforcing steel is presented.

2. EXPERIMENTAL PROGRAM

In total couplers of two different posttensioning systems will be tested.

In a first series the coupler K (Fig. 1) of the posttensioning system D & W (strands) was tested under constant amplitude loading. The stress ranges were chosen as follows:

$$\Delta\sigma_z = 140 \text{ MPa (5 tests)}$$

$$\Delta\sigma_z = 180 \text{ MPa (4 tests)}$$

$$\Delta\sigma_z = 220 \text{ MPa (5 tests)}$$

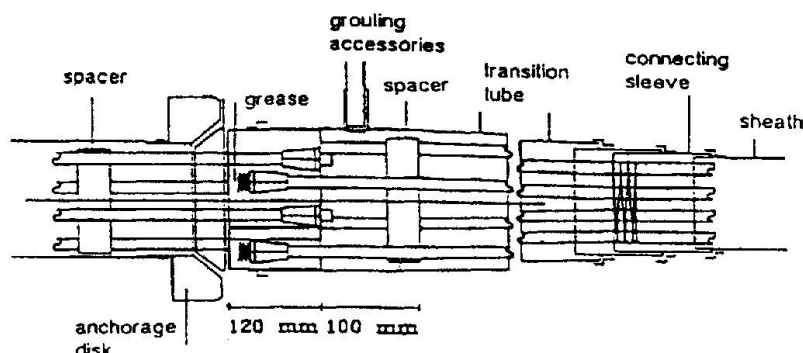


Fig. 1: Coupler K, posttensioning system D & W (strands)

The length of the test beams was 6.0 m and the depth 1.00 m. The beam width of 40 cm was determined by the edge distance for the anchorages given in the approval documents of the posttensioning system. Tendons consisting of 6 strands (type 6806 D & W) were used and the applied prestressing force was chosen to be 650 kN. This value is lower than the nominal value

given by the German approval documents. Fig. 2 shows the test beams, its cross section, and the test setup in the first test series.

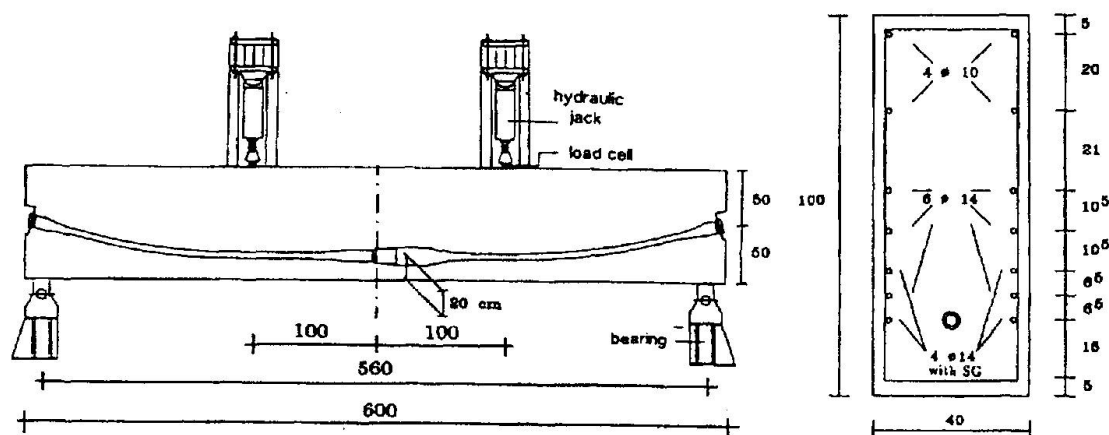


Fig. 2: Test beams, its cross section and test setup

In the second test series the splice device of the tendon of Company BBRV-SUSPA is been tested. Each of the two tendons at both sides of the coupler consist of 16 wires with diameter of 7mm made from cold drawn smooth prestressing steel. All wires of the tendon end in a common steel anchor head. The wires are fixed by cold pressed studs at their ends.

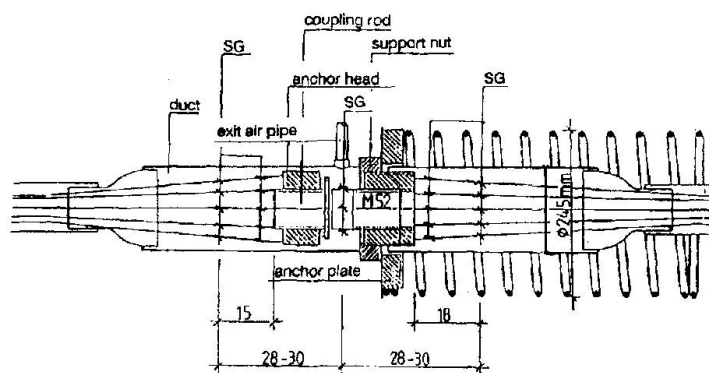


Fig. 3: Coupler B/KI, posttensioning system BBRV-SUSPA II

The most important test parameters (σ_{zmax} , load arrangement, dimension of the test beams) were chosen in such a way that a comparison is possible between the new test results and those obtained by Kordina and Günther.

The experience from the first test series leads to a modification in the construction of the test beam. The type of beams used in the second test series is shown Fig. 4. It consists of clear defined compression and tension chord. The tendon runs in a straight line between the anchors at the ends of the beam in the center of the tension chord. The tendon coupler crosses the coupling joint which is located in the middle of the span length. Additionally four reinforcing bars of diameter 14mm cross the joint. The top compression steel chord is flexurally rigid and connected to the concrete part of the beam. During the test the compression force in the upper chord is measured by load cells. The measurement of the steel strains in the tension chord is performed by strain gauges (SG). Each of the two tendons is equipped with 24 measuring points: 16 in the vicinity of the anchor head and 8 more at a distance of 17 cm apart from it. The force in the coupling spindle is controlled by



four strain gauges distributed over its circumference. Each reinforcing bar is equipped with 7 strain gauges. Their location corresponds to the position of SG on the prestressing wires. During cyclic loading the stress range in some selected wires is continuously controlled.

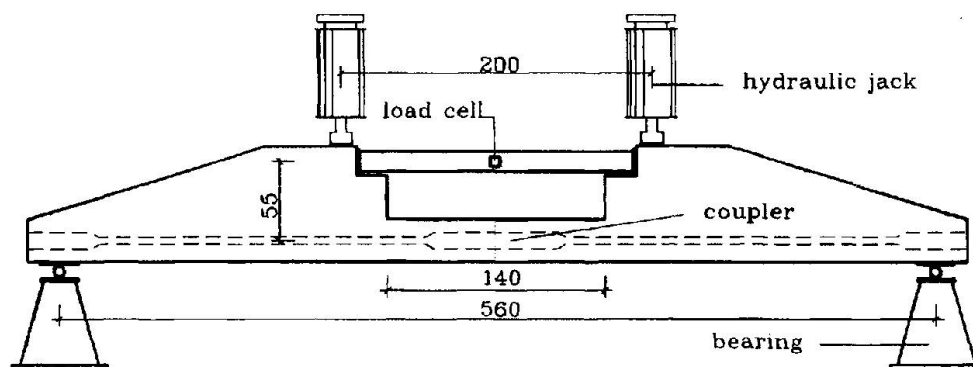


Fig. 4: Test beams for second test series

Up to now eight tests have been carried out. It was found, that the failure of the wires occurred always in the neighbourhood of the anchor head. The fracture developed from the fatigue notches which were located at the inside of the circle over which the wires are distributed. These are the regions of the highest lateral pressure along the wires in the coupling region. The stress redistribution was also observed as in former tests.

3. TEST RESULTS

3.1 Fatigue Behaviour

The statistical analysis of the numbers of cycles N was performed assuming a normal distribution for $\log N$. The results for the first test series are shown in a S-N diagram, Fig. 5. The straight lines connect the mean values. The dotted line represents the results of a linear regression analysis including all data:

$$\log N = 13.634 - 3.603 \log \Delta \sigma \quad (1)$$

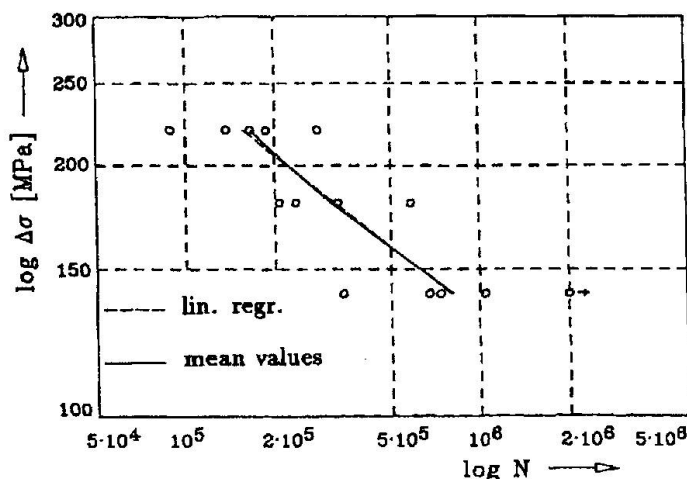


Fig. 5: Fatigue behaviour of the first test series

The first results in the second test series indicate the same tendency as in the first test series. The stress increase in the prestressing steel is significantly lower compared to that of the reinforcing steel.

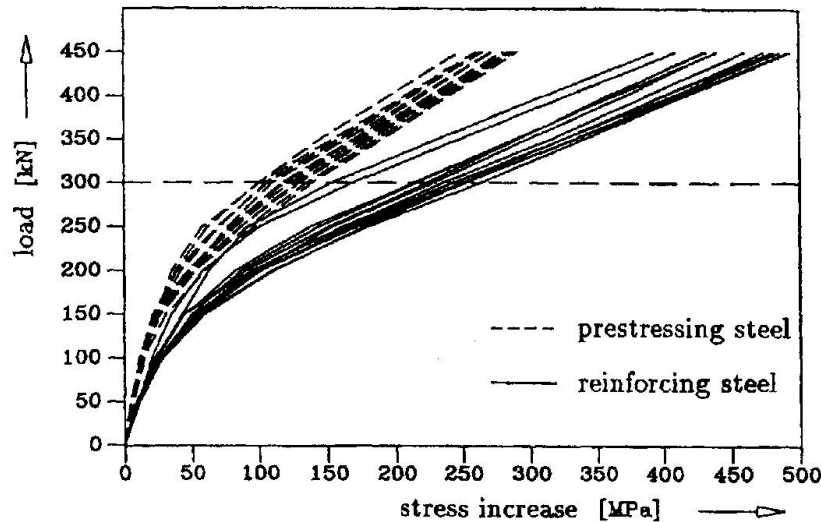


Fig. 7: Stress increases in the reinforcing bars and in the tendon

4. SIMPLE METHOD TO CALCULATE THE STEEL STRESSES

4.1 Background

Because of the different bond behaviour of tendons and reinforcing steel the increase of the stresses in both steel types after the appearance of cracks is different. Considering the compatibility and equilibrium in a cracked prestressed concrete member the following formulas can be stated with the external force F to calculate the actual stresses in tendons and in reinforcing steel.

For a single crack:

$$\sigma_{sR} = \frac{F}{A_s + \xi_1 \cdot A_z} ; \quad \sigma_{zR} = \frac{\xi_1 \cdot F}{A_s + \xi_1 \cdot A_z} \quad (4)$$

where

$$\xi_1 = \sqrt{\xi} \cdot \frac{U_{zw} \cdot A_s}{U_s \cdot A_z} ; \quad \xi = \frac{\tau_{zm}}{\tau_{sm}}$$

For a stabilized crack pattern:

$$\begin{aligned} \sigma_{sR} &= \frac{F - 0,6 \cdot T_{um}}{A_s + A_z} + \frac{0,6 \cdot T_{um}}{A_s + \xi_1 \cdot A_z} \\ \sigma_{zR} &= \frac{F - 0,6 \cdot T_{um}}{A_s + A_z} + \frac{0,6 \cdot \xi_1 \cdot T_{um}}{A_s + \xi_1 \cdot A_z} \end{aligned} \quad (5)$$



The first results in the second test series indicate the same tendency as in the first test series. The stress increase in the prestressing steel is significantly lower compared to that of the reinforcing steel.

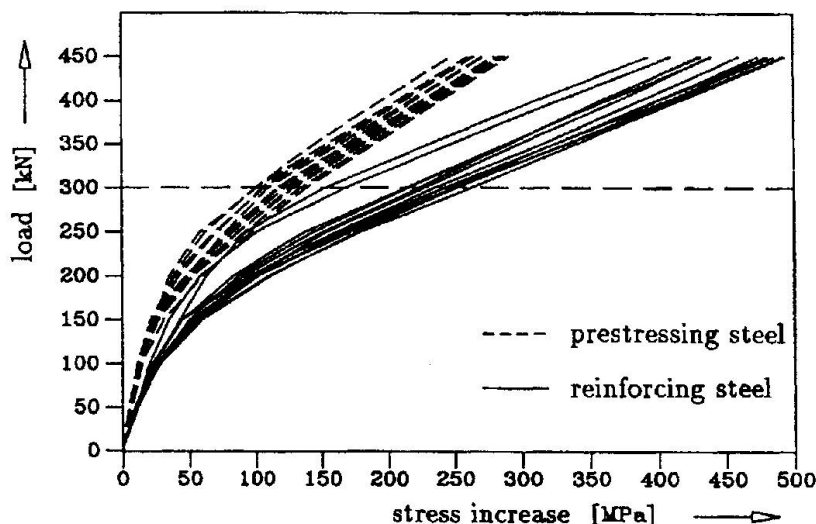


Fig. 7: Stress increases in the reinforcing bars and in the tendon

4. SIMPLE METHOD TO CALCULATE THE STEEL STRESSES

4.1 Background

Because of the different bond behaviour of tendons and reinforcing steel the increase of the stresses in both steel types after the appearance of cracks is different. Considering the compatibility and equilibrium in a cracked prestressed concrete member the following formulas can be stated with the external force F to calculate the actual stresses in tendons and in reinforcing steel.

For a single crack:

$$\sigma_{sR} = \frac{F}{A_s + \xi_1 \cdot A_z} ; \quad \sigma_{zR} = \frac{\xi_1 \cdot F}{A_s + \xi_1 \cdot A_z} \quad (4)$$

where

$$\xi_1 = \sqrt{\xi} \cdot \frac{U_{zw} \cdot A_s}{U_s \cdot A_z} ; \quad \xi = \frac{\tau_{zm}}{\tau_{sm}}$$

For a stabilized crack pattern:

$$\begin{aligned} \sigma_{sR} &= \frac{F - 0,6 \cdot T_{um}}{A_s + A_z} + \frac{0,6 \cdot T_{um}}{A_s + \xi_1 \cdot A_z} \\ \sigma_{zR} &= \frac{F - 0,6 \cdot T_{um}}{A_s + A_z} + \frac{0,6 \cdot \xi_1 \cdot T_{um}}{A_s + \xi_1 \cdot A_z} \end{aligned} \quad (5)$$

These formulas show a stress calculation in prestressed concrete members close to reality, depending on the estimation of the bond force T_{um} and the relation between the mean bond stresses of tendons τ_{zm} and τ_{sm} of the reinforcing steel.

4.2. Calculation of the Mean Bond Stress τ_{zm} and τ_{sm}

The mean bond stress τ_{sm} and τ_{zm} can be calculated with the known crack spacing $s_r = 2 l_{es}$ as follows:

$$\tau_{sm} = \frac{1}{l_{es}} \int_0^{l_{es}} \tau_s(x) dx \quad ; \quad \tau_{zm} = \frac{1}{l_{es}} \int_0^{l_{es}} \tau_z(x) dx \quad (6)$$

For the bond laws according to [6]:

$$\tau_s(x) = C_s \cdot s^{n_s}(x) \quad ; \quad \tau_z(x) = C_z \cdot s^{n_z}(x)$$

It can be written

$$\tau_{sm} = \frac{1}{l_{es}} \int_0^{l_{es}} C_s \cdot s^{n_s}(x) dx \quad ; \quad \tau_{zm} = \frac{1}{l_{es}} \int_0^{l_{es}} C_z \cdot s^{n_z}(x) dx \quad (7)$$

The slip distribution $s(x)$ between two cracks must also be known in order to calculate the mean bond stress. In [5] it was shown that it is possible to describe the slip distribution with the following function

$$s(x) = \frac{w}{2} \cdot \left(\frac{x}{l_{es}} \right)^b \quad (8)$$

The exponent b depends on the load level. For reinforcing steel and deformed tendons b can be calculated as follows:

$$b_s = \begin{cases} 2.85 & \text{For } F \leq F_R \\ 1.85 \cdot (F_R/F)^{1.5} + 1.0 & \text{For } F \geq F_R \end{cases} \quad (9)$$

$$\begin{aligned} n_s &= 0.3; & C_s &= 0.29 \cdot f_{cc} \\ n_z &= 0.3; & C_z &= 0.29 \cdot f_{cm} \end{aligned}$$

for strands:

$$b_z = \begin{cases} 2.70 & \text{For } F \leq F_R \\ 1.70 \cdot (F_R/F)^{1.5} + 1.0 & \text{For } F \geq F_R \end{cases} \quad (10)$$

$$n_z = 0.27; \quad C_z = 0.15 \cdot f_{cm}$$

for smooth tendons:

$$b_z = \begin{cases} 2.40 & \text{For } F \leq F_R \\ 1.40 \cdot (F_R/F)^{1.5} + 1.0 & \text{For } F \geq F_R \end{cases} \quad (11)$$

$$n_z = 0.17; \quad C_z = 0.605 \cdot \sqrt{f_{cm}}$$

With the known slip distribution it is now possible to give the mean bond stress τ_{zm} and τ_{sm} directly:

$$\tau_{sm} = \frac{C_s}{1 + b_s \cdot n_s} \cdot \left(\frac{w}{2} \right)^{n_s}; \quad \tau_{zm} = \frac{C_z}{1 + b_z \cdot n_z} \cdot \left(\frac{w}{2} \right)^{n_z} \quad (12)$$



The relation between τ_{zm} and τ_{sm} is:

$$\xi = \frac{\tau_{zm}}{\tau_{sm}} = k_b \cdot k_s \cdot \frac{C_z}{C_s} \quad (13)$$

where

$$k_s = \left(\frac{w}{2}\right)^{n_z \cdot n_s} \quad k_b = \frac{1 + b_s \cdot n_s}{1 + b_z \cdot n_z}$$

Considering the fact that the crack width in reality is between 0.1 and 0.3 mm, the factor k_s can be approximately replaced by the following constants:

for deformed tendons:	$k_s = 1.00$
for strands:	$k_s = 1.05$
for smooth tendon:	$k_s = 1.34$

4.3. Calculation of the Bond Force T_{um}

The bond force is the part of the force which is transferred from the steel to concrete via the bond after the crack formation. This can be calculated generally as follows

$$T_u = \tau_{sm} \cdot U_s \cdot \frac{s_r}{2} \quad (14)$$

The determination of the the bond force is simple in the case of single cracks because at the end of the transmission length the strain of concrete equals the strain of steel. With this boundary condition the bond force can be expressed with $\alpha = E_s/E_c$ and the reinforcement ratio ρ as follows:

$$T_u = \frac{F}{1 + \alpha_p} \quad (15)$$

In the case of stabilized cracking, the bond force depends on different parameters. Its maximal value is the force which leads to the crack formation in concrete between two adjacent cracks. It can be written as:

$$T_{u,max} = A_{c,ef} \cdot f_{ct} = t_{sm,max} \cdot U_s \cdot \frac{s_{rmax}}{2} \quad (16)$$

where $A_{c,ef}$: effective area of concrete which contributes to the tension capacity of the section

Because the mean bond stress τ_{sm} is a function of the crack width the problem of determination of the bond force T_{um} is solved, if the ratio between the mean w_m and maximal crack width w_{max} as well as the relation between the mean and maximal crack spacing is known.

The assumption of a parabolic distribution curve of the steel stress between two cracks leads to the ratio:

$$\frac{w_m}{w_{max}} = r \cdot \frac{k_1 - 0.33 \cdot (3r - r^2)}{k_1 - 0.67} \quad (17)$$

where r : ratio between the average and maximal crack spacing

$$r = s_{rm}/s_{rmax}$$

k_1 : ratio between the actual load F and the first cracking load F_R ; $k_1 = F/F_R$

The relation between maximal and mean crack spacing for the calculation of the bond force can be assumed as follows:

$$s_{rm} = s_{rmax} \left[1 - 0.5 \cdot \sqrt{1 - \left(\frac{F_R}{F} \right)^t} \right] \quad (18)$$

This assumption is based on the following limitations:

- The properties of single cracks characterize the behaviour of the member in the first cracking load level.
That means: $s_{rm} = 2l_{cs} = s_{rmax}$.
- The mean crack spacing decreases with increasing loads F and tends towards the value of the single transmission length l_{cs} .
That means: $s_{rm} \Rightarrow l_{cs}$.
- The crack pattern changes most strongly around the load level when the first cracking occurs.

Having mathematically fitted the different test results, we can describe the exponent t in eq. (18) depending on the reinforcement ratio ρ as:

$$t = 1 + \frac{2.5}{\rho[\%]} \quad (19)$$

By this the bond force above the first cracking load can be calculated depending on the external loading as follows:

$$T_{um} = A_{c,ef} \cdot f_{ct} \cdot \left[r \cdot \frac{k_1 - 0.33 \cdot (3r - r^2)}{k_1 - 0.67} \right]^{n_s} \cdot r \quad (20)$$

For the repeated loading the bond force can be calculated as follows [6]:

$$T_{um,lw} = T_{um} \cdot \left(\frac{F}{F_{max}} \right) \cdot \frac{1}{(1+r_n)^{0.07}} \quad (21)$$

with $r_n = \log(10 L_w) + L_w/20000$
 L_w = number of cycles.

4.4 Comparison: Test - Calculation

The increase of the steel stresses measured in the first test series is averaged.

The comparison of these averaged values with the calculated stresses as explained above shows a good agreement (Fig. 8). For this calculation the bond stiffness of the tendons in the coupling region was reduced to 50%.

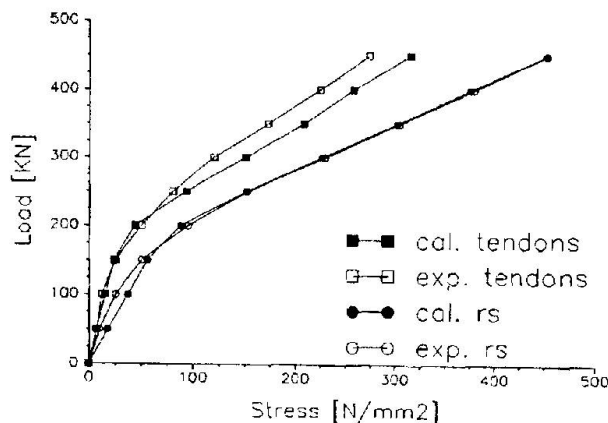


Fig. 8: Comparison Test-Calculation of the stress increase



5. CONCLUSION

The results of the first test series show that only a small reduction in the fatigue strength compared to that of wedge anchors tested in the air. Due to the better bond properties the stress increase in reinforcing steel is higher than that in the tendons. The consequence of this fact is a considerable support for the tendons by the ordinary reinforcement. Furthermore the discontinuity of the curvature within the joint region will be reduced. For the practical application of couplers, it is advisable to provide a minimum of ordinary reinforcement according to German DIN 4227.

The different increase of steel stress in tendons and reinforcing steel can be calculated with the presented simple method.

Literature

1. PATZAK, M.: Die Bedeutung der Reibkorrosion für nicht ruhend belastete Verankerungen und Verbindungen metallischer Bauteile des konstruktiven Ingenieurbaus. Universität Stuttgart. Mitteilungen des Sonderforschungsbereiches 64, Weitgespannte Flächentragwerke. Heft 53 (1979).
2. KORDINA, K., GÜNTHER, J.: Dauerschwellversuche an Koppelankern unter praxisähnlichen Bedingungen. Bauingenieur 57, S. 103-108 (1982).
3. NÜRNBERGER, U., PATZAK, M.: Metallische Verankerungen für dynamisch beanspruchte Zugglieder. Universität Stuttgart. Mitteilungen des Sonderforschungsbereiches 64, Weitgespannte Flächentragwerke. Heft 44 (1978).
4. STURM, R.: Zur Ermüdungsfestigkeit einbetonierter Spanngliedkopplungen und deren Beanspruchung unter besonderer Berücksichtigung der Spannungsumlagerung bei gemischter Bewehrung. Dissertation Darmstadt 1992.
5. TUE, N., KÖNIG, G.: Calculating the Mean Bond and Steel Stress in Reinforced and Prestressed Concrete Members, Darmstadt Concrete Vol. 6 1991.
6. TUE, N.: Zur Spannungsumlagerung im Spannbeton bei der Rißbildung unter statischer und wiederholter Belastung, Dissertation Darmstadt 1992.

Tensile Force of Locked Coil Ropes with Broken Profile Wires

Résistance à la traction de câbles clos présentant des ruptures de fils

Zugkraft von verschlossenen Seilen mit gebrochenen Profildrähten

Gabor OPLATKA

Prof. Dr.

Swiss Fed. Inst. of Technology
Zurich, Switzerland



Gabor Oplatka, born 1935, received his Mech. Eng. degree at the ETH Zurich. He is currently Head of the Section Ropeways at the Institute of Lightweight Structures and Ropeways of the Swiss Fed. Inst. of Technology, Zurich.

SUMMARY

The tests were carried out with five differently locked ropes. Adjacent wires of the same cross-section were severed in turn. The re-establishing of the tensile force in a severed wire was observed. Among others, the following statements could be made: The re-establishing of the tensile force in a broken wire remains more or less similar. The practically full tensile force is reached at a distance of 1.5 to 2.5 lay lengths. If an adjacent wire breaks in the same cross-section of the rope, the re-establishing length of both wires is double.

RÉSUMÉ

On a fait des essais sur cinq différents câbles clos. Des fils voisins de la même section du câble ont été perforés l'un après l'autre. On a observé la recroissance de la force de traction dans un fil perforé. Entre autre, les constatations suivantes ont pu être faites: La recroissance de la force de traction dans un fil cassé reste à peu près la même. La force de traction pratiquement complète est atteinte après 1,5 à 2,5 pas de câblage. Si un fil voisin dans la même section du câble est cassé, la longueur de recroissance dans les fils est double.

ZUSAMMENFASSUNG

An fünf verschiedenen, verschlossenen Seilen wurden Versuche durchgeführt, indem man benachbarte Drähte im selben Querschnitt nacheinander durchtrennte. Dabei beobachtete man den Wiederaufbau der Zugkraft im durchtrennten Draht. Es konnten u.a. die folgenden Feststellungen gemacht werden: Die Zunahme der Zugkraft erfolgt in einem gebrochenen Einzeldraht jedesmal etwa gleich. Die praktisch volle Zugkraft wird nach 1,5 bis 2,5 Schlaglängen erreicht. Bricht ein Nachbardraht im selben Querschnitt des Seiles, so verdoppelt sich die Aufbauänge in beiden Drähten.



1. PROBLEM

Wire breaks only mean a local weakening of a rope. As a result of the friction with the adjacent wires, the tensile force in the broken wire re-establishes itself, which means that at a certain distance the wire has again reached its full carrying force. This distance is called the critical length (l_{cr}).

The aim of the present investigation was to collect data regarding the regularity of this force re-establishing also in cases where several adjacent wires are broken. This should make it possible to use the number and distribution of the wire breaks as well as the design data of the structure in order to calculate the weakening of the rope. This is, of course, an important but not the only criteria for the evaluation of the further usability. The chronological increase of the wire breaks [1], the reason of the wire breaks, the danger of springing out of the wires from the cover layer [2], the deformations of the rope, etc., must also be considered.

Theoretical considerations, for example [3], imply that the tensile force in the broken wire (S_g) increases with the distance from the break spot (l) after

$$S_g = k_1 (e^{\mu k_2 l} - 1)$$

while k_1 and k_2 are constants which depend on the construction data and μ is the coefficient of the friction acting between the wires.

When determining the constants and the coefficients of friction, however, one meets with difficulties and therefore depends on measurements.

2. ROPES TESTED

The tests were carried out on the five ropes mentioned in Table 1.

In order to assess the degree of prestressing (elastic deformation) displayed by the shaped wires the ropes to be tested were marked out into sections measuring about five lay lengths and taken apart. The stress-relieved wires were then measured as to rope diameter, length of lay and distortion. The results of these measurements are listed in Table 2.

Rope no.	1	2	3	4	5
Diameter d (mm)	29.0	39.5	32.5	33.0	23.0
Construction	1+5+7+ +13+18 Z	1+6+12+ +18+21 Z	1+6+12+ +18+24+ +25 Z	(3+3) +9+ +15+21+ +21 Z	1+4+8+ +14+23 Z
Length of lay of outer layer λ (mm)	255	333	272	265	235
Effect. breaking force (kN)	760	1560	1010	≈1050	522

Table 1 Main data of ropes used for tests

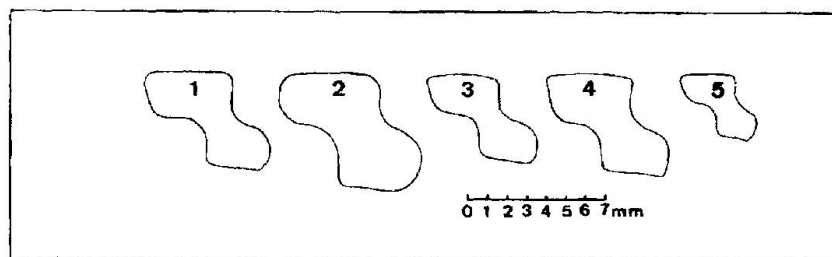


Fig.1 Type and size of shaped wires used in the five tested ropes

Rope no.	1	2	3	4	5
$(\Delta\lambda/\lambda) \cdot 100$	+1.0	+1.8	+2.1	+1.9	+1.9
$(\Delta d/d) \cdot 100$	-7...-14	-11...-14	-6...-15	-10...-14	-7...-17
φ/λ	≈ 0	untwist 22.2°	untwist 8.1°	untwist 19.2°	untwist 8.7°

Table 2 Degree of elastic deformation (prestressing) of Z-wires after removal from unloaded ropes
(λ = lay length, d = rope diam., φ = angle of distortion)

3. METHODS OF MEASUREMENT APPLIED

In the tensioned ropes adjacent wires of the same cross-section of the rope were severed one after the other by means of a carbide tipped drill. During this process the behaviour of the tensile force in the severed wire was observed.

Two different methods were applied in determinating the tensile force of the single wires, namely:

3.1 Strain gauges (rope 1)

Strain gauges were glued on the outer surface of the shaped wires in their longitudinal direction. Circuit wiring and information processing took place in the usual way. The calibration was carried out as follows:

The rope with ends held in cast sockets was put into a tensile testing machine. After ten variations of the rope tensile force between 2 and 40 % of the breaking strength the different measuring bridges were set up and the amplifications were adjusted in such a way that the signals during the change of the rope tensile force were of an equal size for all the measuring bridges. This method is based on the assumption that, in case of central loading of the rope, shaped wire which are intact show the same stress and its change on all the spots but that the single measuring chains (strain gauge, amplifier, galvanometer) show deviations from one to the other.



3.2 Measuring of the wire displacement (ropes 2, 3, 4 and 5)

If sharply defined markings (hairlines) situated across the rope axis are placed on the surface of the rope, the displacement (V) of the broken wire can be read from them with an accuracy of $1/10$ mm.



Fig.2 The displacement of a broken wire can be determined by means of the markings. The picture shows the displacement of two adjacent broken wires at a distance of one lay length from the break spot (test 3, phase b). Attention should be paid to the fact that the displacement of the two wires was of equal size although they had broken one after the other.

Considering the difference of the wire displacement of two adjacent markings (a and b), the contraction of the wire on the stretch in question is

$$\varepsilon = V_a - V_b$$

which is proportional to the decrease of the tensile force in the wire. This means neglecting as a second order effect the fact that, as a result of the wire breaks, the distance between the markings on the intact wires also changes. The calibration is carried out by determining the distances between markings as a function of the tensile force.

Such markings are, of course, also suited for the display of wire breaks which occur in not observable spots on the cover layer of locked coil ropes. This applies, for example, to cast sockets and supporting shoes [4].

4. TESTS CARRIED OUT

The tests were carried out in detail as follows:

Rope no.1

Test 1A: The strain gauges were situated at the following distance from the wire break spot:

- Wire no. "n": 0.1, 0.5, 1, 2, 10, 20 lay lengths
- Wire no. "n + 1": 0.1 lay length
- Wire no. "n + 9": 180° opposite the break spot of the wire "n".

Between the cast sockets the rope measured 30 lay lengths. The break spot was at a distance of 8 lay lengths from the cast socket.

After the calibration described under 3.1 the rope was, step by step:

- a) unloaded $S = 0$
- b) loaded $S = 0.4 \cdot S_B$ (100 %)

- c) unloaded ($S = 0.02 \cdot S_B$); wire "n" spot-drilled at spot "0": tensile force increased till $S = 0.4 \cdot S_B$; the spot-drilled wire "n" broke at $S = 0.17 \cdot S_B$.
- d), e) and f) unloaded once ($S = 0.02 \cdot S_B$) and again loaded with $S = 0.4 \cdot S_B$
- g) unloaded till $S = 0.02 \cdot S_B$; subsequently moved (knocked with a hammer, subjected to the passage of a cross load): tensile force increased to $S = 0.4 \cdot S_B$
- h) twice unloaded and loaded (according to d)

The results are shown in Fig.3 and 4.

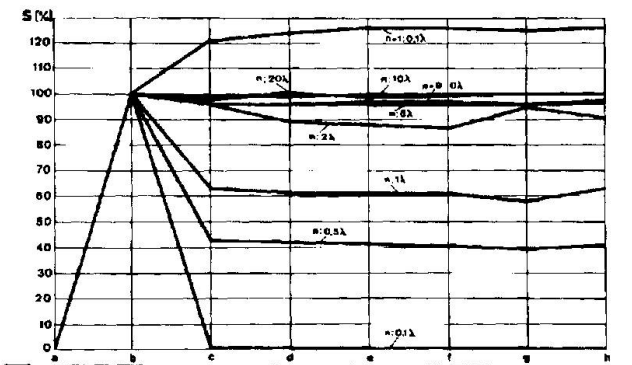


Fig.3 The tensile force in the wires "n"; "n + 1" and "n + 9" during the phases of test 1A. The length indication (λ) gives the distance in lay lengths between the measuring point and the break spot of the wire "n".

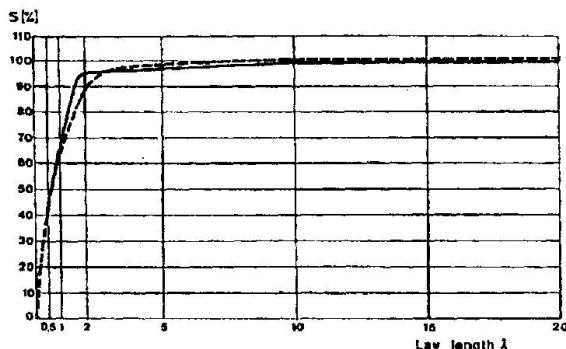


Fig.4 Behaviour of the tensile force in wire "n" after the breaking of the wire (phase c, full line) and after six repeated pulsating loads of the rope (phase h, broken line). It is remarkable that the pulsating load has changed the force behaviour only negligibly.

Test 1B: Like test 1A, but with a concentration of the measuring points near the break spot. The strain gauges were situated:

- on wire "n" at: 0.1, 0.25, 0.5, 0.75, 1.0, 1.5, 2.0, 3.0, 5.0, 8.0 lay lengths
- on wire "n + 9": 180° opposite the break spot of wire "n"

After calibration, step by step,

- a) the rope was unloaded $S = 0$ and loaded by $S = 0.4 \cdot S_B$ (100 %);
- b) the wire "n" was severed at the spot "0";
- c) the rope tensile force was lowered to $S = 0.02 \cdot S_B$ and again increased to $S = 0.4 \cdot S_B$;
- d) the wire "n + 1" was severed at the spot "0";
- e) the wire "n + 2" was severed at the spot "0";
- f) the wire "n + 3" was severed at the spot "0".

The tensile force behaviour of the wires up to phase d was about equal to that in test 1A. Subsequently it became apparent that in such cases where several adjacent wires are broken measuring the tensile force by strain gauge is not possible any more. Besides the tensile force, bending and torsion of the wire also change. The strains caused in this process cannot be separated by strain gauge.

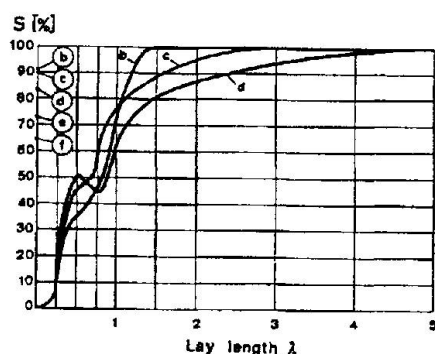


Fig. 5 Test 1B, behaviour of the tensile force in wire "n" after the phases b, c and d. It shows that the tensile force in the wire itself following the break of the adjacent wire is fully re-established after 5 lay lengths. In the break plane the circles are indicating the tensile force in wire "n + 9" (opposite the break spot) after the corresponding test phases.

Test 1C: Like test 1A, but the tensile force was measured on both sides of the break spot. The strain gauges were fixed accordingly:

- On wire "n" on both sides of the break spot at: 0.1, 0.5, 1.0, 2.0 and 4.0 lay lengths.
- On wire "n + 9": 180° opposite the break spot of wire "n".

After calibration, step by step,

- a) the rope was unloaded $S = 0$ and loaded with $S = 0.4 \cdot S_B$ (100 %);
- b) the wire "n" was severed at the spot "0";
- c) the wire "n + 1" was severed at the spot "0". In this process, wire "n-1" which was damaged during the cutting off of wire "n" also broke.
- d) the wire "n + 2" was severed on the spot "0";
- e) the rope tensile force lowered six times to $S = 0.02 \cdot S_B$ and again increased to $S = 0.4 \cdot S_B$. This produced practically no tensile force change in the broken wires.

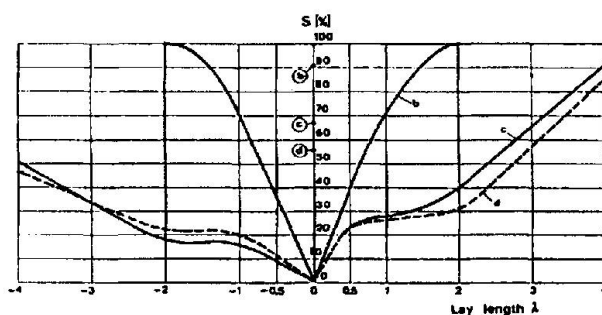


Fig. 6: Test 1C. The tensile force in the cut-off wire "n" is proceeding symmetrically on the left and right side of the break spot. When totally three or four adjacent wires have been cut off (phase c and d), there is no symmetry any more. The circles on the break plane are indicating the tensile force in wire "n + 9" (opposite the break spot) after the corresponding test phases.

Rope no. 2

The cross hairlines according to chapter 3.2 were placed on both sides of the designated break spots at distances of 0.1, 1.0, 2.0, 3.0, 4.0 and 5.0 lay lengths.

Free rope length approx. 800 m.

Rope tensile force = $0.24 \cdot S_B = \text{const.}$

After calibration, step by step,

- a) the wire "n" was severed;
- b) the break spot was subjected to the passage of a carriage with six soft-lined rollers (diameter 80 mm; load 3.0 kN/roller);
- c) the wire "n + 1" was severed and the break spots filled with lead;
- d) the break spots were subjected to four passages of a carriage as mentioned under b);
- e) the break spot was passed over with an engaged track rope brake (see Fig. 8).

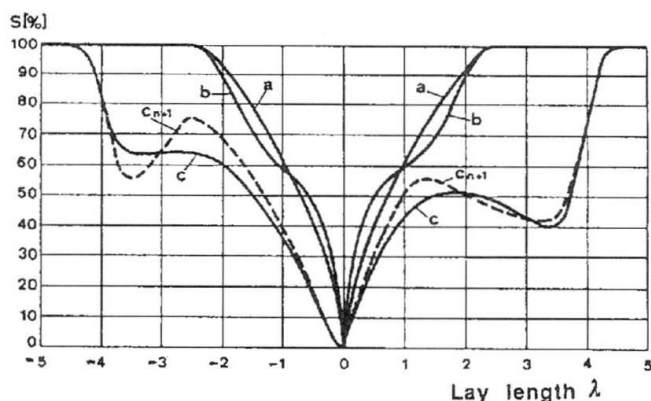


Fig. 7: Rope no.2. Re-establishing of the tensile force in wire "n" on both sides of the break spot: a) after the break of wire "n"; b) after the passage of the rope with rollers and c) after the break of the adjacent wire. The tensile force behaviour in the wire "n + 1" which broke in phase c (broken line) differs only negligibly from that of wire "n".



Fig. 8: The minimal gap between the wires and the lead filling shows that the stress of the two adjacent broken wires has not been relieved because of the passage of loaded rollers (d) and because of a track rope braking (e). Data of the braking: Shoe lining material = multicomponent bronze; shoe length 260 mm; shoe pressure 90 kN.

Rope no.3

The cross hairlines according to chapter 3.2 were placed on both sides of the designated break spot at distances of 0.1, 1.0, 2.0, 3.0, 4.0, 5.0, 6.0 and 7.0 lay lengths.

Free rope length approx. 800 m.

Rope tensile force = $0.30 \cdot S_B = \text{const.}$

After calibration, step by step,

- the wire "n" was severed;
- the wire "n + 1" was severed;
- the break spot was subjected to two passages of the carriage, as described under test 2, point b;
- the wire "n - 1" was severed.

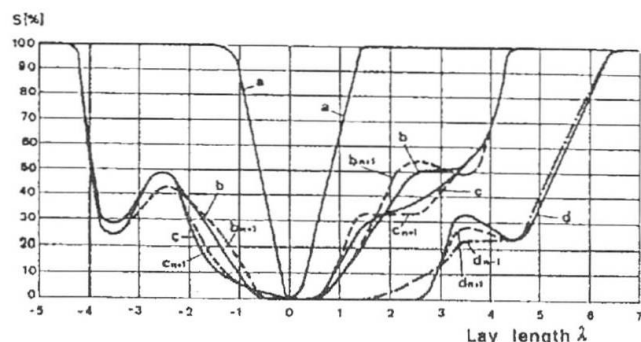


Fig. 9: Rope no.3. Re-establishing of the tensile force in the broken wires with increasing distance from the break spot during the different phases. Again the tensile force behaviour in the adjacent broken wires differs only negligibly from that of wire "n".



Rope no.4

Measuring method and markings like rope no.3.
Free rope length approx. 800 m.
Rope tensile force = $0.29 \cdot S_B = \text{const.}$

After calibration, step by step,

- a) the wire "n" was severed;
- b) the wire "n + 1" was severed;
- c) the wire "n + 2" was severed.

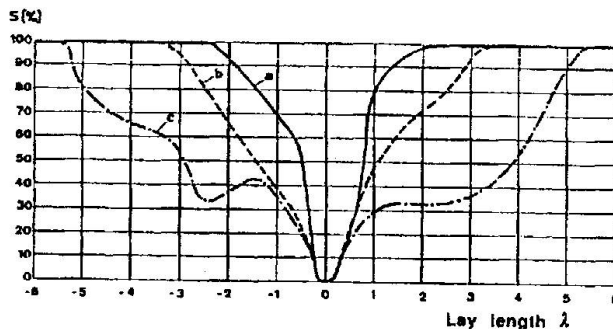


Fig.10: Rope no.4. Re-establishing of the tensile force in wire "n" with increasing distance from the break spot after the cutting off of wire "n" (a), wire "n + 1" (b) and wire "n + 2" (c).

Rope no.5

Cross hairlines according to chapter 3.2 at 0.1 and after each lay length.
Free rope length approx. 32 lay lengths.
Rope tensile force = $0.29 \cdot S_B = \text{const.}$

- a) wire "n" severed
- b) wire "n + 1" severed

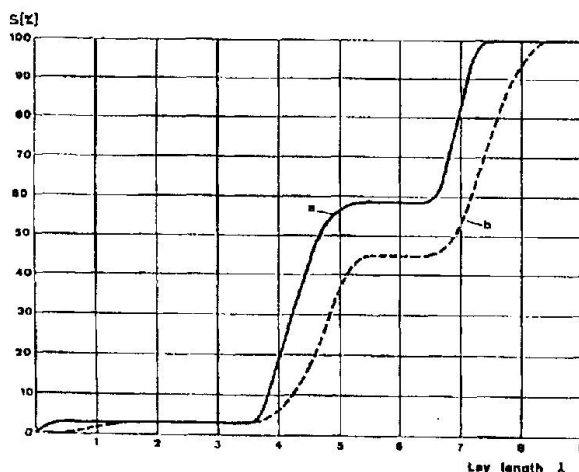


Fig.11: Rope no.5. Re-establishing of the tensile force in the broken wire "n" after its cutting off and after the break of the adjacent wire (b). The fact that the tensile force is only re-established after 8 lay lengths is due to the irregular and loose twisting of the cover layer. From the unloaded rope even a single broken Z-wire could be easily removed.

5. OBSERVATIONS AND CONCLUSIONS

In view of the limited number of findings no generally valid rules can be formulated. However, within the test conditions the following statements may be made:

- In a broken single wire the re-establishing of the tensile force occurs more or less in the same way each time if the cover layer has been firmly twisted. Half of the initial tensile force is reached at a

distance of 0.5 to 0.8, the practically full tensile force after 1.5 to 2.5 lay lengths.

- If the cover layer is loose, as it was the case with rope 5, the critical length can amount to a multiple of the above value.
- If an adjacent wire breaks in the same cross-section of the rope,
 - the re-establishing behaviour of the tensile force in both broken wires is the same.
 - the critical length is doubled and its scattering also increases. Again after exclusion of rope no.5 half of the tensile force was reached after 1 to 4, the full tensile force after 3.5 to 5 lay lengths.
- A rope with wire breaks behaves similarly to a notched homogenous tension bar:
 - In the wire lying near the break spot, the tensile force is increased superproportionally to the decrease of the cross-section.
 - The tensile force is decreased in the wire lying opposite the break spot.

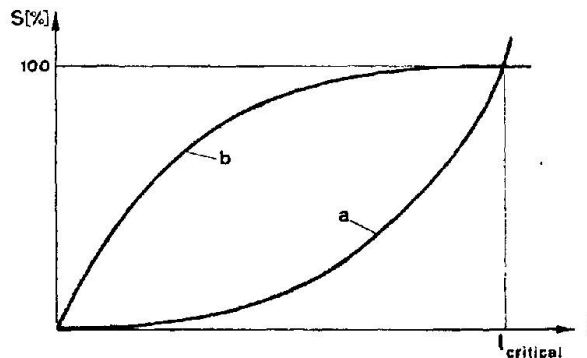


Fig.12: Qualitative behaviour of the re-establishing of tensile force in the broken wire:

- a) expected, neglecting the internal rigidity of the wire;
- b) measured.

- The re-establishing behaviour of the tensile force (S) does not follow, as expected, an exponential curve (a) but rather a saturation curve (b) (Fig.12). This indicates that the re-establishing in the broken wire is not primarily caused by the friction between the wire and the core of the rope (which is due to its spiral-shaped wrapping) but rather by the friction with the adjacent wires caused by the change of form (torsion and bending) which occurred due to the break of the not ideally preformed wire. This means that the internal rigidity of the wire should not be neglected during the theoretical analysis of the problem.

This change of wire form (torsion and bending) is also the reason why the tensile force cannot be measured with strain gauges near the break spot.

- The pulsating bending and tensile stress of the rope but also the track rope braking do not change the tensile force distribution along the broken wire in a significant way. This means that no important increase of the critical length has to be expected during operation.

Practical experience seems to confirm these observations. Gaps of wire breaks have not or have only minimally changed during nine years in the case of five other track ropes in operation. In a double fix anchored track rope where the range of stress amounts to 20 % of the base tensile force a gap grew during these nine years from 20 to 23 mm. These observations should, however, be continued and extended to other ropes.



7. REFERENCES

- [1] OPLATKA, G.: Die zeitliche Folge von Drahtbrüchen in auf Wechselbiegung beanspruchten Drahtseilen.
3rd International Congress of Cable Transport (OITAF), Lucerne 1969.
- [2] OPLATKA, G.: On the Springing Out of Broken Shaped Wires from the External Layer of Full-Lock Coil Ropes.
International Aerial Tramway Review, no. 5/1978
- [3] KAWECKI, Z.: Some problems of quantitative evaluation of indications obtained by means of the electro-magnetic inspection of wire ropes.
Ropeway Review, Oct.-Dec. 1963.
- [4] NETH, A.: Contribution to the discussion at the 4th International Congress of Cable Transport (OITAF), Vienna 1975.
Documentation, page 139.
- [5] DAVIDSON, W.: Investigation and calculation of the remaining tensile strength in wire ropes with broken wires.
Ingeniörsvetenskapsakademien, Handlingsar nr. 214.
- [6] SERGEEV, S.T.: Stalnie kanati (Steel Wire Ropes)
Published by "Technika", Kiev 1974.
Pages 174 - 183 and 190 - 193, Russian.
- [7] CHAPLIN, R.,
TANTRUM, H.: The influence of wire break distribution on strength.
OIPEEC Round Table Conference, East Kilbride/Glasgow, June 19-22nd, 1985.
- [8] KAWECKI, Z.: Magnitnaia defectoscopia stalnih kanatow (Magnetical Defectoscopy of Steel Wire Ropes).
Published by "Nedra", Moscow 1974.
Pages 98 - 111, Russian.